Oxygen-Dependent Regulation of a Diguanylate Cyclase SadC Lacking Canonical Sensory and Regulatory Domains in *Pseudomonas aeruginosa*

Dissertation

der Mathematisch-Naturwissenschaftlichen Fakultät

der Eberhard Karls Universität Tübingen

zur Erlangung des Grades eines

Doktors der Naturwissenschaften

(Dr. rer. nat.)

vorgelegt von

Przemyslaw Piotr Olejnik

aus Gniezno/Polen

Tübingen

2024

Gedruckt mit Genehmigung der Mathematisch-Naturwissenschaftlichen Fakultät der Eberhard Karls Universität Tübingen.

Tag der mündlichen Qualifikation:	05.05.2025
Dekan:	Prof. Dr. Thilo Stehle
1. Berichterstatter/-in:	Dr. Sandra Schwarz
2. Berichterstatter/-in:	Prof. Dr. Karl Forchhammer

Table of Contents

1. Abbreviations

°C	a degree Celsius
µg	microgram
µl	microliter
A	alanine
BACTH	Bacterial Adenylate Cyclase Two-Hybrid
C	cysteine
c-di-GMP	bis-(3'-5')-cyclic dimeric guanosine monophosphate
CF	cystic fibrosis
CIP	calf intestinal alkaline phosphatase
ddH_2O	double distilled water
DGC	diguanylate cyclase
DMSO	dimethyl sulfoxide
DNA	deoxyribonucleic acid
dNTPs	deoxynucleotide triphosphates
DSS	disuccinimidyl suberate
EDTA	ethylenediaminetetraacetate
g	gram
GTP	guanosine-5'-triphosphate
HRP	horseradish peroxidase
IPTG	isopropyl-β-Dthiogalactopyranoside
kbp	kilobasepair(s)
kDa	kiloDalton
l	liter
M	molar
MANT-GTP	2'/3'-O-(N-Methyl-anthraniloyl)-guanosine-5'-triphosphate
MBP	maltose-binding protein
mg	milligram
min	minute
ml	milliliter
mM	millimolar
nm	nanometer
OD	optical density
OdaA	oxygen-dependent activator of alginate production, PA4330
OdaI	oxygen-dependent inhibitor of alginate production, PA4331

PCR	polymerase chain reaction
rpm	revolutions per minute
s	second
SadC	surface adhesion defective, PA4332
$SadC_{cyt}$	Cytosolic part of SadC (nucleotides 880-1464)
SDS	sodiumdodecylsulfate
SDS-PAGE	sodium dodecyl sulphate–polyacrylamide gel electrophoresis
SOC medium	super optimal catabolite repression medium
Tab.	table
TBE	Tris/Borate/EDTA buffer
Tris	2-Amino-2-(hydroxymethyl)propane-1,3-diol
U	enzyme unit
V	volt
v/v	volume/volume
X-gal	5-bromo-4-chloro-3-indolyl-β-D-galactopyranoside

2. Summary

Pseudomonas aeruginosa enhances alginate synthesis in response to oxygen limitation by a mechanism that is currently not fully understood. It was previously found that the membrane-bound diguanylate cyclase (DGC) SadC stimulates alginate synthesis in the lack of oxygen. The C-terminal cytoplasmic part of SadC ($SadC_{cyt}$) containing the GGEEF domain has substantially higher DGC activity when purified from bacteria grown under anaerobic conditions than aerobic conditions. *sadC* is located in a predicted and highly conserved operon with genes encoding a mono-functional enoyl-CoA isomerase (*odaA*, PA4330) and putative dioxygenase reductase (*odaI*, PA4331), which function as a positive and negative regulator of alginate synthesis under oxygen limitation, respectively. It is vital to notice that SadC does not appear to contain oxygen sensing domains. It suggests that SadC and possibly other proteins regulate alginate synthesis in an oxygen-dependent manner. mRNA levels of those genes are not influenced by changes in oxygen tensions. Bacterial Adenylate Cyclase Two-Hybrid assay was performed to study interactions that occur between SadC, $SadC_{cyt}$, OdaA, and OdaI. Results indicate that OdaA interacts with SadC and itself in the presence and absence of oxygen. No interaction between OdaI and SadC was observed, suggesting that the inhibitory effect of OdaI on alginate synthesis is not based on direct interaction with SadC. Moreover, we show that a transmembrane domain of SadC is critical for its functionality.

In this work, cysteine residues (C390, C420, C421, and C478) of $SadC_{cyt}$ were substituted with alanine. It was found that in the case of mutant $SadC_{cyt\ C420A\ C421A}$, the binding efficiency of GTP was enhanced. That can mean that oxygen may modify cysteine residues of SadC and influence in that way its functionality. It was hypothesized that the activity of the SadC may be altered in aerobic and anaerobic compared to microaerophilic conditions, which were previously shown to be optimal for the growth of *P. aeruginosa.*

Through mRNA sequencing, significant transcriptional changes across numerous genes in *P. aeruginosa* were identified, particularly highlighting impact of deletion of SadC on alginate biosynthesis genes. This global analysis underscored the intricate regulatory network mediated by SadC, suggesting its pivotal role in bacterial adaptation to varying oxygen conditions and its influence on alginate production pathways.

3. Zusammenfassung

Pseudomonas aeruginosa verstärkt die Alginatsynthese als Reaktion auf Sauerstoffmangel durch einen Mechanismus, der derzeit nicht vollständig verstanden ist. Frühere Untersuchungen zeigten, dass die membrangebundene Diguanylatcyclase (DGC) SadC die Alginatsynthese bei Sauerstoffmangel stimuliert. Der C-terminale zytoplasmatische Teil von SadC ($SadC_{cyt}$) mit der GGEEF-Domäne zeigte eine deutlich höhere DGC-Aktivität, wenn er aus Bakterien gereinigt wurde, die unter anaeroben Bedingungen und nichtunter aeroben Bedingungen gewachsen waren. SadC befindet sich in einem vorhergesagten und stark konservierten Operon mit Genen, die für eine monofunktionelle Enoyl-CoA-Isomerase (OdaA, PA4330) und einen hypothetische Dioxygenasen-Reduktase (OdaI, PA4331) kodieren. Diese fungieren unter Sauerstoffmangel als positiver bzw. negativer Regulator der Alginatsynthese. Es ist wichtig zu anzumerken, dass SadC keine Sauerstoffsensordomänen zu enthalten scheint. Dies legt nahe, dass SadC und möglicherweise andere Proteine die Alginatsynthese in einer sauerstoffabhängigen Weise regulieren. Die mRNA-Level dieser Gene werden nicht durch Veränderungen der Sauerstoffkonzentration beeinflusst. Bacterial Adenylate Cyclase Two-Hybrid Assays wurden durchgeführt, um die Interaktionen zwischen SadC, $SadC_{cyt}$, OdaA und OdaI zu untersuchen. Die Ergebnisse zeigten, dass OdaA sowohl in Anwesenheit als auch in Abwesenheit von Sauerstoff mit SadC und sich selbst interagiert. Es wurde keine Interaktion zwischen OdaI und SadC beobachtet, was darauf hindeutet, dass der hemmende Effekt von OdaI auf die Alginatsynthese nicht auf einer direkten Interaktion mit SadC basiert. Zudem wurde gezeigt, dass eine transmembrane Domäne von SadC für seine Funktionalität entscheidend ist. In dieser Arbeit haben wir Cystein-Reste (C390, C420, C421 und C478) von $SadC_{cyt}$ durch Alanin ersetzt. Es wurde herausgefunden, dass die Bindungseffizienz von GTP im Fall des mutierten $SadC_{cyt}$ C420A C421A erhöht war. Das könnte bedeuten, dass Sauerstoff die Cystein-Reste von SadC modifiziert und so seine Funktionalität beeinflusst. Wir haben die Hypothese aufgestellt, dass die Aktivität von SadC unter aeroben und anaeroben Bedingungen, verändert sein könnte. Durch mRNA-Sequenzierung wurden starke transkriptionelle Veränderungen in zahlreichen Genen von *P. aeruginosa* identifiziert, wenn *sadC* deletiert ist und die Bakterien unter anaeroben Bedingungen kultiviert wurden.. Diese globale Analyse unterstreicht das komplexe regulatorische Netzwerk, das durch SadC vermittelt wird, und deutet auf seine zentrale Rolle bei der bakteriellen Anpassung an unterschiedliche Sauerstoffbedingungen sowie seinen Einfluss auf die Alginatproduktionswege hin.

4. Introduction

4.1 Cystic fibrosis

Cystic fibrosis (CF) is an autosomal recessive genetic disease. The incidence is the highest in the Caucasian population and is estimated at 1/3000 and 1/6000 (Scotet et al., 2020; Southern et al., 2007). Dorothy H. Anderson first described the disease in 1938 (Anderson, 1938). In 1989, it was revealed that CF is caused by mutations in the *CFTR* gene (cystic fibrosis transmembrane conductance regulator) (Kerem et al., 1989; Riordan et al., 1989; Rommens et al., 1989). The CFTR protein is an ABC transporter, a phosphorylation and ATP-gated anion channel which increases the flow of chloride and thiocyanate anions across the membrane and is localized to the apical side of the epithelial cell in several organs such as lungs, pancreas, or testicles (Elborn, 2016).

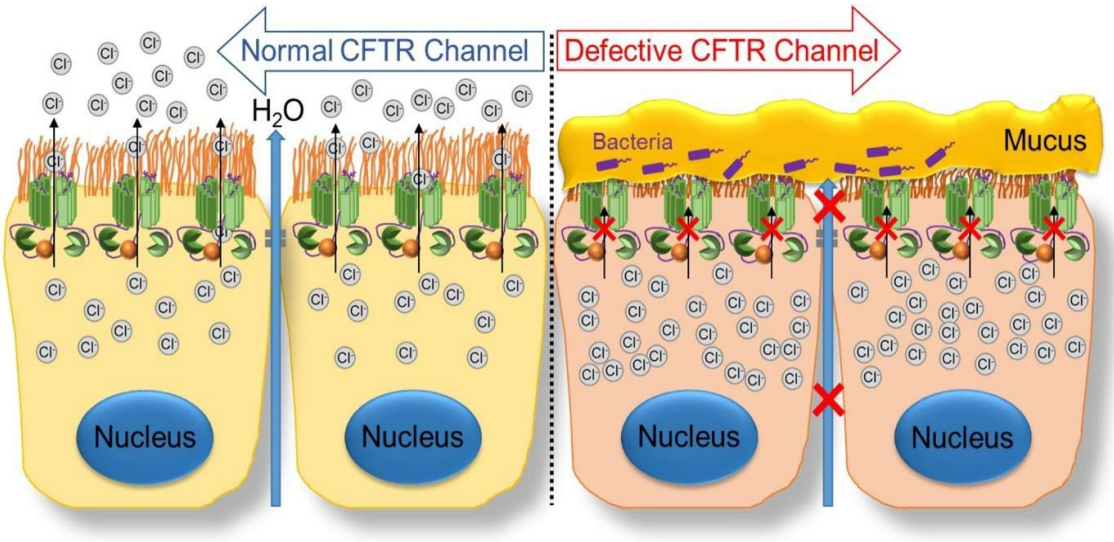

Figure 1 Lung epithelium of healthy individuals with functional CFTR protein (left) and CF patients with dysfunctional CFTR protein (right). Normally functioning CFTR protein allows movement of chloride anions to the outside of cell, and as a consequence movement of sodium cations (not shown) and water which results in the right airway surface liquid (ASL) composition and functional MCC. On the other hand, dysfunctional CFTR protein does not allow movement of chloride ions. Because of that, sodium cations also do not move outside of the cell, and water does not hydrate ASL. That leads to buildup of thick, vicious and dehydrated mucus outside of cells and impeded MCC, leading to colonization of lungs by pathogens (Harutyunyan et al., 2018).

Although deletion of the phenylalanine residue Phe508del is the most common mutation in the *CFTR* gene and occurs in more than two-thirds of CF cases, there are approximately 2,000 other known disease-causing mutations (Antoniou & Elston, 2016; Davidson & Porteous, 1998; Elborn, 2016). *CFTR* mutations can be grouped into six classes based on their functional consequences: total or partial lack

of a functional CFTR protein (class I); misfolding of the protein and disturbed trafficking to the cell membrane (class II); non-responding gating mechanism to intracellular signals (class III); reduced ion conductance (class IV); reduced synthesis of the protein (class V) and a shortened half-life of a protein (class VI) (Boyle & De Boeck, 2013; Turcios, 2020).

There are existing two mechanisms which assure clearance of healthy lungs: mucociliary clearance (MCC) and cough reflex. The MCC allows a clearance of lung from inhaled particles, including pathogens. The MCC is based on production of airway surface liquid (ASL), which consists of periciliary sol layer (PCL) and overlying mucus gel layer. Cilia are present on the surface of airways beating in a coordinate fashion within periciliary sol layer. During the movement, cilia penetrate mucus gel layer and propel it towards larynx, where the mucus becomes swallowed or coughed out.

In lungs, functional CFTR protein allows the transport of chloride and thiocyanate ions across a cell membrane into ASL. Sodium cations follow chloride cations through epithelial sodium channel (ENaC) and increase total electrolyte concertation in ASL, which results in water movement out of the cell via osmosis. In CF, disrupted CFTR protein is not able to transport chloride and thiacyanate anions which results in disrupted chloride secretion, sodium reabsorption, and water transport are disrupted, leading to mucus dehydration and impaired MCC (Figure 1) (Stoltz et al., 2015). That causes airflow obstructions, clogs in the airways, and colonization of bacteria in a mucus, resulting in chronic infections and inflammation, which over the years can lead to increased damages and respiratory failure (Malhotra et al., 2019; Stoltz et al., 2015; Turcios, 2020).

4.1.1 Oxygen limitation in CF lungs

In healthy individuals, the mucosal surfaces of the lungs are well-oxygenated. Contrastingly, the lungs of cystic fibrosis (CF) patients, as well as those with asthma or chronic obstructive pulmonary disease, often present with conditions such as stagnant mucus and infection-induced inflammation. These, coupled with the high oxygen demand from cellular activity, lead to hypoxia within the mucus and the lung epithelial layer (Figure 2) (Page et al., 2021; Worlitzsch et al., 2002). Local lung hypoxia plays a crucial role in the disease and influences host-pathogen interactions (Page et al., 2021).

In human cells, a response to hypoxia is governed by, e.g., hypoxia-inducible factor (HIF), which is recognized as a central transcriptional regulator for hypoxia. HIF is a DNA-binding protein regulating the expression of hundreds of genes in response to hypoxia (Page et al., 2021). It is expressed in, e.g., innate immune cells like

macrophages, neutrophils, and epithelial cells (Colgan et al., 2020; Page et al., 2021). HIF activation leads to the preservation of innate immune functions, prolonged survival of neutrophils, more significant macrophage response to bacterial lipopolysaccharide, and aggravated inflammatory response (Frede et al., 2006; M et al., 2020; Page et al., 2021; Walmsley et al., 2005). Although processes triggered by hypoxia are essential to resolve infections, the immune response may be exaggerated, leading to tissue damage in chronic respiratory diseases (Page et al., 2021).

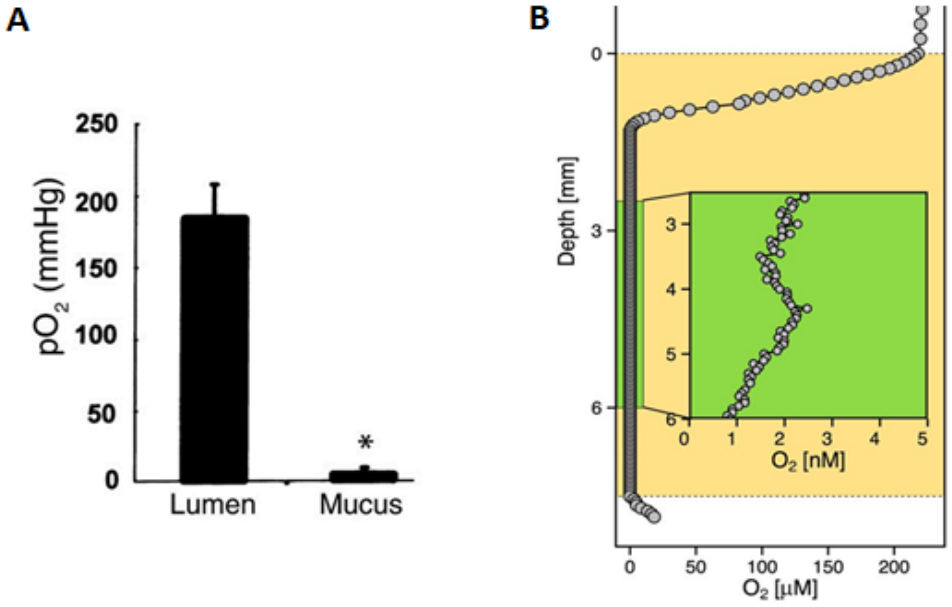

Figure 2 (A) Oxygen concentrations, measured *in vivo*, in the airway lumen and mucus of CF patients. The oxygen concentration in mucus is low, which creates local hypoxia (Worlitzsch et al., 2002). (B) The profile of oxygen concentration, measured *ex vivo*, in the sputum of paediatric patients consists of a thin aerobic surface, whereas deeper levels are hypoxic (Cowley et al., 2015).

Due of hypoxia, secretion of mucus and mucus plugging increase, and the number of secretory cells compared to ciliated cells is changed, strengthening the effects of CFTR protein dysfunction in CF patients (Mall, 2016; Page et al., 2021; Turcios, 2020). Furthermore, epithelium necrosis in obstructed airways triggers neutrophilic inflammation, resulting in hypoxia strengthening (Fritzsching et al., 2015). Additionally, low oxygen tensions in lung epithelium lead to elevated epithelial permeability, increasing susceptibility to pathogens (LaFemina et al., 2014; Page et al., 2021)

Moreover, through HIF transcriptional factor, low oxygen tensions cause increased expression of Platelet-activating factor receptor (PAFR) in the epithelium (Shukla et al., 2015). Pathogenic bacteria use this protein as an adhesion molecule, which enables better adherence to the epithelium, and is associated with a faster course of pneumonia and quicker lung function decline (Grigg et al., 2017; Page et al., 2021).

Besides described consequences, hypoxia also leads to an elevated biofilm formation by *P. aeruginosa* and other pathogens (Nguyen & Oglesby-Sherrouse, 2016); dysregulation in airway glucose homeostasis, which increases glucose availability to pathogens (Baker et al., 2007; Brennan et al., 2007); enhanced replication of viruses (Page et al., 2021) and imbalanced release of inflammatory factors, like proteases or reactive oxygen species (ROS), which may additionally lead to excessive damages of tissue (Gibbs et al., 1999; Page et al., 2021).

4.1.2 Infections in CF lungs

Retention of sticky, dehydrated mucus in CF lungs leads to chronic obstructions of airways, colonization of lungs by pathogenic bacteria, and finally, acute and chronic infections. Chronic infections are the reason for approximately 95% of deaths of CF patients (Hauser et al., 2011). In young patients, a lung microbiome is diverse. Still, with years of chronic infections, the diversity of bacteria in the lungs becomes less varied, and airways become colonized mainly by typical CF pathogenic bacteria such as *P. aeruginosa*, *Achromobacter xylosoxidans*, *Burkholderia cepacia,* and *Staphylococcus aureus* (Figure 3) (Lipuma, 2010; Registry, 2020; Turcios, 2020).

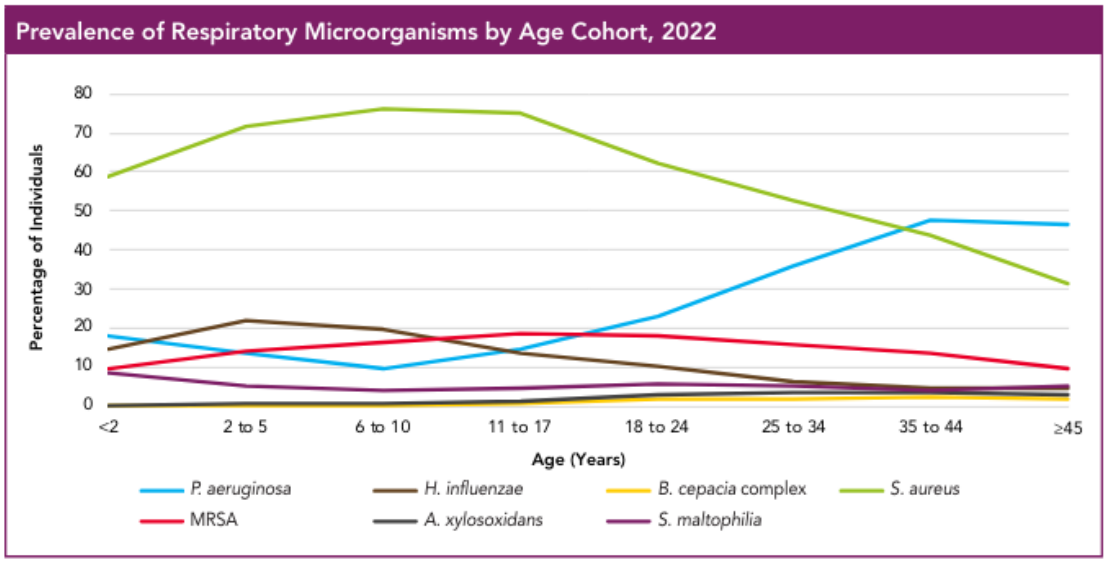

Figure 3 Occurrence of bacteria in lungs of CF patients by age. During the lifespan of patients, *P. aeruginosa* becomes one of the major pathogens infecting the lungs of CF patients (Registry, 2022).

Besides bacterial infections, CF patients are vulnerable to viral ones. Conditions with a respiratory syncytial virus (RSV), human rhinovirus, influenza virus A and B, and parainfluenza virus are the most common (Blanchard & Waters, 2019;

Wat & Doull, 2003). The severity of viral infections is more significant in CF patients than in healthy individuals (Schogler et al., 2016; Wat & Doull, 2003). In general, viral infections increase the occurrence of pulmonary exacerbations, cause a drop in lung function and increase inflammatory markers (Flight et al., 2014; Wat & Doull, 2003). Interestingly, viral/bacterial coinfections are very common. Viruses positively influence a new acquisition, conversion to chronic infection, or increased biofilm formation by *P. aeruginosa* (Blanchard & Waters, 2019; Hendricks et al., 2016; Johansen & Hoiby, 1992).

Another group of microorganisms, which infects the lungs of CF patients, is fungi. *Aspergillus fumigatus* is the most commonly diagnosed fungi, with prevalence oscillating around 15% (Turcios, 2020). The presence of *A. fumigatus* in CF lungs can be asymptomatic but can also cause allergic bronchopulmonary aspergillosis (ABPA), which displays asthma-like symptoms (Elphick & Southern, 2014; Stevens et al., 2003; Turcios, 2020).

4.1.3 Treatment of bacterial infections in CF patients

The management of bacterial infections in CF patients primarily revolves around the prevention and control of infections through antibiotic therapy. CF patients should be regularly tested for presence of pathogens in sputum, including performance of antibiogram. Once a pathogen is detected, antibiotic treatment is started basing on an individual situation of the patient and record of past infections. In this case, therapy aims an eradication of pathogen. In case of chronic infections, antimicrobial therapies usually fail to eradicate the pathogen. The implementation of long-term treatments aims to control the infection and attempts to prevent the deterioration of patients' respiratory functions, even if complete eradication is not possible. One of the common schemes of long-term treatment of *P. aeruginosa* infections is inhalation of aztreonam and tobramycin in a 1-month on and 1-month off pattern (Allen et al., 2020; Ng et al.; Wat & Doull, 2003).

The prevention of infections is as important as the pharmaceutical treatment. It is crucial to include respiratory clearance treatments and chest physiotherapy to improve impaired MCC. It is necessary to maintain high hygienic regime of nebulizers and airway clearance devices used for treatment. Pathogens can be easily transferred between CF patients, therefore their contact should be reduced to minimum. It is also recommended to prevent the spread of infections by often handwashing, usage of medical masks (especially in healthcare facilities) and avoidance of in-person socialization (Saiman et al., 2013; Turcios, 2019; Wat & Doull, 2003).

4.2 *Pseudomonas aeruginosa*

P. aeruginosa is a, gram-negative, facultative anaerobic, rod shaped bacterium which colonizes multiple natural environments. It is considered as an opportunistic pathogen, which causes serious infections mostly in patients with cystic fibrosis and traumatic burns. Moreover, *P. aeruginosa* easily survives on moist surfaces like medical equipment or sanitary facilities, causing cross-infections in health care facilities (Hogardt & Heesemann, 2013; Registry, 2020; Valentini et al., 2018).

P. aeruginosa is the most common bacterium isolated from adult CF patients (up to ~70%) (Registry, 2020). Initially, isolates of that bacterium resemble those from the natural environment and are nonmucoid, present at low density, and are usually susceptible to antibiotics. Over the years of chronic infection, *P. aeruginosa* converts to mucoid phenotype, with a high alginate secretion and tolerance to antibiotics and the immune system of patients. Antibiotic therapies aiming at the eradication of nonmucoid *P. aeruginosa* are usually successful. At the same time, a mucoid phenotype can cause chronic infection, be rarely eradicated, and is associated with a rapid decline in lung function, high morbidity, and reduced life expectancy of the CF patients (Douglas et al., 2009; Emerson et al., 2002; Rosales-Reyes et al., 2021; Turcios, 2020).

4.2.1 Genetic and phenotypic adaptations of *P. aeruginosa* in lungs of CF patients

In comparison to the natural environment, in CF lungs, *P. aeruginosa* encounters new selective pressure due to, e.g., host immune system, a shortage of some nutrients, oxygen gradient, presence of antibiotics and other pharmaceuticals, or competition with other pathogens (Rossi et al., 2021). These factors force *P. aeruginosa* to adapt to new conditions encountered in the lungs of CF patients. The selective pressure in the CF airways makes *P. aeruginosa* to switch from planktonic lifestyle associated with acute infections to biofilm-related lifestyle which plays a major role in chronic persistent infections (Valentini et al., 2018). Interestingly, those changes share a significant similarity from independent patients across the whole globe (Kordes et al., 2019; Rossi et al., 2021). The most common changes occur in DNA repair processes, energy metabolism, acquisition of limited nutrients, antibiotic and stress resistance, or biofilm formation and are described in the following chapters (Rossi et al., 2021).

4.2.1.1 Genetic adaptations

Usually, primary isolates of *P. aeruginosa*, which colonizes CF lungs, persist for long periods and dominate. Interestingly, the coexistence of more than one variant is possible. Over time of the infection, other clones of *P. aeruginosa* invade the lungs. It is unlikely that they are competitive enough to replace a primary variant, which has already started adapting to a specific CF lung environment over the time of chronic infection (Kordes et al., 2019; Marvig et al., 2013; Rossi et al., 2021).

Interestingly during the early stages of infection, *P. aeruginosa* shows a hypermutator phenotype, gained by mutations in genes like *mutS* and *mutL,* which are involved in DNA repair processes (Marvig et al., 2013; Marvig et al., 2015). Over time *P. aeruginosa* adapts to new conditions, accumulation of adaptive mutations becomes slower and compensatory mutations appear, decreasing mutation rate and transforming bacterium into a more stable and adopted phenotype (Rossi et al., 2021).

Genetic studies revealed the most frequently mutated genes in adaptation to CF lungs. They include genes engaged in biofilm lifestyle (*algU*, *morA* or *mucA*), antibiotic resistance (*gyrA*, *gyrB*, *mexZ*, *mexB*, *mpl,* and *nfxB*), decreased virulence factor synthesis (*mpl* and *ykoM*), quorum sensing (*lasR*), and other regulatory systems (e.g., *gacA*, *gacB* or *rpoN*) (Klockgether et al., 2018; Marvig et al., 2015; Rossi et al., 2021).

4.2.1.2 Nutrients acquisition and glucose metabolism

In CF lungs, *P. aeruginosa* encounters an environment rich in nutrients, which leads to high rates of cellular growth and high biomass production. Even though the availability of nutrients like iron or zinc ions, which are crucial cofactors for the functioning of multiple enzymes, is deficient and limits the growth of *P. aeruginosa* (Alonso et al., 1999; Palmer et al., 2007; Rossi et al., 2021). The expression of proteins involved in zinc-sequestering and uptake systems or iron-scavenging systems provide *P. aeruginosa* higher availability of restricted, essential nutrients (Rossi et al., 2018).

Clinical CF isolates of *P. aeruginosa* show an inability to assimilate and metabolize glucose, although cultured in media with high concentrations of that carbohydrate. In CF lungs, glucose homeostasis is disturbed, and glucose concentration is elevated, which seems not to correspond with impaired metabolism of glucose by *P. aeruginosa* CF isolates (Baker et al., 2007; Brennan et al., 2007; La Rosa et al., 2018). A reduction of glycolysis and funnelling TCA cycle to the assimilation of amino acids and lactate lead to a lower synthesis of electron donors in the electron transport chain and most likely results in improved resistance to oxidative stress (Crabbe et al., 2019; La Rosa et al., 2018; Rossi et al., 2018; Rossi et al., 2021).

4.2.1.3 Development of antibiotic resistance and tolerance

Due to improved and intense treatment, including often or even continuous antibiotic therapy, the life expectancy of CF patients is close to 50 years (Registry, 2022; Scotet et al., 2020). High usage of antibiotics can cause raising resistance development towards them by all pathogens, including *P. aeruginosa* (Figure 4). Several mechanisms help bacteria to develop antibiotic resistance. Spontaneous mutations in antibiotic targets, like mutations in ribosomal genes or gyrase gene, can cause resistance towards tobramycin or fluoroquinolone, respectively. There are also known cases where the acquisition of mobile genetic elements results in resistance (Botelho et al., 2019; Halfon et al., 2019; Hooper & Jacoby, 2015; Rossi et al., 2021). The development of antibiotic resistance involves several factors: decreased cell membrane permeability, the expression of genes such as β-lactamases like AmpC, efflux pumps including MexAB-OprM, MexCD-OprJ, MexEF-OprN, and MexXY, as well as biofilm formation, which impedes molecule diffusion and alters bacterial metabolic activity (Botelho et al., 2019; Ciofu & Tolker-Nielsen, 2019; Rossi et al., 2021).

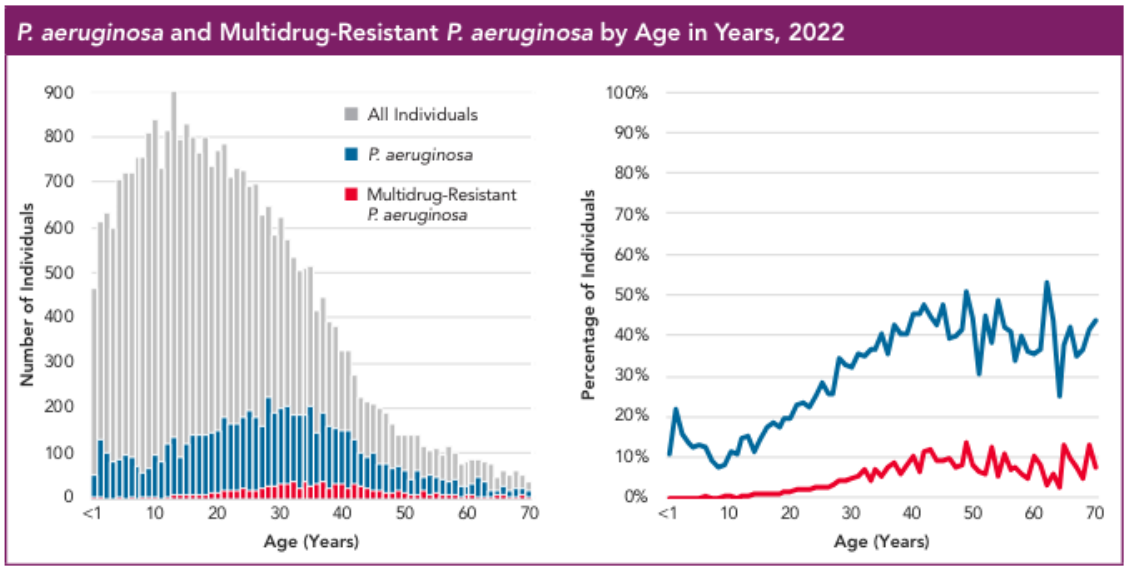

Figure 4 Number (left) and percentage (right) of individuals colonized by *P. aeruginosa* and multidrug-resistant *P. aeruginosa* by age in CF patients. The occurrence of *P. aeruginosa* infections increases with the age of CF patients. Due to frequent antibiotic treatments, *P. aeruginosa* often becomes multidrug-resistant (Registry, 2022).

P. aeruginosa can also diversify to subpopulations that play a high survival role during exposure to antibiotics. One of the mechanisms is to develop a group of cells, called persisters, which stop growth and replication during exposure to an antibiotic and resume normal functions after a stop of treatment. Interestingly, no genetic changes were observed between subpopulations, which could explain the formation of persisters

by *P. aeruginosa* (Balaban et al., 2019; Rossi et al., 2021). *P. aeruginosa* can also use another mechanism to increase resistance toward antimicrobials substantially. A heteroresistance phenotype emerges in exposure to antibiotics, by a tandem replication of specific genes, which occurs at low frequency, only in a part of the bacterial population and elapses after an exposure. That mechanism is responsible for increased resistance towards polymyxin and carbapenem (Andersson et al., 2019; He et al., 2018; Hermes et al., 2013; Rossi et al., 2021).

4.2.1.4 Alternative respiratory pathways

P. aeruginosa seems to respond to conditions in CF lungs within a continuum along with oxygen tensions and produce energy through a mixture of microaerophilic and anaerobic respiration (Alvarez-Ortega & Harwood, 2007; Rossi et al., 2021). Although oxygen respiration provides the highest yields in energy, *P. aeruginosa* prefers microaerophilic conditions and can actively create such an environment with lower oxygen transfer, most likely by secretion of yet unidentified substances (Kim et al., 2003; Sabra et al., 2002; Schobert & Jahn, 2010). When oxygen is lacking, and cannot be utilised as an electron acceptor, *P. aeruginosa* can switch to other alternative respiratory pathways, with a preference in an order: denitrification and arginine or pyruvate fermentation (Schobert & Jahn, 2010).

Four different reductases are essential for denitrification: NarGHI, NirS, NorCB, and NosZ and catalyse reductions of nitrate (NO_3^-), thought nitrite (NO_2^-) and nitric oxide (NO), to dinitrogen (N_2) (Zumft, 1997). For induction of denitrification in *P. aeruginosa,* a presence of nitrate or nitrite in concentrations from 10 to 700 µM is necessary and such can be found in CF lungs (Fritz et al., 2007; Hassett, 1996; Palmer et al., 2007; Schobert & Jahn, 2010). Interestingly, besides energy generation, the denitrification pathway is also engaged in maintaining a certain NO level by nitrite reductase NirS and nitric oxide reductase NorCB. NO is a very reactive free radical, toxic for cells above some concertation. Although it is an essential signalling molecule for biofilm dispersal, it is a part of the host immune response towards bacteria. Hence, nitric oxide reductase plays a vital role in neutralizing host immune response and maintaining optimal concertation of NO in cells (Kakishima et al., 2007; Pullan et al., 2008; Schobert & Jahn, 2010; Spiro, 2007).

Simultaneously with denitrification, arginine fermentation is induced in *P. aeruginosa*. Mucus in CF lungs is rich in amino acids, including arginine. Analyses of the transcriptome of *P. aeruginosa* in CF sputum revealed an increased expression level of *arcDABC* operon, which encodes proteins required for arginine fermentation (Platt et al., 2008; Schobert & Jahn, 2010; Son et al., 2007).

The last type of alternative respiration pathway in anaerobic conditions is pyruvate fermentation which provides enough energy only for the survival of *P. aeruginosa* (Eschbach et al., 2004). *P. aeruginosa* PA14, under aerobic and microaerobic conditions, secrets pyruvate in the late stationary phase of growth. Pyruvate diffuses into deeper anoxic parts of biofilm and supports the survival of bacterial cells located there (Price-Whelan et al., 2007; Schobert & Jahn, 2010).

4.2.1.5 Biofilm formation

Most bacteria, including *P. aeruginosa*, can attach to biotic and abiotic surfaces and create a biofilm. A biofilm matrix encases bacteria and builds up more than 90% of whole biofilm biomass and consists of exopolysaccharides (Psl, Pel, alginate), extracellular DNA (eDNA), proteins, and lipids (Donlan, 2002; Ryder et al., 2007; Thi et al., 2020). Biofilm formation is one of the strategies of bacteria to survive limiting conditions, like changes in temperature, nutrient availability, resistance towards host immune system or antibiotics, or protection from desiccation. Additionally, biofilm provides a platform for quorum sensing (a process by which bacteria communicate with each other using chemical signals) and sharing by bacteria populations common goods, like nutrients, enzymes, or cytosolic proteins (Thi et al., 2020). *P. aeruginosa* creates biofilms to persist, survive and grow in such environments as CF lungs, wounds, and medical and industrial equipment (Thi et al., 2020).

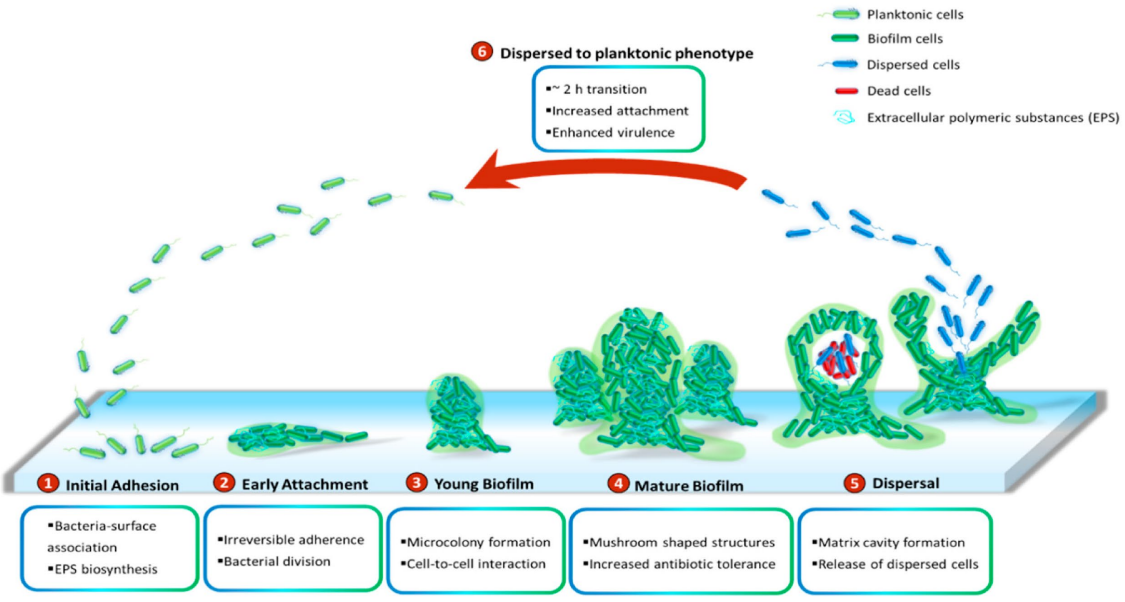

Figure 5 The model of stages of biofilm formation (Thi et al., 2020).

The commonly proposed model of formation of biofilm consists of six stages: bacteria adhere to a surface, which can be reversible, and for *P. aeruginosa* attachment

is material-specific (stage I); bacteria adhere to a surface in an irreversible manner (stage II); bacteria start intense propagation and form structures called microcolonies (stage III); biofilm matures, and microcolonies develop into mushroom-like structures (stage IV); mushroom-like structure disrupts due to cell autolysis which results in freeing dispersal cells (stage V); dispersal cells spread and colonized new spaces (stage VI). Biofilm formation cycle repeats (Figure 5) (Thi et al., 2020).

4.2.1.6 Alginate synthesis

Alginate is an anionic linear polymer consisting of β-1,4-mannuronic acid and α-L-guluronic acid (Hay et al., 2014). Alginate plays a role in the maturation of biofilm (although it is not essential for its formation), maintains hydration of bacteria under desiccating conditions, impedes the diffusion of antimicrobials, and protects from host immune system defence and reactive oxygen species (Hay, Gatland, et al., 2009; Hay et al., 2014; Hodges & Gordon, 1991; Learn et al., 1987; Li et al., 2010; Nivens et al., 2001; Wozniak et al., 2003). Biosynthesis of alginate is energetically costly. Therefore, it is controlled by a complex regulatory network at the transcriptional, posttranscriptional, and posttranslational levels (Hay et al., 2014; Wozniak et al., 2003).

Alginate synthesis is conducted by a polymerization/secretion complex which spans from the inner to the outer cell membrane. A fructose-6-phosphate synthetised *via* gluconeogenesis serves as substrate for synthesis. Three cytosolic enzymes, AlgA, AlgC and AlgD, catalyse four reactions to produce GDP-mannuronic acid from fructose-6-phosphate. Next, GDP mannuronic acid becomes polymerized by a complex of glycosyl-transferase/polymerase (Alg8) and copolymerise Alg44 localised in the inner membrane. That results in the synthesis of nascent alginate chain (poly-M) which is next translocated through periplasm by multiprotein scaffold of AlgX, AlgG and AlgK. Complex of these proteins guides the nascent alginate chain through periplasm and protects it from the activity of alginate lyase, AlgL. Additionally, nascent alginate chain becomes modified by O-acetylation and epimerization during the transport through periplasm. Nascent alginate is O-acylated by the mutual activity of AlgI, AngJ, AlgF and most likely also Algx, whereas epimerization is conducted by AlgG. It is worth to note, that those modifications are not essential for alginate synthesis, but they modify alginate properties.

The O-acetylation increases the water holding capacity, whereas epimerization of M residues to G residues results in modification of gel properties, which include stiffness, swelling and porosity. In the last step, mature alginate is being secreted by a beta barrel porin, AlgE. It was proposed that proteins forming alginate biosynthesis machinery form a multiprotein complex as presented at Figure 6 (Hay et al., 2013).

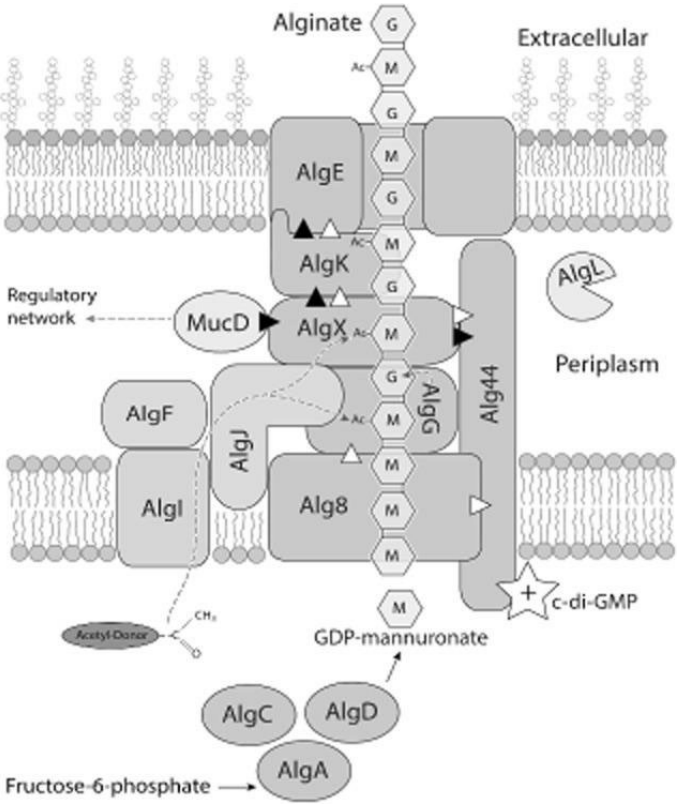

Figure 6 Schematic representation of the alginate biosynthesis machinery, spanned from the inner to the outer membrane of the *P. aeruginosa*. The O-acetylation conducted by AlgI, AlgJ AlgF and AlgX and the epimerization processed by AlgG are presented as dashed lines. PilZ domain of Alg44 is additionally presented, as well as MucD which was shown to interact with AlgX. Letters M and G refer to alginate residues (Hay et al., 2013).

All except one of the genes involved in alginate biosynthesis are localized in a 12-gene operon (*algD*, *alg8*, *alg44*, *algK*, *algE*, *algG*, *algX*, *algL*, *algI*, *algJ*, *algF,* and *algA*). This operon is regulated by an AlgT-dependent promoter placed upstream of *algD*. AlgT, a gene coding for an alternative sigma factor σE is located in another operon (*algT-mucA-mucB-mucC-mucD*), together with other genes involved in regulating AlgT activity (Hay et al., 2014; Malhotra et al., 2019). AlgT is engaged in response to envelope stress and, besides positive regulation of alginate synthesis, is predicted to control the expression of 290 open reading frames in *P. aeruginosa* (Martin et al., 1994; Wood & Ohman, 2015).

Transcriptional regulation of alginate synthesis is complex and involves numerous sigma factors, two-component systems, and DNA binding proteins (Hay et al., 2014). For example, the housekeeping sigma factor RpoD has to be sequestrated by AlgQ, an anti-sigma factor. Another way, RpoD blocks the interaction

between AlgT and RNA polymerase, which enables the transcription of alginate synthesis operon (Yin et al., 2013).

In nonmucoid *P. aeruginosa*, the protein AlgT is regulated by an anti-sigma factor called MucA, which keeps it inactive. However, in a process known as the RIP (regulated intramembrane proteolysis) cascade, several proteases come into play to degrade MucA and activate AlgT. These proteases include AlgW, MucP, ClpXP, and ATP-dependent cytosolic proteases, such as RipC. This cascade of proteolytic events ultimately allows AlgT to become active and carry out its cellular functions (Hay et al., 2009). Under uninduced conditions, AlgW cannot initiate the RIP cascade by the cleavage of MucA, which is protected by MucB bounded to it. Envelope stress alters trafficking, localization, and stability of outer membrane proteins and liposaccharides, which leads to activation of RIP cascade and release of AlgT into the cytoplasm (Hay et al., 2014; Qiu et al., 2008; Qiu et al., 2007).

AlgT competes with sigma factor RpoN, which also binds to the *algD* promoter and acts as a repressor of alginate synthesis under specific conditions, like nitrogen-rich conditions (Boucher et al., 2000). Interestingly, in a mucoid mutant (muc23/PAO579), alginate synthesis is driven by RpoN but not AlgT (Hay et al., 2014).

Other DNA binding proteins (AmrZ, AlgQ, AlgP, CysB, Vtr) regulate transcription of alginate synthesis operon. They increase the expression of the *algD* operon by latching onto the promotor region (Baynham et al., 2006; Delic-Attree et al., 1997; Hay et al., 2014; Yin et al., 2013). Transcription of the *algD* operon can also be enhanced by KinB-AlgB and FimS-AlgR two-component signal transduction systems. Those systems get activated by unknown environmental cues leading to the release of AlgB and AlgR, increasing the expression of genes located in the *algD* operon (Hay et al., 2014; Leech et al., 2008).

Alginate synthesis is also controlled post-transcriptionally by small RNAs (sRNA), which bind to regulatory protein RsmA. That represses the translation of various mRNA, affecting alginate synthesis. The expression of sRNA is controlled by the GacS-GacA two-component system, which influences, e.g., biofilm formation, quorum sensing, or virulence. A disruption of the GacS-GacA system causes a reduction of alginate synthesis in *Pseudomonas* spp. (Ghaz-Jahanian et al., 2013; Hay et al., 2014; Lalaouna et al., 2012; Moll et al., 2010).

On the posttranslational level, alginate polymerization is positively regulated by the second messenger c-di-GMP, which binds to a PilZ domain of Alg44. That protein consists of the already mentioned PilZ domain and transmembrane domain, leading to the periplasmatic domain. Alg44 participates in alginate polymerization and modifications (acetylation and epimerization) (Hay et al., 2014; Moradali et al., 2017;

Oglesby et al., 2008). Alg44 and Alg8 constitute an alginate polymerase activated by c-di-GMP by binding to a PilZ domain of Alg44 (Moradali et al., 2017).

It was also proposed that alginate synthesis can be indirectly regulated by substrate availability and competition by different pathways. The reaction catalysed by AlgC seems to be a limiting step in alginate synthesis. AlgC displays phosphomannomutase and phosphoglucomutase activities and converts 6-phosphate to mannose-1-phosphate and glucose-6-phosphate to glucose-1-phosphate. Next, mannose-1-phosphate is used as a substrate by AlgA, PslB, and WbpW in alginate, Psl, and B-band LPS synthesis, respectively. Competition between those pathways may indirectly influence alginate synthesis (Byrd et al., 2009; Hay et al., 2014; Ma et al., 2012; Shinabarger et al., 1991).

4.2.1.7 Mucoid phenotype of *P. aeruginosa*

The mucoid phenotype was first described by Sonnenschein in 1937 and was called a “capsulated” variant of *P. aeruginosa* (Cetin et al., 1965; Malhotra et al., 2019). Mucoid variants were reported in multiple *P. aeruginosa* infections across organ systems, like urinary tract infections, ocular diseases, non-CF bronchiectasis, and most importantly, cystic fibrosis lung infections (Malhotra et al., 2019). Mucoidy is recognized by a constitutive overproduction of alginate, which in most cases is primarily caused by a mutation in the *mucA* gene (mutant *mucA22* where gene deletion of guanine results in a frameshift and premature termination of translation). That results in a truncated and nonfunctional MucA, which no longer sequestrates the transcriptional factor AlgT (Malhotra et al., 2019; Urtuvia et al.,2017). Even though mutations in MucA are the most common, there are known cases of mutations in *mucB* and *mucD,* which cause destabilization of the MucA-AlgT complex (Figure 7) (Boucher et al., 1997; Malhotra et al., 2019). Due to mutations in *mucA*, *mucB,* and *mucD*, AlgT can freely bind to RNA polymerase and initiate transcription of alginate synthesis operon (Boucher et al., 1996; Boucher et al., 1997; Malhotra et al., 2019).

Interestingly, *mucA22* mutation is found in 70% of non-mucoid isolates from CF

lungs with chronic infection. It is caused by a reversion from mucoid to nonmucoid phenotype by second-site mutation, which mainly suppresses the functionality of AlgT. However, other second-site mutations in AlgO were described. There are also known cases of third- and forth-site mutations that restore mucoid phenotype and cause another reversion, respectively (Bragonzi et al., 2009; Ciofu et al., 2008; Damkiaer et al., 2013; DeVries & Ohman, 1994; Malhotra et al., 2019; Sautter et al., 2012).

Mucoid *P. aeruginosa* demonstrates higher tolerance against antimicrobials, advantages in evading the immune system response, and downregulation of flagella expression, which helps to avoid immune detection (Garrett et al., 1999; Limoli et al., 2014; Malhotra et al., 2019; Pier et al., 2001; Young et al., 2011). Numerous reports indicate the coexistence of mucoid and nonmucoid variants in CF lungs. It suggests that diversity in the population of *P. aeruginosa* may lead to selective advantages in colonizing lungs (Bjarnsholt et al., 2009; Ciofu et al., 2008; Clark et al., 2015; Damkiaer et al., 2013; Malhotra et al., 2019; Malhotra et al., 2018; Tai et al., 2017).

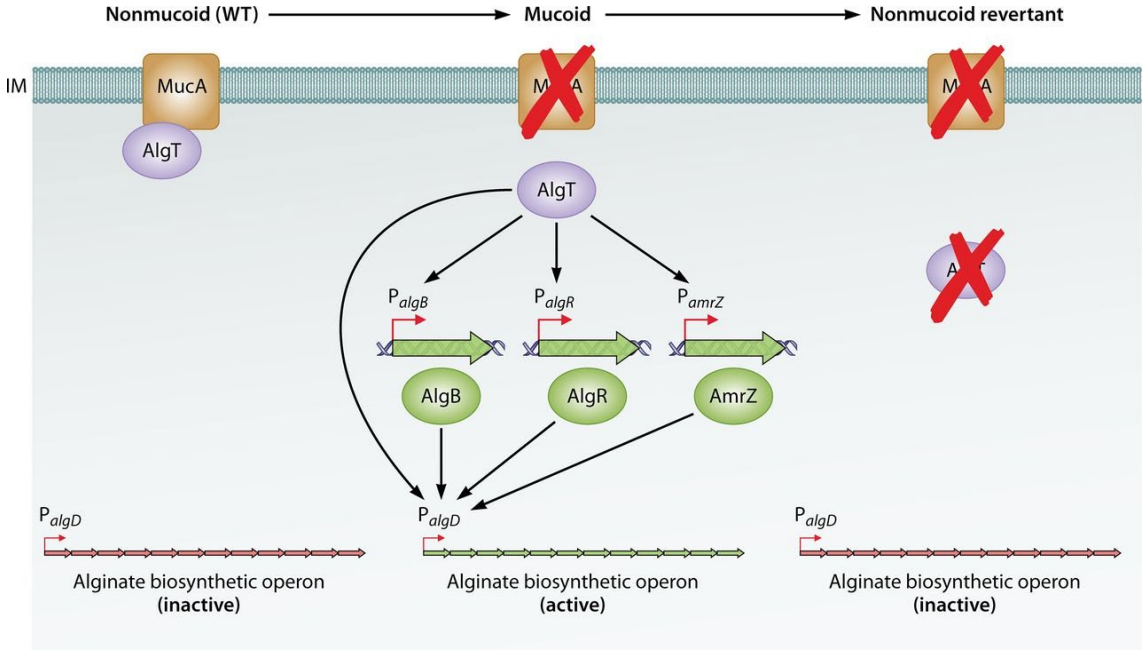

Figure 7 In *P. aeruginosa*, the genes needed to make alginate are usually inactive. AlgT, a protein that starts alginate production, is blocked by another protein, MucA, at the inner membrane. When a mutation damages MucA, AlgT is freed and triggers alginate production by: i) directly activating the alginate gene cluster, and ii) turning on other key genes that are crucial for alginate production. However, *P. aeruginosa* can switch back to a non-alginate-producing state if a new mutation affects AlgT, shutting down alginate production again (Malhotra et al., 2019).

4.3 The second messenger c-di-GMP

C-di-GMP is a second messenger in bacteria. It was discovered in 1987 as an activator of cellulose synthesis in *Gluconacetobacter xylinus* (Jenal et al., 2017; Petchiappan et al., 2020; Ross et al., 1987). C-di-GMP is involved in the regulation of cell cycle, cell morphology, exopolysaccharide production, antimicrobial tolerance, quorum sensing, chemotaxis, virulence, and transition between planktonic and surface-attached lifestyles. In general, high concentrations of c-di-GMP lead to sessile lifestyle,

whereas bacteria with low c-di-GMP concertation stay in a planktonic mode of growth (Ha & O'Toole, 2015; Hecht & Newton, 1995; Hengge, 2016; Lori et al., 2015; Matsuyama et al., 2016; Petchiappan et al., 2020).

Concentrations of c-di-GMP are balanced in the cell by diguanylate cyclases (DGCs) and phosphodiesterases (PDEs). DGSs are responsible for synthesizing c-di-GMP from two molecules of GTP by the GGDEF domain. Hydrolysis of c-di-GMP can be proceeded by two types PDEs: EAL and HD-GYP domain-containing. Hydrolysis products are respectively linear di-GMP (5'-pGpG) or two molecules of GMP. Often proteins are bifunctional and contain both DGC and PDE domains. A broad group of enzymes has GGDEF, EAL, HD-GYP, and other regulatory domains to modulate their activity precisely (Chen et al., 2018; Hengge, 2009; Jenal et al., 2017; Petchiappan et al., 2020).

In *P. aeruginosa,* there are predicted 18 DGCs, 8 PDEs, and 16 DGC/PDE fusion proteins (Petchiappan et al., 2020; Valentini & Filloux, 2016). To precisely control concentrations of c-di-GMP, the activity of all the proteins involved in its synthesis and hydrolysis is modulated by various mechanisms like expression control, allosteric regulation, feedback inhibition, protein-protein interactions, or post-translational modifications (Chen et al., 2018; Paul et al., 2007; Petchiappan et al., 2020; Trimble & McCarter, 2011; Zahringer et al., 2013).

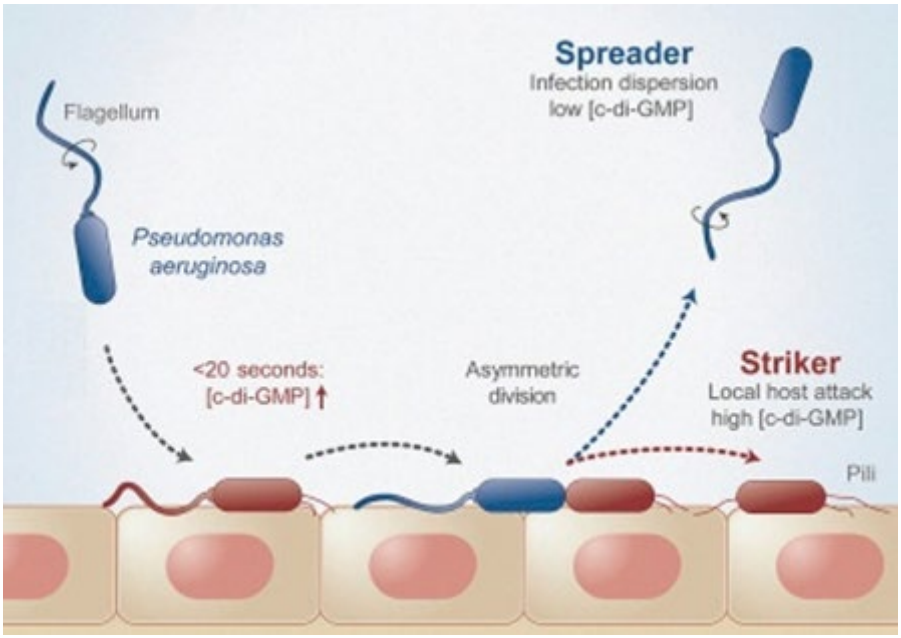

Figure 8 Asymmetric division of *P. aeruginosa*. Once the bacterium encounters the surface, c-di-GMP levels rapidly increase. The bacterium divides asymmetrically to a pillated, sessile progeny (striker) and a motile cell that colonizes other sites (spreader) (Laventie et al., 2019).

Specific DGCs and PDEs were associated with a particular phenotype caused by, e.g., environmental cues. However, not all described proteins have an impact on total c-di-GMP concentrations in bacterial cells. It is proposed that concentrations of c-di-GMP are spatially and temporally sequestrated (Hengge, 2009; Petchiappan et al., 2020). That means that DGCs and PDEs can be spatially sequestrated in a cell and localized at a specific site or in distinct multi-protein complexes, creating local pools of c-di-GMP. Many proteins involved in c-di-GMP metabolism are regulated depending on environmental conditions, e.g., nutrient availability, and are only expressed or active at specific timepoints. Additionally, it has been shown that c-di-GMP effectors have a different affinity to it. That all makes c-di-GMP signalling tightly regulated and allows bacteria to adapt and react precisely to environmental cues, conduct development of cells, and ensure effective communication within a population of cells (Dahlstrom et al., 2018; Dahlstrom & O'Toole, 2017; Hengge, 2009; Petchiappan et al., 2020; Rodesney et al., 2017; Sarenko et al., 2017).

There are multiple reports about the heterogeneous distribution of c-di-GMP in cells, biofilms, and planktonic cultures. Localization of specific enzymes at the cell poles and their cooperation leads to an asymmetric distribution of c-di-GMP. This can result in an asymmetric cell division and differentiation of daughter cells into the spreader, with low c-di-GMP levels and planktonic lifestyle, and striker, with high c-di-GMP concentrations and sessile lifestyle (Figure 8) (Laventie et al., 2019). Also, global c-di-GMP levels increase highly during cell settlement to a surface, converting from planktonic to a surface-associated lifestyle (Nair et al., 2017; Petchiappan et al., 2020). Interestingly, c-di-GMP levels differ in different regions of a biofilm – lower sections of biofilm, with access to higher concentrations of nutrients and lower oxygen tensions, display high c-di-GMP levels (Klauck et al., 2018). Moreover, a heterogeneous distribution of c-di-GMP was observed among cells of isogenic populations of bacteria. That is considered to increase the persistence of a population to different stressors, like exposure to antimicrobials (Petchiappan et al., 2020; Valentini & Filloux, 2016).

4.3.1 The diguanylate cyclase SadC of *P. aeruginosa*

Diguanylate cyclase SadC (surface adhesion defective; PA4332) is an inner membrane-bound protein that contains GGEEF and several transmembrane domain (TM domain). TM domain is crucial for the spatial control of c-di-GMP pools synthesized by SadC (Merritt et al., 2007;; Zhu et al., 2016). SadC was found to be involved in regulating many processes in *P. aeruginosa* and is often described as a central

regulator of the surface mode growth. It stimulates biofilm formation and inhibits swimming, swarming, and twitching motilities and is linked to the patho-adaptative transition by switching from motile to sessile lifestyle (McCarthy et al., 2017; Zhu et al., 2016). So far, SadC was observed to promote Psl synthesis, enhance pyoverdine biosynthesis, take part in stress response caused by tellurite and ethanol, and take part in the regulation of liposaccharide modifications (Chen et al., 2015; Chua et al., 2015; Lewis et al., 2019; McCarthy et al., 2017; Zhu et al., 2016).

In past years, SadC was observed to interact with multiple proteins in multiple processes in a cell. It was found that SadC acts upstream of SadB and downstream of RsmA, as part of the Gac/Rsm pathway, in a biofilm formation (Moscoso et al., 2014). SadC was shown to interact with NbdA, a membrane phosphodiesterase involved in degrading c-di-GMP. Interestingly, NbdA contains an MHYT domain, which can potentially sense diatomic gases such as NO, CO, and O_2 (Scherhag et al., 2023). SadC interacts with WarA and plays a central role in transitioning from acute to chronic infection phenotypes (McCarthy et al., 2017). In planktonic cultures, SadC interacts with PilO (part of type 4 pili), and that protein inhibits SadC activity, but during adhesion to a surface, interaction is reduced and replaced by one with MotC (a stator of a flagellar motor), which stimulates SadC activity and results in the initiation of biofilm formation (Baker et al., 2019; Webster et al., 2021). The interaction between SadC and PilY1 was observed to influence swarming motility by synthesizing local c-di-GMP pools (Kuchma et al., 2010; Kuchma et al., 2012). Recent findings highlight regulatory role of SadC in nitrogen-fixing biofilm formation in *Pseudomonas stutzeri* and its broader biofilm regulation mechanisms, with RsmA binding to its mRNA for posttranscriptional control (Shang et al., 2021).

It has been shown that alginate synthesis in *P. aeruginosa* is triggered by the availability of oxygen and that non-mucoid strain PAO1 synthesizes alginate under anoxic conditions *in vitro* and *in vivo* in the lungs of mice with chronic infection (Bragonzi et al., 2005; Worlitzsch et al., 2002). It has been shown that c-di-GMP is necessary for alginate synthesis (Bragonzi et al., 2005). The transposon mutagenesis screen revealed that SadC is essential for alginate synthesis under anoxic conditions (Bastian, 2008; Bragonzi et al., 2005; Merighi et al., 2007; Schmidt, 2015). Under anoxic conditions, SadC regulates alginate synthesis also in a planktonic culture, which shows that stimulus activating SadC-dependent response is independent of adhesion to the surface (Schmidt et al., 2016). Similar observations were made when *P. aeruginosa* was grown in the presence of ethanol and tellurite as stress factors. In those experiments, planktonic cultures of *P. aeruginosa* synthetised alginate when treated with an ethanol or tellurite salts (Chua et al., 2015; Lewis et al., 2019).

It is considered that alginate synthesis under anaerobic conditions is regulated at the posttranslational level. Up-regulation of alginate synthesis under anaerobic conditions is not caused by an increased expression of alginate synthesis genes nor expression levels of *sadC* (Schmidt, 2015). Additionally, SadC does not seem to contain any oxygen-sensing domains (Schmidt et al., 2016). A mutant PAO1 Δ*sadC* showed deficient alginate synthesis under anaerobic conditions. The disruption of the GGEEF domain in a mutant PAO1 $SadC_{GAAEF}$ disables alginate synthesis in the absence of oxygen (Schmidt, 2015; Schmidt et al., 2016). MBP-$SadC_{cyt}$ fusion protein expressed and purified from *E. coli* under anaerobic conditions is also significantly more active than one purified from cultures grown in the presence of oxygen. That could be caused by an impact of the enzymatic machinery of *E. coli* on MBP-$SadC_{cyt}$ in an oxygen-dependent manner (Schmidt et al., 2016).

It was proposed that a receptor of c-di-GMP, synthesized by SadC to increase alginate production, is Alg44, which harbours a c-di-GMP-binding domain PilIZ (Schmidt et al., 2016). Interestingly, another protein, MucR (PA1727), with DGC and PDE activity was reported to interact with Alg44. MucR was proposed to synthesize c-di-GMP during growth in a biofilm and degrade it in a planktonic mode of growth (Li et al., 2013; Schmidt, 2015). MucR contains MHYT domain, with putative carbon monoxide, nitric oxide, and oxygen sensing activity and was reported to suppress alginate synthesis in the presence of nitrate (Hay, Remminghorst, et al., 2009; Schmidt et al., 2016; Wang et al., 2015). It is possible that different signals trigger the DGC activity of SadC and MucR and that both proteins signal through Alg44 (Schmidt et al., 2016) or that SadC does not activate Alg44 directly.

4.3.1.1 PA4330 is required for alginate synthesis, whereas PA4331 inhibits alginate synthesis in the presence of O_2

A genetic neighbourhood of SadC was investigated, because SadC does not contain any domains which could be responsible for oxygen sensing. SadC is located in an operon with two other genes: *odaA* (oxygen-dependent activator of alginate production, PA4330) and *odaI* (oxygen-dependent inhibitor of alginate production, PA4331). Localization of these genes in one operon suggests a functional association of these proteins. Moreover, the DNA sequence of the PA4330-4332 operon is highly conserved and shares very high similarities between clinical isolates from patients worldwide, and from sequestial isolates from same patients collected over the years of chronic infection. This suggests its importance for the survival or pathogenesis of *P. aeruginosa* (Schmidt, 2015).

OdaI is predicted to serve as a cytoplasmic ferredoxin reductase, housing essential domains such as FAD, NAD, and a [Fe-S] binding domain, characterized by four cysteine residue motifs (Cys4). Notably, the [Fe-S] binding domains can not only function as an oxygen sensor but could also operate as a crucial electron transfer unit within the system. (Schmidt, 2015; Unden et al., 2013).

Mutants PAO1 Δ*odaI* and PAO1 $OdaI_{C72A\ C74A}$ (mutations that disrupted the [Fe-S] binding domain) synthesize alginate in aerobic and anaerobic conditions. In an *in vitro* assay with purified SadC and OdaI, it was observed that OdaI inhibits the DGC activity of SadC in the presence of oxygen. Accordingly, it has been proposed that PA4331 plays a role in detecting oxygen levels, either through a modification of SadC or through structural interactions between SadC and OdaI (Bastian, 2008; Schmidt, 2015; Schmidt et al., 2016).

OdaA, the third gene in the operon consisting of SadC and OdaI, OdaA, was reported to be essential for alginate synthesis in the lack of oxygen. A mutant PAO1 Δ*odaA* was not able to synthesize alginate and shows a similar phenotype to PAO1Δ*sadC* (Schmidt, 2015; Schmidt et al., 2016). Recently, the crystal structure of OdaA was solved, indicating that OdaA creates a homotrimer, and it was shown that OdaA binds acyl-CoA esters. It was proposed that OdaA functions as mono-functional enoyl-CoA isomerase. A *cis-trans* isomerization of unsaturated fatty acids is a crucial mechanism responding to environmental stress, cellular signaling, and pathogenesis. It was hypothesized that OdaA could be involved in quorum sensing by synthesizing diffusible signal factors (DSFs). DSFs are *cis* saturated fatty acids that take part in biofilm formation, antibiotic resistance, and the synthesis of virulence factors (Zhao et al., 2021).

4.4 Oxygen sensing in bacteria

Molecular oxygen is a terminal electron acceptor in the anaerobic respiratory chain and is essential for most organisms to survive and produce cellular energy. During aerobic respiration, oxygen becomes reduced to H_2O, and that reaction provides energy for a cell in the form of ATP. Too high oxygen concertation lead to oxidative stress and the presence of reactive oxygen species (ROS), which destroy cellular machinery. On the other hand, low oxygen tensions or lack of oxygen causes inefficient aerobic respiration and triggers adaptation to the environment by switching energy metabolism to anaerobic respiration. As a result of changing oxygen tensions, organisms evolved complex molecular systems for oxygen sensing. Especially some bacteria can quickly adapt to different oxygen concertation in an environment. Facultative anaerobes can

easily change the electron acceptor from oxygen to molecules like nitrate, pyruvate, or asparagine (Taabazuing et al., 2014).

Changes in an energy metabolism require a change in cellular machinery to adapt cell metabolism to specialized pathways like nitrogen fixation, hydrogen production, or sulphate reduction. Enzymes engaged in those pathways are often metalloproteins and are highly sensitive to molecular oxygen. For oxygen sensing, bacteria usually utilize proteins containing Fe-S clusters or hemes to regulate gene expression by altered binding to DNA affinity. At the same time, in higher organisms, oxygen sensing also leads to altered protein/protein binding affinities (Taabazuing et al., 2014).

Bacteria extensively utilize heme-based sensors, enabling the reversible binding of molecular oxygen. This process leads to structural changes and affects the binding of sensor to DNA or other proteins. There are known well-studied heme-based sensors like FixL, *Ec*Dos, *Ax*PDEA1, or HemAT (Chang et al., 2001; Delgado-Nixon et al., 2000; Gilles-Gonzalez & Gonzalez, 1993; Hou et al., 2000; Taabazuing et al., 2014). On the other hand, oxygen binding to Fe-S clusters causes degradation of the cluster, and the regulation takes place by sensor protein synthesis, cluster degradation, and cluster formation. Changes in the cluster composition cause alteration of binding affinity to DNA and proteins. Some well-studied examples of proteins containing Fe-S cluster are FNR, NreB, ArnR, and WhiB (Bhat et al., 2012; Kiley & Beinert, 1998; Mullner et al., 2008; Nishimura et al., 2008; Taabazuing et al., 2014).

So far, bacterial oxygen sensing has been recognized to function in two modes: direct transcriptional control and two-component signalling cascade. An oxygen sensor FNR from *E. coli* is a well-studied example of direct transcriptional control. In that case, a sensor serves both as an oxygen sensor and a transcriptional factor. Binding O_2 to a homomeric FNR, with $[Fe_4\text{-}S_4]^{2+}$ form of the cluster, results in its degradation to a monomer $[Fe_2\text{-}S_2]^{2+}$ and diminished DNA binding affinity. Dimeric FNR promotes, as a transcriptional factor, the expression of genes involved in anaerobic metabolism and represses ones involved in aerobic metabolism (Kiley & Beinert, 1998; Sutton et al., 2004; Taabazuing et al., 2014).

Two components of signalling cascades were primarily found in prokaryotes, with some examples in eukaryotes. Those systems consist of a sensory protein, in that case, an oxygen sensor, and a response regulator protein. Sensing proteins contain at least a sensing domain and histidine kinase (HK) domain. Binding oxygen to a sensory domain causes ATP-dependent autophosphorylation on the HK domain and following transfer of a phosphoryl group to the response-regulator protein. As a result, depending on a specific two-component signalling cascade, the expression

of target genes can be stimulated or repressed. One of the representatives of such a system is FixL/FixJ two-component signalling cascade from *Sinorhizobium meliloti*. Oxygen is sensed through a PAS (PerARNT-Sim) domain on FixL protein, which contains heme. Due to autophosphorylation of FixL and phosphoryl transfer to FixJ, FixL dimerizes and stimulates expression of specific genes of *fixK* promoter (Galinier et al., 1994; Gao & Stock, 2009; Gouet et al., 1999; Monson et al., 1992; Taabazuing et al., 2014).

Prolyl hydroxylation is another known way of oxygen-sensing. Since recently, it was considered that only eukaryotes could use that post-translational modification, and prokaryotes were known to consume free L-proline as a substrate (Gorres & Raines, 2010; Schnicker et al., 2017). A homolog of human prolyl hydroxylase was identified in *P. aeruginosa* and *Pseudomonas putida* and named *Pseudomonas* prolyl hydroxylase (PPHD) (Schaible et al., 2020; Scotti et al., 2014). It was found that PPHD in *P. aeruginosa* influences virulence and antibiotic resistance in link to environmental oxygen tensions (Dickinson et al., 2017; Schaible et al., 2020; Schaible et al., 2017; Scotti et al., 2014). Prolyl hydroxylase was also described in *Bacillus anthracis* (Schaible et al., 2020; Schnicker et al., 2017). In those bacteria, mentioned hydroxylases were found to modify elongation factor Tu (TufB), which demonstrates that also bacteria can use proline hydroxylation in post-translational regulation of gene expression (Schnicker et al., 2017; Scotti et al., 2014). In general, prolyl hydroxylases (PHD) catalase a prolyl-4-hydroxylation and require Fe (II), α-ketoglutarate (αKG), and molecular oxygen for activity. In the reaction, the substrate is oxidized, αKG becomes decarboxylated, and succinate and carbon dioxide are synthesized as side products. Consequently, one atom from molecular oxygen is incorporated into the substrate, creating 4-hydroxyproline (Schnicker et al., 2017; Scotti et al., 2014). So far, another alternative enzymatic activity of PHDs has not been described, although steric hindrance is proposed as one of the possible mechanisms of target regulation, besides performing prolyl hydroxylation (Wong et al., 2013; Xie et al., 2009).

5. Aim

Alginate is an important virulence factor of *P. aeruginosa,* and the lack of oxygen triggers its synthesis. It can be a strategy of *P. aeruginosa* to survive in the early stages of infection before conversion to mucoid strains (Bragonzi et al., 2005; Worlitzsch et al., 2002). It has been shown that the protein SadC is the main regulator of alginate synthesis under anaerobic conditions. Together with OdaA and OdaI, which are expressed from the same operon, it is necessary to control alginate synthesis under anaerobic conditions. OdaA was shown to be critical for alginate synthesis under aerobic synthesis, whereas OdaI inhibits alginate production in the presence of alginate. The current stage of knowledge explains that regulation in a limited way (Bastian, 2008; Schmidt, 2015; Schmidt et al., 2016). Therefore, an oxygen-dependent regulation of alginate synthesis by SadC was further investigated in this work. The specific aims of the project are:

1. To study interactions between SadC, cytosolic part of SadC ($SadC_{cyt}$), OdaA, and OdaI under aerobic and anaerobic conditions.
2. To investigate the role of cysteine residues (C390, C420, C421, C478) of $SadC_{cyt}$ on its functionality.
3. To conduct mRNA sequencing to analyze the transcriptional effects of SadC deletion under varying oxygen levels in *P. aeruginosa*.

6. Materials

6.1 Media

LB medium

25.00 g	Difco™ LB Broth, Miller	(BD, USA)

ddH_2O was added to a volume of 1 l, and a medium was autoclaved

LB agar

40.00 g	Difco™ LB AGAR, Miller	(BD, USA)

ddH_2O was added to a volume of 1 l, and a medium was autoclaved

McConkey agar

51.50 g	MacCONKEYAgar No. 2	(Oxoid Limited, UK)

ddH_2O was added to a volume of 1 l, and a medium was autoclaved

Freezing medium

25.00 g	Difco™ LB Broth, Miller	(BD, USA)
100.00 g	Glycerol	(Merck Millipore, USA)

ddH_2O was added to a volume of 1 l, and a medium was autoclaved

SOC medium

20.00 g	Tryptone	(ThermoFisher Scientific, USA)
5.00 g	Yeast Extract	(Merck Millipore, USA)
0.50 g	NaCl	(Merck Millipore, USA)
2.50 ml	1 M KCl	(Merck Millipore, USA)

ddH_2O was added to a volume of 970 ml and autoclaved. Following solutions were added:

10.00 ml	sterile 1 M $MgCl_2$	(Merck Millipore, USA)
20.00 ml	sterile 1 M glucose	(Merck Millipore, USA)

6.2 Buffers and solutions

SDS-PAGE loading buffer

2x Laemmli Sample Buffer (Bio-Rad, USA)

DNA loading buffer

BlueJuice Gel Loading Buffer (ThermoFisher Scientific, USA)

5x TBE buffer

54.00 g	Tris base	(Merck Millipore, USA)
27.5 g	Boric acid	(Merck Millipore, USA)
20 ml	0.5 M EDTA (pH 8.0)	(AppliChem GmbH, Germany)

ddH_2O was added to a final volume of 1 l

1M $CaCl_2$

111.00 g	$CaCl_2$	(Merck Millipore, USA)

ddH_2O was added to a final volume of 1 l, and a solution was autoclaved

50% glycerol

500.00 g	glycerol	(Merck Millipore, USA)

ddH_2O was added to a final volume of 1 l, and a solution was autoclaved

0.1M $CaCl_2$ + 15% glycerol

100.00 ml	sterile 1 M $CaCl_2$	this study
300.00 ml	sterile 50% glycerol	this study

Sterile ddH_2O was added to a final volume of 1 l

Amylose column buffer

11.6 g	NaCl	(Merck Millipore, USA)
2.4 g	Tris-HCl	(Carl Roth, Germany)
1.8 g	EDTA	(AppliChem GmbH, Germany)
0.7 ml	2-mercaptoethanol	(AppliChem GmbH, Germany)

ddH_2O was added to a final volume of 1 l, and the pH was adjusted to 7.4

Amylose elution buffer

11.6 g	NaCl	(Merck Millipore, USA)
3.4 g	maltose	(Merck Millipore, USA)

2.4 g	Tris-HCl	(Carl Roth, Germany)
1.8 g	EDTA	(AppliChem GmbH, Germany)
0.7 ml	2-mercaptoethanol	(AppliChem GmbH, Germany)

ddH_2O was added to a final volume of 1 l, and the pH was adjusted to 7.4

50 mM Tris-HCl buffer

6.00 g	Tris-HCl	(Carl Roth, Germany)

ddH_2O was added to a final volume of 1 l, and the pH was adjusted to 8.0

20mM phosphate buffer pH 7.4

2.42 g	K_2HPO_4	(Merck Millipore, USA)
0.83	KH_2PO_4	(Merck Millipore, USA)

ddH_2O was added to a final volume of 1 l

2x GTP binding reaction buffer

1.26 g	$MnCl_2$	(Merck Millipore, USA)
5.80 g	NaCl	(Merck Millipore, USA)
15.76 g	Tris-HCl	(Carl Roth, Germany)

ddH_2O was added to a final volume of 1 l, and the pH was adjusted to 8.0

10x SDS PAGE running buffer

30.30 g	Tris base	(Carl Roth, Germany)
144.00 g	Glycine	(Carl Roth, Germany)
10.00 g	SDS	(Carl Roth, Germany)

ddH_2O was added to a final volume of 1 l

Transfer buffer

3.02 g	Tris base	(Carl Roth, Germany)
14.40 g	Glycine	(Carl Roth, Germany)
200.00 ml	methanol	(AppliChem GmbH, Germany)

ddH_2O was added to a final volume of 1 l

10x TBST buffer

12.11 g	Tris base	(Carl Roth, Germany)
87.66 g	NaCl	(Merck Millipore, USA)
5.00 ml	Tween-20	(SERVA Electrophoresis, Germany)

ddH_2O was added to a final volume of 1 l and the pH adjusted to 7.6

5% skim milk in 1x TBST buffer

5.00 g	skim milk	(TSI Consumer Goods, Germany)
95.00 ml	1x TBST	this study

PMSF 1 mM

1,7 mg	PMSF	(AppliChem GmbH, Germany)
10.00 ml	isopropanol	(AppliChem GmbH, Germany)

a solution was aliquoted and stored at -20°C

Lysozyme 10 mg/ml

100.00 mg	lysozyme	(Merck Millipore, USA)

ddH_2O was added to a final volume of 10 ml, and a solution was aliquoted and stored at -20 °C

1M Tris-HCl pH 7.5

157.6 g	Tris-HCl	(Carl Roth, Germany)

ddH_2O was added to a final volume of 1 l, and the pH was adjusted to 7.5

1M KCl

74.55 g	KCl	(Merck Millipore, USA)

ddH_2O was added to a final volume of 1 l

1M $MgCl_2$

95.21 g	$MgCl_2$	(Merck Millipore, USA)

ddH_2O was added to a volume of 1 l, and a solution was autoclaved

1M glucose

180.16 g	glucose	(Merck Millipore, USA)

ddH_2O was added to a final volume of 1 l, and a solution was autoclaved

6.3 Water

Nuclease free water

Nuclease-Free Water, for Molecular Biology (Sigma Aldrich, Germany)

ddH_2O

Ampuwa®, Sterile Water for Irrigation (Fresenius Kabi Deutschland GmbH, Germany)

6.4 Enzymes

Table 1 Enzymes and their concentration used in this work.

Enzyme	Stock solution concentration	Final concentration	Manufacturer
CIP	5 U/µl	0.15 U/µl	NEB, USA
*Hind*III	20 U/µl	0.6 U/µl	NEB, USA
MangoMix™	10 X	1 X	Bioline USA
Pfu Turbo DNA Polymerase	2.5 U/µl	0.05 U/µl	Agilent Technologies, USA
Phusion DNA Polymerase	2 U/µl	0.04 U/µl	ThermoFisher Scientific, USA
ReproFast DNA Polymerase	5 U/µl	0.1 U/µl	Genaxxon Bioscience, Germany
T4 DNA ligase	400 U/µl	20 U/µl	NEB, USA
*Xba*I	20 U/µl	0.6 U/µl	NEB, USA
5x In-Fusion Master Mix	5 X	1 X	Takara Bio, USA

6.5 Other reagents

Table 2 Other reagents and their concentrations used in this work.

Reagent	Manufacturer
amylose resin	NEB, Germany
DMSO	Carl Roth, Germany
dNTPs 2 mM	ThermoFisher Scientific, USA
GeneRuler 1kb	ThermoFisher Scientific, USA
GTP	ThermoFisher Scientific, USA
IPTG	ThermoFisher Scientific, USA
maltose	Merck Millipore, USA
MANT-GTP	Invitrogen, USA
Precision Plus Protein™ Dual Color Standards	Bio-Rad, USA
SYBR Safe	Invitrogen, USA
DNA/RNA Shield™	Zymo Research, USA

6.6 Antibiotics

Table 3 Antibiotics and their concentrations used in this work.

Antibiotic	Stock solution concentration	Final concentration	Manufacturer
ampicillin	100 mg/ml in ddH_2O	100 µg/ml	SERVA Electrophoresis GmbH, Germany
kanamycin	50 mg/ml in ddH_2O	50 µg/ml	Carl Roth, Germany
gentamicin	10 mg/ml in ddH_2O	15 µg/ml (for *E.coli*) 75 µg/ml (for *P. aeruginosa*)	Merck Millipore, USA

6.7 Antibodies

Table 4 Antibodies used in this work.

Antibody	Dilution	Manufacturer
MBP-SadC$_{cyt}$	1:500 000	Massimo Merighi, Harvard University, USA
Goat-anti-rabbit HRP conjugate	1: 10 000	Dako, Germany

6.8 Kits

Table 5 Kits used in this work.

Kit	Manufacturer
DNA Clean & Concentrator-5	Zymo Research, Germany
Pierce™ BCA Protein Assay Kit	ThermoFisher Scientific, USA
Quick-gDNA™MiniPrep	Zymo Research, Germany
SilverQuest™ Silver Staining Kit	Invitrogen, USA
Zyppy™PlasmidMiniprep	Zymo Research, Germany

6.9 Bacterial strains

Table 6 Bacterial strains used in this work.

Strains	Genotype/characteristics	Source or reference
E. coli		
BL21	*fhuA2 [lon] ompT gal (λ DE3) [dcm] ΔhsdS λ DE3 = λ sBamHIo ΔEcoRI-B int::(lacI::PlacUV5::T7 gene1) i21 Δnin5*	Bioline, USA
BTH101	*F - cya-99 araD139, galE15 galK16 rpsL1 (Str r) hsdR2 mcrA1 mcrB1*	Euromedex, France
DH5α	*F- Φ80lacZΔM15 Δ(lacZYA-argF) U169 recA1 endA1 hsdR17(rk-, mk+) phoA supE44 thi-1 gyrA96 relA1 λ-*	Invitrogen, USA
DHM1	*F - cya-854 recA1 endA1 gyrA96 (Nal r) thi1 hsdR17 spoT1 rfbD1 glnV44(AS)*	Euromedex, France
SM10(λpir)	*thi thr leu tonA lacY supE recA::RP4-2-Tc::Mu Km λpir*; kanamycin resistant	Simon R. et al.,1983
P. aeruginosa		
PAO1	reference strain, wild type, wound isolate	ATCC15692
PAO1 Δ*sadC*	markerless deletion mutant of *sadC* (PA4332)	This work

6.10 Plasmids

6.10.1 pKNT25

This bacterial two hybrid system vector is a derivative of the low copy-number plasmid pSU40 and contains a kanamycin resistance cassette and allows expression of desired genes under control of the *lac* promoter. pKNT25 encodes the first 224 amino acids of the adenylate cyclase CyaA from *Bordetella pertussis* (T25 fragment). A multiple cloning site (MCS) is located upstream of the T25 sequence enabling fusions of genes to the N-terminus of the T25 fragment (Euromedex).

6.10.2 pUT18

The bacterial two hybrid system vector pUT18 is derived from the high copy-number plasmid pUC19 and harbors an ampicillin resistance cassette. pUT18 carries the T18 fragment encoding amino acids 225-399 of the CyaA from *B. pertussis* with an upstream MCS and *lac* promoter. The plasmid allows expression of genes fused to the N-terminus of the T18 fragment (Euromedex).

6.10.3 pMCSG19

The expression vector pMCSG19 allows protein expression under control of the *T7* promoter fused at the N-terminus to the maltose binding protein (MBP) and a 6xHis tag. Additionally, the presence of a TEV and TVMV protein cleavage sites allows separation of the protein of interest from the MBP (Donnelly et al., 2006).

6.10.4 pEXG2

The pEXG2 plasmid is a suicide vector used for the construction of chromosomal mutations *via* allelic exchange. It is mobilizable and carries the *sacB* gene encoding levansucrase as a counter selectable marker which converts sucrose to levans that are harmful to Gram negative bacteria (*Rietsch et al. PNAS 2005*).

Table 7 Plasmids used in this work.

Plasmid	Source	Antibiotic
BACTH System experiment		
pKNT25	Euromedex	kanamycin
pUT18	Euromedex	ampicillin
pKT25-zip	Euromedex	kanamycin
pUT18C-zip	Euromedex	ampicillin
pKNT25::PA4330	this work	kanamycin
pKNT25::PA4331	this work	kanamycin
pKNT25::PA4332	this work	kanamycin
pKNT25::PA4332$_{883\text{-}1464}$	this work	kanamycin
pUT18::PA4330	this work	ampicillin
pUT18::PA4331	this work	ampicillin
pUT18::PA4332	this work	ampicillin
pUT18::PA4332$_{883\text{-}1464}$	this work	ampicillin
Cysteine mutants of SadC$_{cyt}$		
pMCSG19	DNASU Plasmid Repository, (Donnelly et al., 2006)	ampicillin
pMCSG19::MBP-His-PA4332$_{883\text{-}1464}$	(Schmidt et al., 2016)	ampicillin
pMCSG19::MBP-His-PA4332$_{883\text{-}1464\ C390A}$	this work	ampicillin
pMCSG19::MBP-His-PA4332$_{883\text{-}1464\ C420A\ C421A}$	this work	ampicillin
pMCSG19::MBP-His-PA4332$_{883\text{-}1464\ C478A}$	this work	ampicillin
Chromosomal deletion of *sadC*		
pEXG2	Rietsch et al. 2005	gentamicin
pEXG2::ΔPA4332	This work	gentamicin

6.11 Primers

All the primers were delivered by Integrated DNA Technologies, Inc., USA.

Table 8 Primers used in this work.

Name	Sequence (5'- 3')
BACTH System experiment	
pUT18_pKNT25_F	cggataacaatttcacacagg
pKNT25_R	cggcgtttgcgtaaccag
pUT18_R	gtcgatgcgttcgcgatc
PA4330_nostart_BACTH_HindIII#1	cgttgcataagcttgagcgagctgattcgggtcg
PA4330_nostop_BACTH_XbaI#2	cgttgcattctagagtggcgaacctggagaaatccg
PA4331_nostart_BACTH_HindIII#1	cgttgcataagcttgcctgacatacgggtcggc
PA4331_nostop_BACTH_XbaI#2	cgttgcattctagagtggcgtggggcaggaacagg
PA4332_nostart_BACTH_HindIII#1	cgttgcataagcttgaactgcagggcatcggc
PA4332_nostop_BACTH_XbaI#2	cgttgcattctagagtggcactggtgacctcccagg
PA4332_cytosolic_nostart_BACTH_HindIII#1	cgttgcataagcttgcggcaacgcatgcgccag
Cysteine mutants of $SadC_{cyt}$	
PA4332_C390A_for	gcggtggcgcgttccgccctgcgcgatggcgac
PA4332_C390A_rev	gtcgccatcgcgcagggcggaacgcgccaccgc
PA4332_C420A_C421A_for	gaacagctggaaagcgccgcggagcgcctgcgcctg
PA4332_ C420A_C421A _rev	caggcgcaggcgctccgcggcgctttccagctgttc
PA4332_C478A_for	ggcggacgaaaccgcgccgacgccacctgggag
PA4332_C478A_rev	ctcccaggtggcgtcggcgcggtttcgtccgcc
Chromosomal sadC deletion mutant	
PA4332 ko IF HindIII pEXG2 F	aatgtaaagcaagctgcgacatcgacttcgaccttg
PA4332 ko IF overlap R	ttcagcatgcttgcggctcgagttgggctccgtcccgtaatgg
PA4332 ko IF overlap F	aactcgagccgcaagcatgctgaaagtgcctgacatacgggtcgg
PA4332 ko IF HindIII pEXG2 R	cgacctgcagaagcttcgctcgccaggtagtggtc
PA4332 inside R	ccagcacgtagaacaccatg
PA4332 outside F	tgcacaccggcagcgaggcg

6.12 Equipment

Table 9 Equipment used in this work.

Equipment	Model	Manufacturer
-80°C freezer	HERAfreeze™	Heraeus Holding, Germany
Agarose gel chamber	Mini-SUB® Cell GT System	BIO-RAD, USA
Agarose gel chamber	Wide Mini-SUB® Cell GT	BIO-RAD, USA
Chromatography system	ÄKTA Prime Plus	GE Healthcare Life Science, Germany
Bench-top centrifuge	Eppendorf Centrifuge 5415 R	Eppendorf, Germany
Blotting system	Trans-Blot® SD Semi-Dry Transfer Cell	BIO-RAD, USA
Clean bench	HeraSafe KS18	Thermo Fisher Scientific, USA
Fridge and freezer	Es Series	Thermo Scientific, USA
Chemiluminescence imaging	Fusion Solo S 3	Vilber, France
Heating block	Eppendorf Thermomixer Comfort	Eppendorf, Germany
Incubator	Kelvitron®t	Heraeus, Germany
Microplate reader	Infinite® M200 PRO	Tecan Group Ltd., Switzerland
Mini-Centrifuge	Mini Spin Plus	Eppendorf, Germany
Orbital Shaker	MaxQ 4450	Thermo Fisher Scientific, USA
UV-VIS-Photometer	BioPhotometer D30	Eppendorf, Germany
Pipette controller	Accu-Jet® Pro	Brand, Germany
Pipettes	Eppendorf Reference (10 µl)	Eppendorf, Germany
Pipettes	Eppendorf Research (1000 µl, 100 µl)	Eppendorf, Germany

Pipettes	Eppendorf Research Plus (1000 µl, 100 µl, 10 µl)	Eppendorf, Germany
Platform shaker	Unimax 1010	Heidolph, Germany
Power supplier	Power Pac 200/300	BIO-RAD, USA
Precision scale	Kern PCB 1000-2	KERN & SOHN, Germany
SDS-PAGE gel chamber	Criterion™	BIO-RAD, USA
Thermocycler	C1000 TouchTM Thermal Cycler	BIO-RAD, USA
Vortex	REAX Control	Heidolph, Germany
Size exclusion chromatography column	HiLoad 16/600 Superdex 200 pg	GE Healthcare Life Science, Germany
Electroporation system	Gene Pulser	BIO-RAD, USA
Anaerobic jar	Anaerocult™	Merc Millipore, Germany

6.13 Consumables

Table 10 Consumables used in this study.

Model	Manufacturer
14ml Polystyrene Round Bottom Tube	Corning, USA
15 ml Polypropylene Conical Tube	Greiner Bio-one, Germany
50 ml Polypropylene Conical Tube	Corning, USA
96-well Sensoplate Plus	Greiner Bio-one, Germany
Anaerobic Indicator - Resazurin	bioMérieux SA, France
Bottle Top Vacuum Filter 500 ml; 0.22 µm	Corning, USA
BRAND® Disposal Bag	Merc Millipore, Germany
Corning® Costar® Stripette® Serological Pipettes	Corning, USA
Corning® PET Storage Bottle	Corning, USA
Criterion™ TGX™ Precast Gel	BIO-RAD, USA

Cryo.s™ Vials	Greiner Bio-one, Germany
Descosept AF	Dr. Schuhmacher, Germany
Extra Thick Blot Filter Paper	BIO-RAD, USA
Gene Pulser/MicroPulser Electroporation Cuvette	BIO-RAD, USA
Kimwipes™ Delicate Task Wipes	Kimberly-Clark Professional, USA
Nitrile, Powder free Medical Examination Gloves	ABENA, Dennmark
Parafilm® M	Omnilab, Germany
PCR Tube Strip	Biozym, Germany
Pipette Tips 100 -1000 µl	Ratiolab, Germany
Pipette Tips 10-100 µl	Sarstedt, Germany
Pipette Tips 0,5-10µl	Starlab, Germany
Pure Nitrocellulose Membrane unsupported; 0.45 µm	AppliChem, Germany
Safe Lock Tubes 1.5 and 2 ml	Eppendorf, Germany
Sterile Filter Pipette Tips 100 -1000 µl and 10-100 µl	Nerbe Plus, Gemany
Sterile Filter Pipette Tips 0,5-10µl	Biozym, Germany
Sterilization Indicator Tape	Merc Millipore, Germany
UV Cuvette 2.7 ml; 10 mm	Sarstedt, Germany

6.14 Software

Table 11 Software used in this study.

Software	Manufacter
Adobe Illustrator CS5	Adobe Systems, USA
Adobe Photoshop CS6	Adobe Systems, USA
DNASTAR Lasergene 12 Core Suite	DNASTAR, USA
GraphPad Prism 7	GraphPad Software, Inc, USA
Paint	Microsoft Corporation, USA
Tecan i-control 2.0	Tecan Group Ltd., Switzerland
Vision Capt	Vilber, France

7. Methods

7.1 Cultivation of bacteria

1.1.1 Cultivation on agar plates

Unless stated otherwise, *E. coli* was cultivated on LB or MacConkey agar plates supplemented with antibiotics where necessary. *P. aeruginosa* was grown on LB agar plates in the presence of antibiotics where required. The bacteria were incubated overnight at 37°C.

1.1.2 Cultivation in liquid media broth

Bacteria were grown in LB or TSB broth supplemented with antibiotics and 20 mM KNO_3 where necessary in 14 ml culture tubes or in Erlenmeyer flasks inoculated with a single colony from an agar plate or from a freezing stock. For 3 ml cultures 14 ml polystyrene tubes were used and for larger culture volumes Erlenmeyer flasks. Cultures were grown overnight in a shaker at 200 rpm and 37°C.

7.1.1 Cultivation in a fermenter for transcriptome analysis

P. aeruginosa wild type and Δ*sadC* mutant were grown overnight in 50 ml TSB medium supplemented with 20 mM KNO_3 under aerobic conditions at 200 rpm and 37°C. The cultures were used to inoculate 1000 ml TSB plus 20 mM KNO_3 each, in a bioreactor vessel in parallel of a Biostat® Bplus batch bioreactor system (Sartorius) at OD_{600} 0.05. Before inoculation and during aerobic incubation the medium was flushed with filtered air at an aeration rate of 1.5 l/min. The oxygen concentration was continuously measured with an oxygen electrode (Oxyferm FDA 225, Hamilton). The bacteria were incubated at 37°C and agitation and the pH was kept at pH 7±1. When the cultures reached an OD_{600} of 1.0±0.2 aliquots were aseptically drawn into DNA/RNA Shield™ (Zymoresearch). The cultures were then flushed with N_2. After two hours of anaerobic incubation, aliquots of the cultures were again aseptically drawn into DNA/RNA Shield™.

1.1.3 Exponential phase cultures for $SadC_{cyt}$ purification

A freezing stock of *E. coli* BL21 containing the desired plasmid was used to inoculate 30 ml of LB supplemented with the appropriate antibiotic. After overnight incubation at 37°C in a shaker at 180 rpm, the culture was used to inoculate 300 ml of LB supplemented with the appropriate antibiotic at an OD_{600} of 0.05 and grown in a shaker

at 180 rpm and 37°C. Recombinant protein expression was induced with 0.5 mM IPTG after 3 hours, and cells were harvested by centrifugation when the culture reached an OD_{600} of 1.0.

1.1.4 Cryopreservation

Bacteria grown overnight in LB with supplemented antibiotic where necessary were centrifuged for 5 min at 3 000 rpm, and the supernatant was discarded. The bacterial pellet was resuspended in 1 ml of freezing medium, transferred to a 2 ml CRYO.S™ freezing tube (Greiner Bio-One GmbH, Germany), and placed at -80°C.

7.1.2 Measurement of optical density (OD)

The optical density (OD) of liquid cultures was measured at 600 nm with an Eppendorf BioPhotometer® D30 (Eppendorf, Germany). If a measured value exceeded 1.0, the sample was diluted and measured again.

7.2 Molecular biology methods

7.2.1 Genomic DNA extraction

Genomic DNA was extracted from 2 ml of an overnight bacterial culture using a Quick-gDNA™MiniPrep according to the manufacturer's instructions. Extracted DNA was stored at -20°C.

7.2.2 Plasmid DNA extraction

Plasmid DNA was extracted from *E. coli* grown overnight in 2 ml LB supplemented with required antibiotic, using the Zyppy™ PlasmidMiniprep Kit according to the manufacturer's instructions. Plasmid DNA was eluted with 30 µl ddH_2O and stored at -20°C.

7.2.3 Measurement of DNA concentration

The concentration and purity of genomic and plasmid DNA was measured with a NanoDrop™ One (ThermoFisher Scientific, USA).

7.2.4 Polymerase Chain Reaction (PCR)

7.2.4.1 PCR using high fidelity DNA polymerases

For the generation of expression constructs and mutants, DNA was amplified using high fidelity DNA polymerases (Table 12). The samples were prepared on ice and the PCR reactions were performed using the cycling conditions indicated in Table 13.

Table 12 Composition of performed PCRs.

Component	Volume (µl)	
	ReproFast, *Pfu* Turbo	Phusion
nuclease-free water	32	27
buffer	5	50
DMSO	5	
dNTPs 2mM	5	
DNA (1-500 ng/µl)	1	
primer F (50 µM)	0,5	
primer R (50 µM)	1	
Total volume	**50**	

Table 13

PCR cycling conditions. * - temperature was dependent on used primers.

Temperature	Duration	Step	Cycles
95 °C	300 s	initial denaturation	-
95 °C	60 s	denaturation	29 cycles
X °C *	30 s	annealing	
72 °C	60 s/kbp	extension	
72 °C	420 s	final extension	-
4 °C	∞	-	-

7.2.4.2 Colony PCR

Transformation of bacteria was verified by colony PCR using a Taq Polymerase (MangoMix™, Bioline, USA). For this, a fraction of a colony was picked from an LB agar plate and resuspended in the PCR reaction (Table 14). The PCR cycling conditions used were the same as for PCR using high fidelity DNA polymerases (Table 13).

Table 14 Composition of a colony PCR reaction.

Component	Volume (µl)
MangoMix™	7,5
nuclease free water	5
DMSO	1,5
primer F	0,5
primer R	0,5
total volume	**15**

7.2.5 DNA agarose gel electrophoresis

For analytical DNA gel electrophoresis a solution of 1% agarose in 0.5x TBE buffer was heated, cooled down, supplemented with SYBR® Safe DNA Gel Stain (dilution 1:30,000) and poured into a gel electrophoresis tray. 5-10 µl of DNA or PCR reaction sample was mixed with 6x loading dye when necessary and loaded onto the gel. The GeneRuler 1 kb Plus was used as a molecular size standard. The DNA was separated at 100 V for 30 min, visualized by excitation of the SYBR Safe dye at 360 nm and imaged using the FAS V Gel Documentation System.

7.2.6 DNA purification and concentration

Linearized plasmid DNA and PCR DNA products were purified and concentrated using the DNA Clean & Concentrator®-5 kit. DNA was eluted with ddH_2O and stored at -20°C.

In case of In-Fusion® cloning, linearized plasmid DNA and DNA products were purified using QIAquick Gel Extraction Kit.

7.2.7 Molecular cloning using restriction enzymes

7.2.7.1 Restriction digest

To clone genes or DNA fragments into a plasmid, the insert DNA and plasmid were cut with restriction enzymes. Reactions were prepared on ice according to Table 15 and incubated for 3 h at 37 °C. Next, the enzymes were inactivated by heating the samples at 65 °C for 20 min and an aliquot of the samples was analysed by DNA gel electrophoresis. DNA in the remaining sample was purified using the DNA Clean & Concentrator-5 kit and immediately used or stored at -20°C.

Table 15 Composition of restriction digest.

Component	Volume
plasmid or insert DNA	1 µl
restriction enzyme 1	1,5 µl
restriction enzyme 2	1,5 µl
10x buffer	5 µl
nuclease-free water	up to 50 µl
Total	**50 µl**

7.2.7.2 Dephosphorylation

Dephosphorylation of plasmids was performed to prevent self-ligation during T4 ligase incubation. To each restriction digest containing plasmid DNA, 1.5 µl of calf intestinal alkaline phosphatase (CIP) was added for one hour before the end of restriction digest incubation. The enzymes were inactivated by heating the samples at 65 °C for 20 min and purified using the DNA Clean & Concentrator-5 kit and used immediately or stored at -20°C.

7.2.7.3 DNA ligation

The digested plasmid and insert DNA were ligated using the T4 DNA ligase (NEB, USA) at varying insert /plasmid DNA ratios according to Table 16. The samples were incubated at 16 °C overnight and then heat-inactivated at 65 °C for 10 min. Afterward, the ligation reactions were directly used to transform chemically competent *E. coli*.

Table 16 Composition of a DNA ligation reaction.

Component	Volume
digested plasmid DNA	X µl
digested insert DNA	Y µl
T4 DNA ligase	1 µl
10x buffer	2 µl
nuclease-free water	up to 20 µl
Total	**20 µl**

7.2.7.4 In-Fusion® cloning

The plasmid for the generation of a *P. aeruginosa* PAO1 Δ*sadC* was constructed using the In-Fusion cloning technique (Takara Bio). For this, the coding sequence of *sadC* as annotated on Pseudomonas Genome DB (pseudomonas.com) was deleted from nucleotide 337 to 1455. The first 336 nucleotides were not deleted to keep the gene sequence on the opposite strand intact. The start codon of the downstream gene PA4331 in the Δ*sadC* deletion mutant remained intact as well. Approximately 700 bp up- and downstream of nucleotide 337 and 1455, respectively, were amplified and combined using splicing by overlap extension PCR. The plasmid pEXG2 was linearised by restriction digest with *Hind*III. The digested plasmid and spliced PCR product which contains 15 bp at the ends that are complementary to *Hind*III linearized pEXG2 ends were gel purified and 20 ng of insert DNA and plasmid was mixed with the 5x In-Fusion reagent in a total volume of 10 µl. Following incubation at 50°C for 15 min 3 and 7 µl of the reaction were used to transform chemically competent *E. coli* DH5α. The sequence-verified plasmid pEXG2::Δ*sadC* was cloned into *E. coli* SM10(λpir).

7.2.8 Transformation of bacteria

7.2.8.1 Preparation of chemically competent *E. coli*

The *E. coli* strain was streaked onto an LB plate from a freezing stock and incubated overnight at 37°C. Next, 4 ml of LB medium was inoculated with a single colony and incubated overnight at 37°C and 250 rpm. The next day, the culture was used to inoculate 400 ml of LB medium at dilution of 1:100 in a 2 l flask. The culture was grown at 37°C and 250 rpm, until it reached an OD_{600} of 0.4 - 0.6. Next, 50 ml volumes of the culture were transferred to eight 50 ml tubes and placed on ice for 20 min. The bacteria

were centrifuged at 4°C for 10 min at 3,000 rpm. The pellets were resuspended in 24 ml of ice cold 0.1 M $CaCl_2$ and incubated on ice for 30 min. The samples were centrifuged at 4°C for 10 min at 3,000 rpm, after which the pellets were resuspended in 6.4 ml of ice cold 0.1 M $CaCl_2$ containing 15% glycerol. The suspensions were aliquoted (100 µl portions) into pre-chilled microcentrifuge tubes. The bacteria were snap frozen in liquid nitrogen, stored at -80°C, and used for transformation within 6 months

7.2.8.2 Transformation of chemically competent *E. coli*

An aliquot of chemically competent *E. coli* was thawed on ice for 10 min. A ligation mixture was added to the cells and mixed carefully. The sample was incubated on ice for 30 min. Next, a heat shock was performed at 42 °C for 1 min, and the tubes were placed on ice for 5 min. 1 ml of SOC medium was added, and the sample was incubated at 37 °C for 1 h at 250 rpm. The bacteria were centrifuged at 5000 rpm for 3 min, the supernatant was partially discarded (~900 µl), and the pellet was resuspended in the remaining supernatant. Finally, the bacteria were streaked onto LB agar plates supplemented with the appropriate antibiotic and incubated overnight at 37 °C.

7.2.8.3 Preparation of electrocompetent bacteria

The *E. coli* strain was grown overnight at 37 °C, 250 rpm in LB medium (with an antibiotic selection if necessary). Next, 100 ml of LB medium (with an antibiotic selection if necessary) was inoculated to an OD_{600} of 0,05 and cultivated until OD_{600} reached 0,6. The culture was split into two 50 ml tubes and centrifuged for 15 min at 4000 rpm. The pellets were washed twice in 20 ml of sterile ddH_2O. Next, the bacteria were centrifuged, resuspended in 2 ml of 10% glycerol in ddH_2O, centrifuged again, and resuspended in 200 µl of 10% glycerol in ddH_2O. Finally, 100 µl aliquots were prepared in 1.5 ml tubes. Electrocompetent bacteria were immediately used or stored at -80°C.

7.2.8.4 Transformation of electrocompetent bacteria

An aliquot of frozen electrocompetent bacteria was thawed at room temperature, 50 ng of plasmid DNA was added and mixed by stirring with a pipette tip. The mixture was transferred to an electroporation cuvette (Bio-Rad, USA), and the cuvette was placed on ice. Electroporation was performed using the Gene Pulser (Bio-Rad, USA) with the settings: 200 Ω, 25 µF and 2.5 kV. Immediately after the pulse 1 ml of LB was added to the cuvette, and the content was carefully mixed by pipetting. The bacteria were transferred to a 1.5 ml tube and incubated in a shaker at 37 °C for 1 h. After incubation, the cells were centrifuged at 5000 rpm for 3 min. The supernatant was almost completely discarded and the pellet was resuspended in the remaining supernatant and spread onto

an LB agar plate supplemented with the appropriate antibiotic. The plate was incubated overnight at 37 °C.

7.2.9 Sanger DNA sequencing

Sanger DNA sequencing was performed to verify sequences of plasmid inserts (Eurofins Scientific, Luxembourg). The samples were prepared according to the company's guidelines. Sequencing reactions were performed with primers selected to cover the entire sequence of plasmid inserts.

7.2.10 Analysis of DNA sequences

Plasmid insert sequences were analysed using DNASTAR Lasergene (DNASTAR, USA) for quality and accuracy. Only *E. coli* colonies containing plasmids with inserts identical to the desired sequence were stored and used

7.2.11 mRNA sequencing and data analysis

RNAseq (RNA isolation and expression analysis) was performed by BaseClear B.V. (Netherlands). RNA isolation and RNA sequencing analysis were performed individually from 2 samples per condition and strain, and the mean expression values were used to determine the expression fold change between the PAO1 WT and *ΔsadC* mutant, grown and harvested in aerobic and anaerobic conditions. rRNA depletion was performed with Illumina RiboZERO Plus Kit, and a TruSeq strand-specific mRNA library was prepared for Illumina sequencing, which includes 10 million reads per sample. Gene expression values were normalized based on TPM (transcripts per million). Statistical analysis was not performed because single samples were analyzed.

7.2.12 PCR site-directed mutagenesis

To introduce mutations into plasmid inserts, PCR site-directed mutagenesis was performed. The mutations leading for example to a codon substitution in the insert sequence were introduced in the middle of the forward and reverse primer flanked up- and downstream by 15 nucleotides of the original sequence. Next, the template plasmid was amplified with these primers by PCR using the Pfu Turbo DNA polymerase and PCR reaction composition as described in Table 12 and the cycling conditions indicated in Table 17. Afterwards, the methylation-dependent restriction enzyme DpnI was added to the PCR reaction to digest the methylated template plasmid for 3 h at 37°C. The amplified plasmid DNA was purified using the DNA Clean & Concentrator-5 kit and used to transform chemically competent *E. coli* DH5α. Plasmid DNA was isolated from

the colonies and the plasmid insert was analysed for the incorporation of the mutation by Sanger sequencing.

Table 17 PCR conditions for site-directed mutagenesis.

Temperature	Duration	Step	Cycles
95 °C	60 s	initial denaturation	-
95 °C	30 s	denaturation	16 cycles
50 °C	60 s	annealing	
72 °C	60 s/kbp of plasmid	extension	
72 °C	300 s	final extension	-
4 °C	∞	-	-

7.2.13 Mutagenesis of *P. aeruginosa* by allelic exchange

P. aeruginosa PAO1 was transformed with pEXG2::Δ*sadC* *via* conjugation. Transformants having the plasmid integrated into the chromosome were selected on LB agar plates supplemented with 75 μg/ml gentamicin and 25 μg/ml irgasan. Single colonies were picked, incubated overnight in LB without antibiotics to allow for excision of the plasmid and streaked onto 15% sucrose plates to select for plasmid excision. After overnight incubation at 37°C, single colonies were patched onto LB agar containing 75 μg/ml gentamicin and LB agar without antibiotic. Gentamicin sensitive colonies were analysed by colony PCR for the deletion of *sadC* and colonies lacking *sadC* were tested again for gentamicin sensitivity. gDNA was isolated and the gene deletion was verified by PCR using different primers including one primer that anneals outside of the genomic region that was amplified for allelic exchange.

7.3 Protein biochemistry methods

7.3.1 SDS polyacrylamide gel electrophoresis (SDS-PAGE)

Appropriate volumes and concentrations of bacterial lysates, purified protein or bacterial cell suspensions were mixed with 2x SDS loading buffer at equal ratio and incubated at 95 °C for 5 min. For SDS polyacrylamide gel electrophoresis (SDS-PAGE)

Criterion™ TGX™ Precast Gels (Bio-Rad, USA) were loaded with 10 µl of the sample. Precision Plus Protein™ Dual Colour Standards (Bio-Rad, USA) was used as a molecular weight marker. The proteins were separated for 20 min at 80 V and then for 35 min at 185 V in 1x SDS running buffer.

7.3.2 Western blotting

Protein samples separated by SDS-PAGE were transferred from the gel onto a nitrocellulose membrane (AppliChem GmbH, Germany) using transfer buffer and a semi dry blotting device (Bio-Rad, USA). The transfer was conducted at 15 V for 30 min. The membrane was blocked in 5% skim milk for 30 min at room temperature and incubated with the primary antibody diluted in TBST at 4°C overnight. Next, the membrane was washed three times with TBST, each for 5 min at room temperature and then incubated with the secondary horseradish peroxidase (HRP)-conjugated antibody diluted in TBST for 1 h at room temperature. After three washing steps in TBST each for 5 min, the membrane was incubated with the chemiluminescent substrate Clarity Western ECL Substrate (Bio-Rad, USA) for 10 min at room temperature. The chemiluminescent signal was imaged with the FUSION Solo S imaging system.

7.3.3 Silver staining

The SilverQuest™ Silver Staining Kit (Invitrogen, USA) was used to visualize proteins separated by SDS-PAGE according to the manufacturer's instructions. Images of the stained SDS-PAGE gels were acquired using the FUSION Solo S imaging system.

7.3.4 Analysis of cysteine residues in $SadC_{cyt}$

7.3.4.1 Preparation of plasmids and bacterial strains

The C-terminal end of the inner membrane protein SadC ($SadC_{cyt}$) containing the GGEEF domain is located in the cytoplasm and contains four cysteine residues. To express the wild type cytoplasmic domain of SadC in *E. coli* the plasmid pMCSG19::MBP-His-$PA4332_{883-1464}$ was used, which was constructed in previous work (Schmidt et al. 2016). This plasmid was used as a template for site directed mutagenesis to generate constructs that express cysteine to alanine substitutions (Table 18 and Figure 9). The resulting plasmids harbouring mutations leading to a C390A, C420A C421A or C478A exchange were cloned into *E. coli* BL21 by electroporation. The transformation was verified by colony PCR.

Table 18 Primers used for construction of plasmids.

Plasmid	Primer forward	Primer reverse
pMCSG19::MBP-His-SadC$_{cyt}$ C390A	PA4332_C390A_for	PA4332_C390A_rev
pMCSG19::MBP-His-SadC$_{cyt}$ C420A C421A	PA4332_C420A_C421A_for	PA4332_C420A_C421A_rev
pMCSG19::MBP-His-SadC$_{cyt}$ C478A	PA4332_C478A_for	PA4332_C478A_rev

Nucleotide sequence of SadC$_{cyt}$

ATGCGGCAACGCATGCGCCAGCGCCGCTATGCCTTGCAGGCGCACCAGGACA
CGCTGCGCGGCATGATGCGCCAACTGGAAGACCTGGTGGCCACCGACGAACT
CACCGGTCTGTTCAACCGCCGGCATTTCATGCGCATGGCCAGCCGGGCGCTG
GAAGACCTGCTGCCGAACCGGCAGCACGGCCTGGCGCTGATCGACCTCGATC
ACTTCAAGCGGATCAACGACCGCCACGGCCACGCCGCCGGCGATCGGGTCCT
GCAGACCTTCGCCGCGGTGGCGCGTTCCTGTCTGCGCGATGGCGACGTCCTG
GCCCGTTACGGCGGCGAGGAGTTCGTCCTGCTGCTGCCCCACGCCGACGCG
GAACAGCTGGAAAGCTGTTGCGAGCGCCTGCGCCTGGCGTTCCAACAGGCGG
AACCGGTCGGGGTCACGGTGGATACCCTGAGCCTTTCGGTGGGCATGACCCT
GCTGTATGCCGACGACGATCTCGACGAGGCCTTGCAGCGGGCCGACCAGGC
GCTCTACCGTGCCAAGCGCGGCGGACGAAACCGCTGCGACGCCACCTGGGA
GGTCACCAGTGCCTGA

Amino acid sequence of SadC$_{cyt}$

MRQRMRQRRYALQAHQDTLRGMMRQLEDLVATDELTGLFNRRHFMRMASRALE
DLLPNRQHGLALIDLDHFKRINDRHGHAAGDRVLQTFAAVARSCLRDGDVLARYG
GEEFVLLLPHADAEQLESCCERLRLAFQQAEPVGVTVDTLSLSVGMTLLYADDDL
DEALQRADQALYRAKRGRNRCDATWEVTSA Stop

Figure 9 Nucleotide and amino acid sequence of SadC$_{cyt}$ (nucleotides 880-1446, amino acids 295-488 used in experiment with cysteine codons and residues, which were mutated to alanine (marked in red), resulting in construction of pMCSG19::MBP-His-SadC$_{cyt\ C390A}$, pMCSG19::MBP-His-SadC$_{cyt\ C420A\ C421A}$, pMCSG19::MBP-His-SadC$_{cyt\ C478A}$ plasmids.

7.3.4.2 Preparation of soluble cell extracts

Bacterial cell lysates were prepared from *E. coli* BL21 after induction with IPTG (6.1.3). All steps were performed on ice using ice cold buffers. First, 200 ml of the culture was centrifuged at 4600 rpm for 20 min at 4°C. The supernatant was discarded, and the cell pellet was frozen at -20 °C until further processing or was immediately resuspended in 16 ml amylose column buffer containing 100 µg/ml lysozyme and 2 mM PMSF. Next, the sample was incubated rotating at 4 °C for 60 min followed by sonication

10 times for 10 seconds (20-gauge needle, 40% amplitude, Branson Sonifer 250, Gemini B.V., Apeldoorn Zuid, Netherlands). Finally, the sample was centrifuged at 7940 x *g* for 30 min at 4°C. The supernatant was stored at -20°C until further processing.

7.3.4.3 Affinity chromatography using amylose resin

To purify the cytosolic domain of SadC coupled to MBP, amylose resins were used. All steps were performed on ice and using ice cold buffers. For cell lysates obtained from a 200 ml bacterial culture, 5 ml of amylose resin was used (NEB, Germany). Resins were poured into a 12 ml polypropylene column (Qiagen, Germany) and washed eight times with 4 ml of amylose column buffer. Next, the bacterial cell lysate was loaded onto the column. The column was washed 6 times with 6 ml of amylose column buffer. Finally, MBP-SadC$_{cyt}$ proteins were eluted from the column using 4 ml of amylose elution buffer and stored at 4°C until further processing. Aliquots of flow-through and eluate fractions were taken and analysed by SDS-PAGE and Western blotting.

7.3.4.4 Size exclusion chromatography

Protein samples obtained with amylose affinity chromatography were additionally purified by size exclusion chromatography. For this, a Superdex 200 HiLoad 16/600 column coupled with an Äkta Prime Plus System (GE Healthcare Life Sciences, Germany) placed at 4°C was utilized. A degassed amylose column buffer was used with a flow rate of 1.0 ml/min, with a maximal pressure of 0.5 MPa. 1 ml fractions were collected and analysed by SDS-PAGE and Western Blotting. Next, fractions containing the protein of interest were pooled and concentrated with Amicon Ultra-15 centrifugal filter units with a 10 kDa NMWCO (Merc Millipore, Germany). The concentrated samples were frozen at -20 °C until further processing.

7.3.4.5 Protein concentration measurement

The Pierce™ BCA Protein Assay Kit (Thermo Scientific, USA) was used to measure protein concentrations. All steps were performed according to the manufacturer's protocol. The microplate reader Infinite® 200 PRO (Tecan, Switzerland) was utilized to measure the absorbance of the BCA/copper complex at 562 nm.

7.3.4.6 Protein concentration and buffer exchange

To increase the protein concentration of the fractions collected from size exclusion chromatography or to change the buffer of protein samples, Amicon Ultra-15 centrifugal filter units with 10 kDa NMWCO (Merc Millipore, Germany) were utilized. The filter units

were washed once using 15 ml of ddH_2O and centrifugated at 4 000 x g for 15 min. Next, all fractions containing the protein of interest were pooled, loaded onto a filter device, and centrifuged at 4000 x *g* for 15 min. If required, a buffer exchange was additionally performed. Depending on the experiments performed, 15 ml of 20 mM phosphate buffer or 50 mM Tris-HCl was added for buffer exchange, and the sample was centrifuged 4000 x *g* for 15 min. The flow-through was discarded, and the washing step was repeated twice. The concentrated samples were transferred from the filter device to a 1.5 ml tube and stored at 4°C until further processing

7.3.4.7 Protein dimerization assay using chemical crosslinking

Concentrated MBP-$SadC_{cyt}$ protein samples in 20 mM phosphate buffer were used for the dimerization assay. The crosslinking reaction was performed with a protein sample at a final concentration of 20 µM incubated with disuccinimidyl suberate (DSS) (Thermo Scientific, USA) at a final concentration 2 mM in a total volume of 100 µl. The reaction was allowed to proceed for 30 min at room temperature and was stopped by adding 2 µl of 1 M Tris-HCl pH 7.5. The samples were analysed by SDS-PAGE and Western blotting.

7.3.4.8 Guanosin 5'-triphosphate (GTP) binding assay

The GGEEF domain of SadC catalyses the conversion of guanosin 5'-triphosphate (GTP) to c-di-GMP. The binding of GTP to purified MBP-$SadC_{cyt}$ proteins was measured by using the fluorescent GTP analogue (2'-(or-3')-O-(N-Methylanthraniloyl) guanosine 5'-triphosphate (MANT-GTP) as a probe, which contains a MANT fluorophore at the ribose moiety. The experiments were performed using a modified protocol (Spangler et al., 2011) in 96-well microtiter plates. The reaction mixture consisted of 5 µM purified MBP-$SadC_{cyt}$ protein in 50 mM Tris-HCl and 50 µl 2x GTP binding reaction buffer and ddH_2O in a total volume of 100 µl. Additionally, a set of reactions was prepared: i.) consisting only of protein sample and buffer (blank), ii.) additional 10 µM MANT-GTP, iii.) additional 10 µM of GTP to the reaction mixture and iv.) additional 10 µM MANT-GTP and 10 µM of GTP. Samples were incubated in a room temperature in darkness for 30 minutes and then fluorescence was measured using microplate reader Infinite® 200 PRO (Tecan, Switzerland) using an emission and excitation wavelength of 350 nm and 380 to 540 nm, respectively. MANT-GTP, when bound to the active centre or a specific domain of DGCs, including SadC, is characterized by an increased fluorescence emission peaking at 450 nm.

The experiment was performed in three replicates, and values were collected for each replicate. Following this, the value derived from the reaction containing only

protein and buffer (blank) was subtracted from the other samples to mitigate the influence of protein presence on the experimental results. The value obtained for the purified MBP-SadCcyt protein, encompassing all four cysteine residues, was established as the reference point at 100%, with all other values calculated as percentages. Mean values were subsequently determined.

7.3.5 Bacterial Adenylate Cyclase Two-Hybrid (BACTH) System

To investigate protein interactions between SadC, $SadC_{cyt}$, OdaA, and OdaI *in vivo* in *E. coli* the Bacterial Adenylate Cyclase Two-Hybrid (BACTH) system (Euromedex, France) was utilized.

7.3.5.1 Preparation of plasmids and bacterial strains

A set of BACTH plasmids carrying *sadC* (PA4332), $sadC_{cyt}$ ($PA4332_{883-1464}$), *odaA* (PA4330) and *odaI* (PA4331) fused to the T18 and T25 fragments were constructed (Table 19). Genes were amplified from gDNA of *P. aeruginosa* PAO1 using the primers listed in Table 19, cloned into the vectors pKNT25 and pUT18 and used for transformation of *E. coli* DH5α. Colonies were verified for containing the correct plasmids by colony PCR and Sanger sequencing. The adenylate cyclase deficient *E. coli* BTH101 was co-transformed with pKNT25 and pUT18 plasmids carrying the genes of interest by electroporation and incubated on LB agar plates supplemented with 50 µg/ml kanamycin and 100 µg/ml ampicillin. The presence of both plasmids was confirmed by colony PCR. Suspensions of *E. coli* BTH101 co-transformants were spotted onto i) LB agar plates supplemented with 50 µg/ml kanamycin, 100 µg/ml ampicillin and 40 µg/ml X-Gal and ii) MacConkey agar containing 1% maltose. Protein interactions were analysed in the absence and presence of 1 µM IPTG after incubation under anaerobic conditions in anaerobic jars with AnaeroGen™ and an anaerobic indicator strip (Anaerotest® , Millipore) and aerobic conditions for 48 h.

Table 19 Primers used for construction of plasmids.

Plasmid	Primer forward	Primer reverse
pKNT25::PA4330	PA4330_nostart_ BACTH_*Hind*III#1	PA4330_nostop_ BACTH_*Xba*I#2
pUT18::PA4330		
pKNT25::PA4331	PA4331_nostart_ BACTH_*Hind*III#1	PA4331_nostop_ BACTH_*Xba*I#2
pUT18::PA4331		
pKNT25::PA4332	PA4332_nostart_ BACTH_*Hind*III#1	PA4332_nostop_ BACTH_*Xba*I#2
pUT18::PA4332		
pKNT25::PA4332$_{883\text{-}1464}$	PA4332_cytosolic_ nostart_BACTH_*Hind*III#1	
pUT18::PA4332$_{883\text{-}1464}$		

8. Results

8.1 BACTH interaction analysis of SadC, OdaA, and OdaI

The BACTH system is a genetic assay that allows the detection of protein-protein interactions *in vivo* in *E. coli* (Karimova et al., PNAS, 1998). It is based on adenylate cyclase from *Bordetella pertussis*. The enzyme is divided into two subunits, T18 and T25. These subunits cannot heterodimerize to form a functional enzyme unless they are fused to proteins that interact with each other. The coding sequences for both subunits are already located on separate plasmids provided by the manufacturer. Thus, the coding sequences of the investigated proteins can be easily cloned into these plasmids to create a hybrid with either the T18 or T25 subunit. Subsequently, both plasmids are transformed into an *E. coli* strain that lacks adenylate cyclase activity. When the two proteins of interest, fused with the T18 and T25 subunits, interact, the subunits heterodimerize and synthesize cyclic AMP (cAMP). This cAMP activates the expression of genes involved in lactose and maltose metabolism, which can be visualized by growing the bacteria on an appropriate screening or selective agar medium. A stronger interaction between the investigated proteins results in a more pronounced colorimetric effect on the bacterial colonies.

8.1.1 Experimental setup of BACTH experiment

Initially, genes of interest (SadC/PA4332, $SadC_{cyt}$/$PA4332_{880-1446}$, OdaA/PA4330, OdaI/PA4331) were cloned into each of the plasmids, pKNT25 and pUT18. Following this, *E. coli* BTH101 strains were transformed with combinations of these plasmids to generate strains carrying all possible protein pairings. For each transformation, specific combinations of the pKNT25 and pUT18 plasmids, as detailed in Table 20, were used. After successful transformation, the presence of both plasmids in each strain was confirmed using colony PCR.

For this experiment, all the prepared strains were cultured overnight at 37°C in LB. In addition to these, the manufacturer provided positive and negative controls. The positive control, *E. coli* BTH101 carrying pUT18C-zip and pKNT25-zip, uses the leucine zipper motif. This motif is renowned for mediating protein-protein interactions, ensuring an expected positive interaction. Conversely, the negative control, *E. coli* BTH101 with pUT18 and pKNT25, involves subunits that are not fused to any proteins. Consequently, they cannot interact with each other, resulting in no signal.

The following day, 10 µl of each culture was pipetted onto two distinct types of media: i) LB agar containing 50 µg/ml kanamycin, 100 µg/ml ampicillin, and 40 µg/ml X-Gal; ii) MacConkey agar with 1% maltose. Additionally, both types of plates were either supplemented with 1 µM IPTG or left without. Plates were incubated either at room temperature or at 30°C, and under aerobic or anaerobic conditions. For anaerobic conditions, an anaerobic container (Anaerocult™, Merck Millipore, Germany) and an anaerobic condition generator (AnaeroGen™, ThermoFisher Scientific, USA) were used. After 48 hours of incubation, plates were photographed, and the results were processed as outlined in the subsequent chapter. The entire procedure was repeated in three independent experiments.

Table 20 Combination of *E. coli* BTH101 mutants containing two plasmids, utilized in the experiment (white fields).

***E. coli* BTH101**	**pUT18::PA4330**	**pUT18::PA4331**	**pUT18::PA4332**	**pUT18::PA4332$_{cyt}$**
pKNT25::PA4330	pKNT25::PA4330 pUT18::PA4330	pKNT25::PA4330 pUT18::PA4331	pKNT25::PA4330 pUT18::PA4332	pKNT25::PA4330 pUT18::PA4332$_{cyt}$
pKNT25::PA4331	pKNT25::PA4331 pUT18::PA4330	pKNT25::PA4331 pUT18::PA4331	pKNT25::PA4331 pUT18::PA4332	pKNT25::PA4331 pUT18::PA4332$_{cyt}$
pKNT25::PA4332	pKNT25::PA4332 pUT18::PA4330	pKNT25::PA4332 pUT18::PA4331	pKNT25::PA4332 pUT18::PA4332	pKNT25::PA4332 pUT18::PA4332$_{cyt}$
pKNT25::PA4332$_{cyt}$	pKNT25::PA4332$_{cyt}$ pUT18::PA4330	pKNT25::PA4332$_{cyt}$ pUT18::PA4331	pKNT25::PA4332$_{cyt}$ pUT18::PA4332	pKNT25::PA4332$_{cyt}$ pUT18::PA4332$_{cyt}$

8.1.2 Determination of BACTH signal strength and data analysis

As highlighted in the previous chapter, plates were incubated for 48 hours before being photographed. Signal strength was quantified by the researcher using a scale where 0 indicated no signal, 1 represented a moderate signal, and 2 denoted a strong signal (Table 21). For every strain, the peak score achievable was 24. This was determined from three independent experiments and the potential for 8 points across four distinct medium types: supplemented LB agar or MacConkey agar, either with IPTG or without. Each score was subsequently expressed as a percentage of the maximum possible score (**Error! Reference source not found.** and Figure 16). Additionally, Figure 13 and Figure 14 demonstrate representative examples of colonies for each tested combination.

Table 21 Representative colonies showcasing different signal strength values in the BACTH System experiment. Colonies were grown on two primary media: i) MacConkey agar supplemented with 1% maltose, 50 µg/ml kanamycin, and 100 µg/ml ampicillin ii) LB agar containing 50 µg/ml kanamycin, 100 µg/ml ampicillin, and 40 µg/ml X-Gal. Both media types were tested with and without 1 µM IPTG supplementation. The presented colonies were grown on media without IPTG; however, their appearance was consistent with those grown on media supplemented with IPTG.

Medium	Signal strength		
	0	1	2
MacConkey		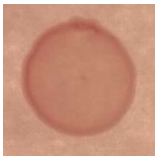	
LB			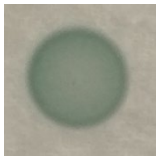

8.1.3 Investigation of the influence of growth conditions in the BACTH experiment

Once *E. coli* BTH101 was chosen, several factors were evaluated for their potential effects on the clarity and intensity of interaction signals on agar plates. These factors included incubation periods (24h, 48h, or 72h), temperature settings (either room temperature or 30°C), the presence or absence of IPTG (either 1 µM IPTG or none), and the type of growth medium (LB agar or McConkey agar). It's noteworthy that the natural leakiness of the *lac* operon rendered the supplementation of IPTG non-essential, as a certain level of expression can occur even without this inducer.

To ensure comprehensive data collection, all experimental conditions were performed under both aerobic and anaerobic environments. The rationale behind this approach was twofold: firstly, an interest in comparing protein interactions in aerobic versus anaerobic conditions, and secondly, to ensure that the observed results and interaction signals are comparable and consistent across both conditions. This ensures that any future experiments aiming to directly compare these two environments will be based on reliable and equivalent data. A 48-hour incubation period was chosen as the most suitable, as it yielded consistent growth across all colonies and clear differentiation in signal intensities (data not shown). Detailed analysis across the varied conditions - encompassing temperature, IPTG levels, and medium types - revealed no

substantial variations in protein interaction signals, as illustrated in Figure 10, Figure 11 and Figure 12.

As a result of the performed analysis, *E. coli* BTH101 was selected as the most suitable strain for the experiments due to its consistent and superior growth characteristics. Furthermore, a 48-hour incubation period was identified as optimal, providing consistent growth across all colonies with clear differentiation in signal strength. Subsequent experiments were conducted using a range of conditions to ensure that the data collected was both comprehensive and reliable. Specifically, these conditions spanned different temperatures (both room temperature and 30°C), IPTG supplementation levels (with 1 µM IPTG or without any supplementation), and growth mediums (LB agar and McConkey agar). This strategy was employed to obtain the most relevant results across different environmental parameters.

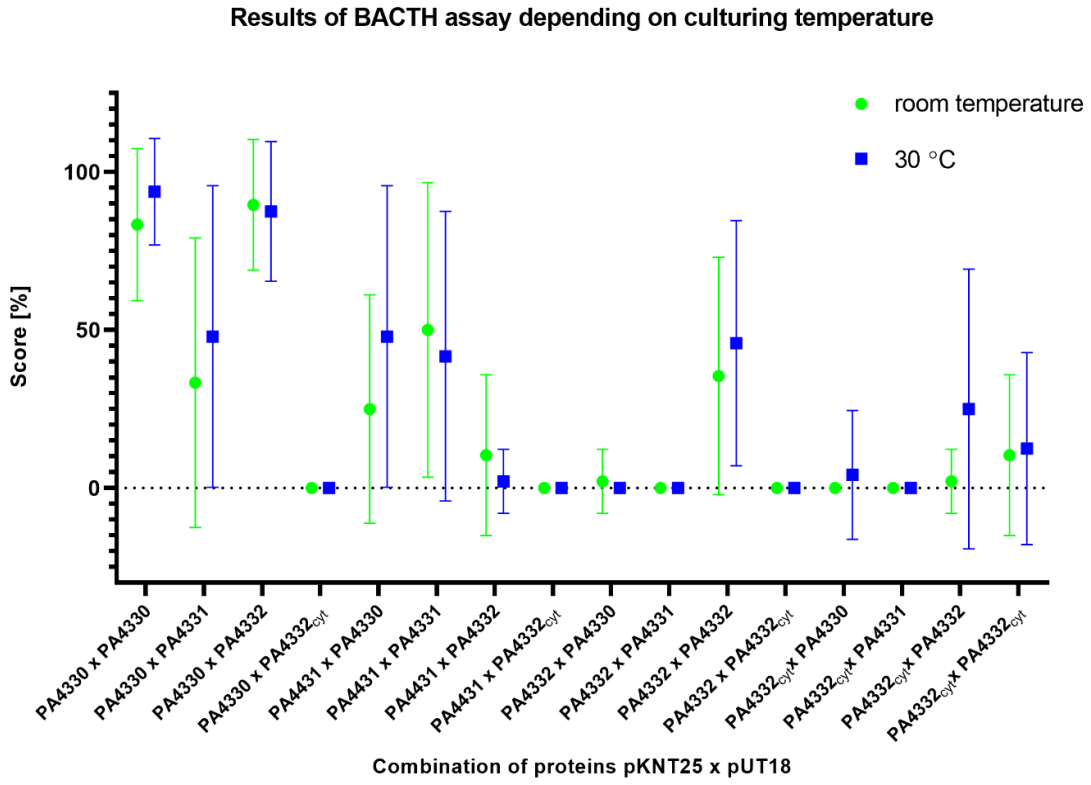

Figure 10 Impact of different culturing temperature on results of BACTH experiment.

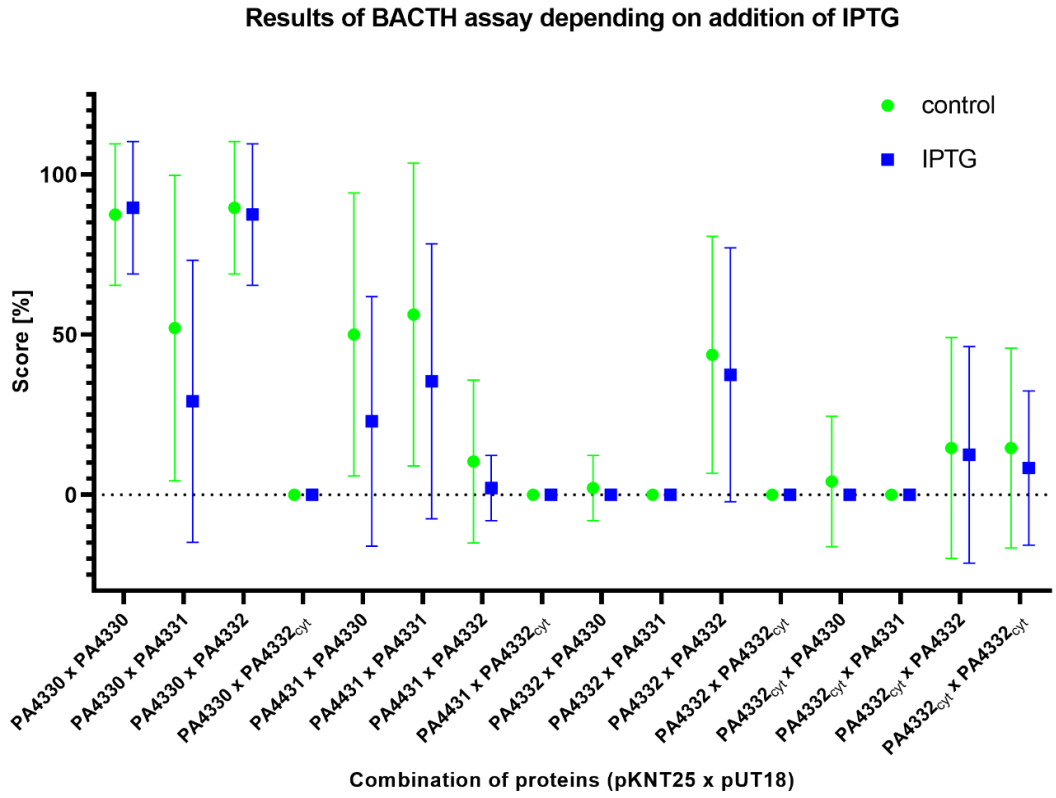

Figure 11 Impact of supplementation of IPTG on results of BACTH experiment.

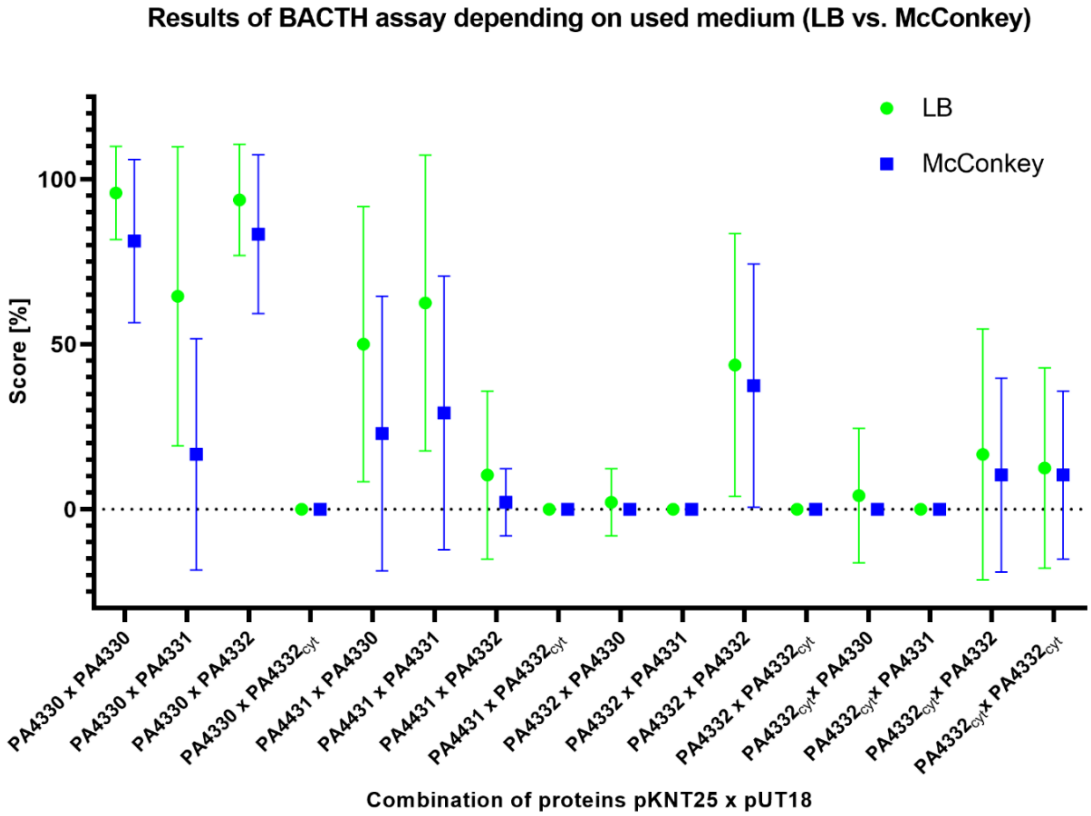

Figure 12 Impact used medium on results of BACTH experiment.

8.1.4 BACTH interaction analysis of SadC, OdaA, and OdaI

In the BATCH experiment, we investigated potential interactions among the proteins SadC, $SadC_{cyt}$, OdaA, and OdaI, considering all possible combinations of these proteins (Table 20). The results discussed in this chapter are based on graphical representations on **Error! Reference source not found.** and Figure 16, which display the outcomes of the various tested combinations. Additionally, the chapters contain tables that outline specific combinations and the values obtained in the experiment.

It's essential to note that each combination of proteins was tested under both aerobic and anaerobic conditions. The BACTH experiment was performed three times (three replicates) to reinforce the robustness of the findings. Results are presented separately for oxygen and temperatures (room temperature and 30°C), with averages calculated under these conditions for media type and IPTG supplementation during analysis.

8.1.4.1 The lack of oxygen stimulates the self-interaction of SadC

Although the molecular structure of SadC has not been resolved yet, experimental findings about other DGCs have shown that dimerization is essential for their catalytic activation, as demonstrated by previous studies (Chan et al., 2004; Paul et al., 2007). BACTH analysis further revealed that the full-length SadC protein demonstrates self-interaction. When the combination pKNT25 x pUT18: SadC x SadC was examined in an *E. coli* strain, signal intensities varied under different conditions. Specifically, at room temperature in the presence of oxygen, the signal was at 8%, but it escalated to 69% under anaerobic conditions. Similarly, at 30°C, the signal intensity was 32% with oxygen and rose to 64% without it (Table 22). These observations suggest that the absence of oxygen significantly enhances the likelihood of SadC self-interaction, potentially boosting its catalytic activity. This trend was observed irrespective of the incubation temperature.

Table 22 Signal intensities in the BACTH experiment for the combination pKNT25 x pUT18: SadC x SadC under different temperature and oxygen conditions.

Combination	Room temperature		30°C	
pKNT25 x pUT18	$+O_2$	$-O_2$	$+O_2$	$-O_2$
SadC x SadC	8%	69%	32%	64%

8.1.4.2 Lack of transmembrane domain of SadC results in impaired self-interaction of SadC

The BACTH experiment underscored the importance of the transmembrane domain in facilitating SadC's interactions (Table 23). For the combination pKNT25 x pUT18: SadC x SadC, the signal intensity was markedly highest than for combinations with at least one Sad_{cyt} (pKNT25 x pUT18: SadC x $SadC_{cyt}$, $SadC_{cyt}$ x SadC and $SadC_{cyt}$ x $SadC_{cyt}$. The combination pKNT25 x pUT18: SadC x SadC yielded 8% at room temperature with oxygen, escalated to 69% without oxygen, 32% at 30°C with oxygen, and reached 64% at the same temperature without oxygen.

However, a different scenario emerged when considering combinations involving at least one variant of SadC devoid of the transmembrane domain. The combination pKNT25 x pUT18: SadC x $SadC_{cyt}$ displayed a complete lack of interaction across all conditions: 0% at room temperature with or without oxygen and 0% at 30°C irrespective of the oxygen presence.

Similarly, the combination pKNT25 x pUT18: $SadC_{cyt}$ x SadC showed limited interactions. There was no detectable interaction at room temperature with oxygen. Still, a slight interaction of 6% was observed without oxygen. Interestingly, this interaction intensified to 50% at 30°C with oxygen and reduced to 21% without oxygen.

Lastly, for the combination pKNT25 x pUT18: $SadC_{cyt}$ x $SadC_{cyt}$, interaction rates were more varied. At room temperature, the interaction was 4% with oxygen and 19% without oxygen. At 30°C, oxygen bolstered the interaction to 29%, while in its absence, the interaction decreased to 11%.

In summary, the absence of the transmembrane domain in SadC distinctly impacts its interaction rates. Specifically, as observed in the various combinations and environmental conditions, the combination pKNT25 x pUT18: SadC x SadC consistently interacted more robustly in tested conditions compared to other combinations: $SadC_{cyt}$ x SadC, namely pKNT25 x pUT18: SadC x $SadC_{cyt}$, pKNT25 x pUT18: $SadC_{cyt}$ x SadC, and pKNT25 x pUT18: $SadC_{cyt}$ x $SadC_{cyt}$ (excluding pKNT25 x pUT18 at 30°C with oxygen). This emphasizes that the transmembrane domain plays an important role in the self-interaction of SadC.

Table 23 Signal intensities in the BACTH experiment for the combinations pKNT25 x pUT18: SadC x SadC, SadC x $SadC_{cyt}$, $SadC_{cyt}$ x SadC and $SadC_{cyt}$ x $SadC_{cyt}$ under different temperature and oxygen conditions.

Combination	Room temperature		30°C	
pKNT25 x pUT18	$+O_2$	$-O_2$	$+O_2$	$-O_2$
SadC x SadC	8%	69%	32%	64%
SadC x $SadC_{cyt}$	0%	0%	0%	0%
$SadC_{cyt}$ x SadC	0%	6%	50%	21%
$SadC_{cyt}$ x $SadC_{cyt}$	4%	19%	29%	11%

8.1.4.3 OdaA self-interacts independently of oxygen tensions

Recent advancements have led to the determination of the crystal structure of OdaA. This revealed that OdaA forms a homotrimer, functioning as a mono-functional enoyl-CoA hydratase (Zhao et al., 2021). The findings align closely with the BACTH experiment results for the combination pKNT25 x pUT18: OdaA x OdaA. High interaction rates were recorded across all conditions: 88% at room temperature with oxygen, 81% in its absence, 93% at 30°C with oxygen, and 89% at the same temperature without oxygen (Table 24).

It is especially noteworthy that the self-interaction efficiency of OdaA remains consistently high across different temperatures and oxygen tensions. This consistency underscores the fact that OdaA's self-interaction is independent of external environmental factors such as oxygen presence and temperature fluctuations.

Table 24 Signal intensities in the BACTH experiment for the combination pKNT25 x pUT18: OdaA x OdaA under different temperature and oxygen conditions.

Combination	Room temperature		30°C	
pKNT25 x pUT18	$+O_2$	$-O_2$	$+O_2$	$-O_2$
OdaA x OdaA	88%	81%	93%	89%

8.1.4.4 The transmembrane domain of SadC is essential for its interaction with OdaA and this interaction is independent of oxygen tensions

The BACTH experiment indicates a robust interaction between OdaA and SadC regardless of oxygen concentrations and temperature variations. In contrast, there is no notable interaction between OdaA and the cytosolic part of SadC ($SadC_{cyt}$), emphasizing the potential importance of the transmembrane domain of SadC in this interaction (Table 25).

In the data from the combination pKNT25 x pUT18: OdaA x SadC, a pronounced interaction is observed. At room temperature with oxygen present, there's a 96% interaction rate. This rate slightly decreases to 88% without oxygen at the same temperature. When the temperature rises to 30°C, interaction peaks at 100% with oxygen and drops to 80% without it. In stark contrast, the combination pKNT25 x pUT18 with SadC and OdaA presents none interaction, in all tested conditions, it is 0%.

For the combination of pKNT25 x pUT18: OdaA x $SadC_{cyt}$, interaction is almost non-existent. At room temperature, irrespective of oxygen presence, no interaction is detected. At 30°C, a slight interaction of 7% is seen with oxygen, but it reduces to 0% without oxygen. Similarly, the combination of pKNT25 x pUT18: SadCcyt x OdaA shows no interaction at room temperature, regardless of oxygen levels. At 30°C, the interaction remains at 0% with oxygen but increases slightly to 7% without it.

An intriguing observation emerges from the data: there is a pronounced interaction for the combination pKNT25 x pUT18: OdaA x SadC, while the interaction is almost negligible for the combination pKNT25 x pUT18 with SadC and OdaA. Notably, this observed potential interaction between SadC and OdaA appears to be independent of oxygen tension. Such a discrepancy could arise from the intrinsic limitations of the BACTH assay, known at times to produce non-specific results. Concurrently, the lack of interaction between OdaA and the cytosolic part of SadC ($SadC_{cyt}$) highlights the significance of SadC's transmembrane domain. While the possibility exists that the observed positive interaction in the combination OdaA x SadC might be a false positive, it's imperative to approach such results with caution when interpreting BACTH assay outcomes. Further confirmation through alternative assays is recommended to validate these findings. However, taking into account the stark contrast between the very strong and very poor interactions, the average interaction strength gravitates towards approximately 46%. This suggests a probable interaction between OdaA and SadC, further underlining the potential importance of the transmembrane domain in facilitating this interaction.

Table 25 Signal intensities in the BACTH experiment for the combinations pKNT25 x pUT18: OdaA x SadC, SadC x OdaA, OdaA x $SadC_{cyt}$ and $SadC_{cyt}$ x OdaA under different temperature and oxygen conditions.

Combination	Room temperature		30°C	
pKNT25 x pUT18	$+O_2$	$-O_2$	$+O_2$	$-O_2$
OdaA x SadC	96%	88%	100%	82%
SadC x OdaA	0%	0%	0%	0%
OdaA x $SadC_{cyt}$	0%	0%	7%	0%
$SadC_{cyt}$ x OdaA	0%	0%	0%	7%

8.1.4.5 OdaI possibly self-interacts under anaerobic conditions

The analysis revealed a distinct behavior of OdaI, suggesting that it may self-interact preferentially in the absence of oxygen. Looking at the details, the change in this interaction, based on oxygen levels, is very noticeable at room temperature. To give a clearer picture, when combination pKNT25 x pUT18: OdaI x OdaI was tested, the self-interaction percentage at room temperature stood at 25% in the presence of oxygen. However, under anaerobic conditions at the same temperature, this interaction leaped to 75% (Table 26).

Interestingly, as the temperature was raised to 30°C, the disparity between the aerobic and anaerobic environments narrowed down. The self-interaction rate of OdaI in the presence of oxygen was 36%, while it was 43% without oxygen. This indicates that the effect of oxygen concentration on OdaI self-interaction diminishes as the temperature rises. These observations provide insights into OdaI's behaviour under different conditions, but caution is essential. The BACTH assay, though instrumental in this research, is not without its limitations. Being an indirect method, it might be susceptible to inaccuracies, possibly skewing the interaction percentages.

Table 26 Signal intensities in the BACTH experiment for the combination pKNT25 x pUT18: OdaI x OdaI under different temperature and oxygen conditions.

Combination	Room temperature		30°C	
pKNT25 x pUT18	$+O_2$	$-O_2$	$+O_2$	$-O_2$
OdaI x OdaI	25%	75%	36%	43%

8.1.4.6 OdaI does not appear to interact with SadC

The experiments largely suggest an absence of interaction between OdaI and SadC or $SadC_{cyt}$ across the tested conditions. For the combination of pKNT25 x pUT18: OdaI x SadC, there was a minor signal of 4% interaction at room temperature with oxygen and a slightly higher signal of 19% in its absence. However, at the raised temperature of 30°C, the interaction signal was completely absent, both in the presence and absence of oxygen (Table 27).

In the reverse combination, pKNT25 x pUT18: SadC x OdaI, there was a negligible interaction of 4% at room temperature with oxygen, but no detectable interaction under any other tested conditions.

Notably, when the experiments extended to the combinations involving $SadC_{cyt}$, the results unequivocally indicated no interaction with OdaI. Both combinations, pKNT25 x pUT18: OdaI x $SadC_{cyt}$ and $SadC_{cyt}$ x OdaI, yielded a 0% interaction signal across all conditions.

These findings predominantly point towards OdaI's lack of interaction with SadC and its variant, $SadC_{cyt}$, under the varied temperature and oxygen levels tested.

Table 27 Signal intensities in the BACTH experiment for the combinations pKNT25 x pUT18: OdaI x SadC, SadC x OdaI, OdaI x $SadC_{cyt}$ and $SadC_{cyt}$ x OdaI under different temperature and oxygen conditions.

Combination	Room temperature		30°C	
pKNT25 x pUT18	$+O_2$	$-O_2$	$+O_2$	$-O_2$
OdaI x SadC	4%	19%	0%	0%
SadC x OdaI	4%	0%	0%	0%
OdaI x $SadC_{cyt}$	0%	0%	0%	0%
$SadC_{cyt}$ x OdaI	0%	0%	0%	0%

8.1.4.7 Moderate signal intensity observed in OdaA and OdaI interaction

The analysis unveiled a moderate signal intensity pointing towards potential interactions between OdaI and OdaA. Interestingly, the data displayed distinct variations based on temperature and oxygen levels. For the combination of pKNT25 x pUT18: OdaA x OdaI, interactions at room temperature showed a lower intensity of 17% with oxygen, but this jumped to 50% in the absence of oxygen. However, at 30°C,

the interaction intensity stood at 50% with oxygen but slightly decreased to 36% without it (Table 28).

In the reverse combination, pKNT25 x pUT18: OdaI x OdaA, the interaction intensity at room temperature remained consistent at 25% regardless of oxygen presence. This consistency shifted at 30°C, where the interaction intensity surged to 75% with oxygen but sharply dropped to 14% when oxygen was absent.

Furthermore, an intriguing observation is the enhanced interaction between the two proteins under aerobic conditions at 30°C, which is in stark contrast to the findings at room temperature. This potential inconsistency, especially concerning oxygen tensions, suggests that if an interaction does occur, it seems most likely to be independent of oxygen levels. Given these nuanced variations, it is crucial to validate the results through alternative methods. The BACTH assay data does hint at a possible interaction between OdaA and OdaI, but further studies would solidify these findings.

Table 28 Signal intensities in the BACTH experiment for the combinations pKNT25 x pUT18: OdaA x OdaI and OdaI x OdaA under different temperature and oxygen conditions.

Combination	Room temperature		30°C	
pKNT25 x pUT18	$+O_2$	$-O_2$	$+O_2$	$-O_2$
OdaA x OdaI	17%	50%	50%	36%
OdaI x OdaA	25%	25%	75%	14%

Protein combination (pKNT25 x pUT18)	Growth conditions: room temperature							
	$+O_2$				$-O_2$			
	LB		McConkey		LB		McConkey	
	+IPTG	-IPTG	+IPTG	-IPTG	+IPTG	-IPTG	+IPTG	-IPTG
SadC x SadC								
$SadC_{cyt}$ x $SadC_{cyt}$								
SadC x $SadC_{cyt}$								

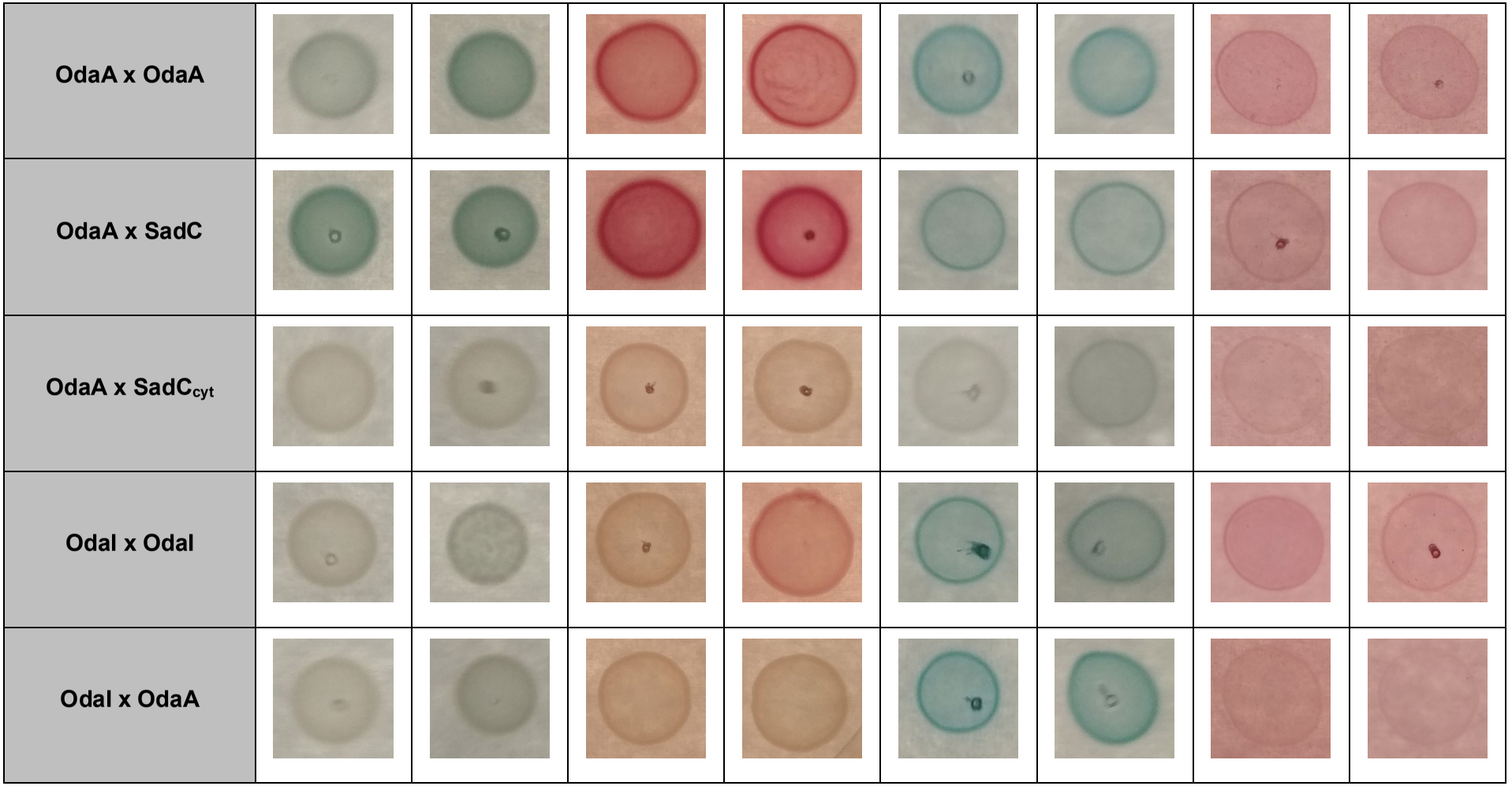

Figure 13 Representative examples of colonies grew at room temperature in the BACTH experiment.

Protein combination (pKNT25 x pUT18)	Growth conditions: 30 °C							
	$+O_2$				$-O_2$			
	LB		McConkey		LB		McConkey	
	+IPTG	-IPTG	+IPTG	-IPTG	+IPTG	-IPTG	+IPTG	-IPTG
SadC x SadC								
$SadC_{cyt}$ x $SadC_{cyt}$								
SadC x $SadC_{cyt}$								

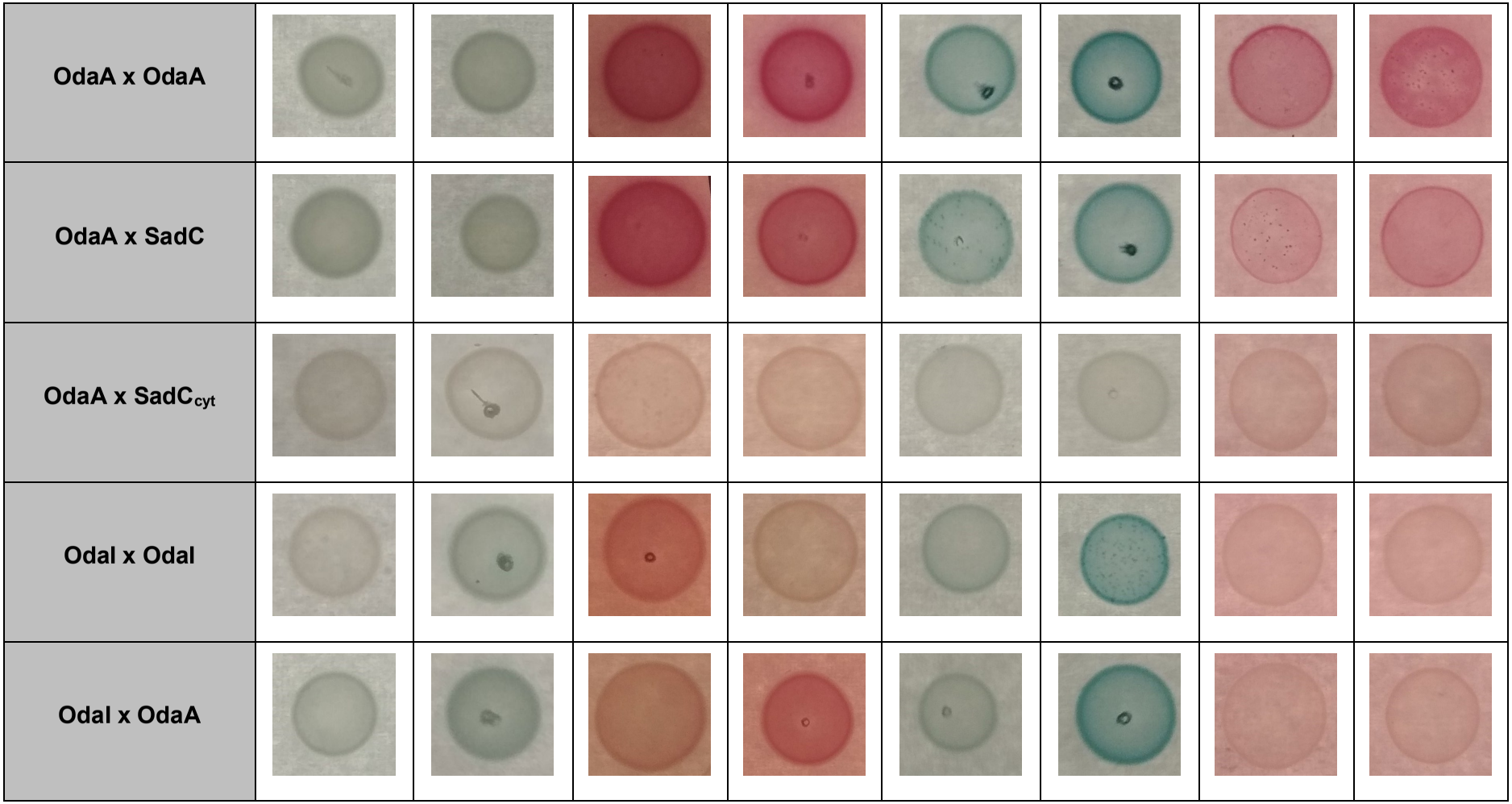

Figure 14 Representative examples of colonies grew at 30 °C in the BACTH experiment.

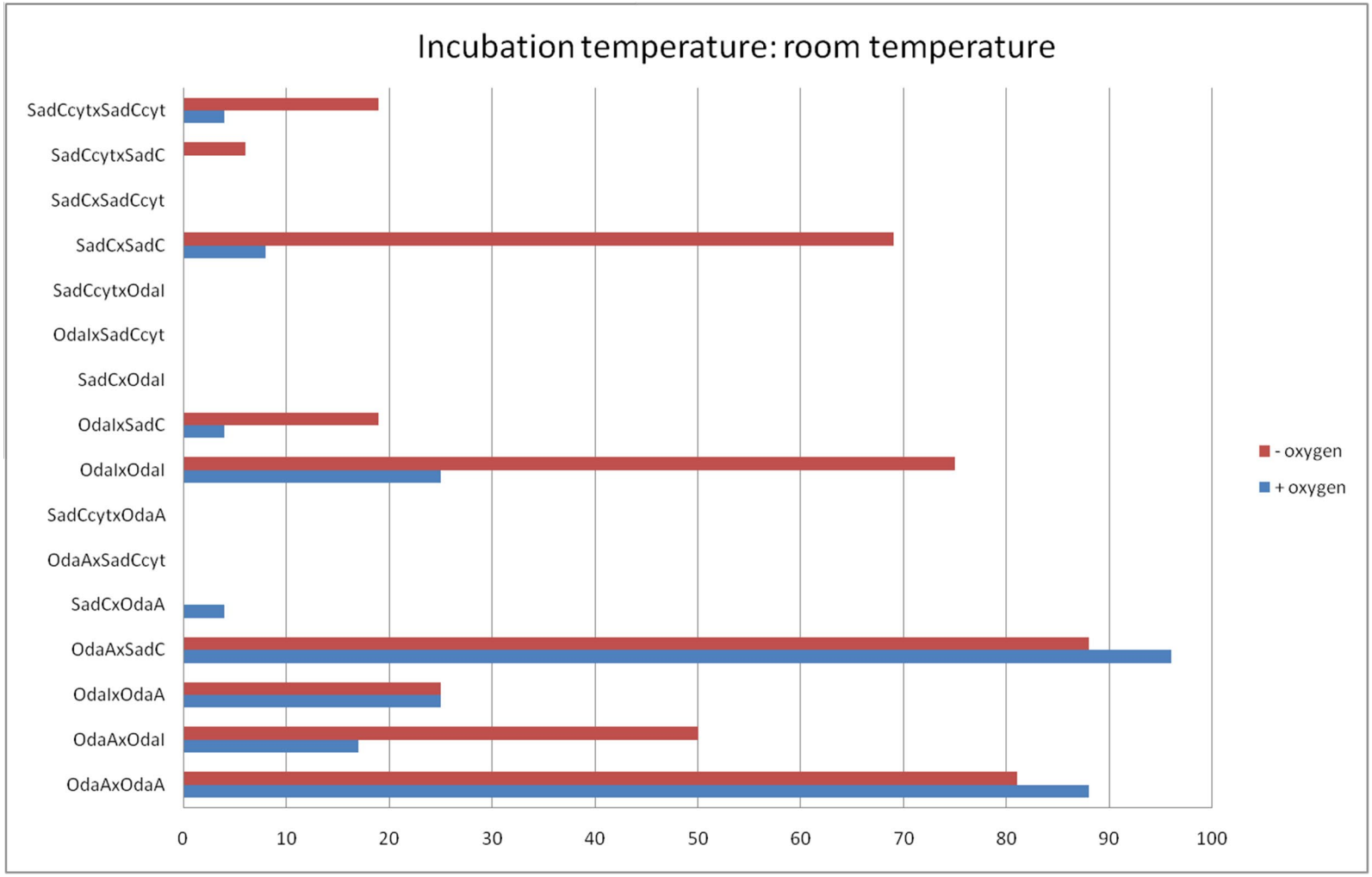

Figure 15 Results of the BACTH System experiment performed at room temperature in aerobic and anaerobic conditions. Descriptions on the *y*-axis refer to plasmids' combination - pKNT25 x pUT18 - carrying listed genes, and values on the *x*-axis refer to a percentage of the maximal possible score in the experiment. The presented results are averages from three independent experiments.

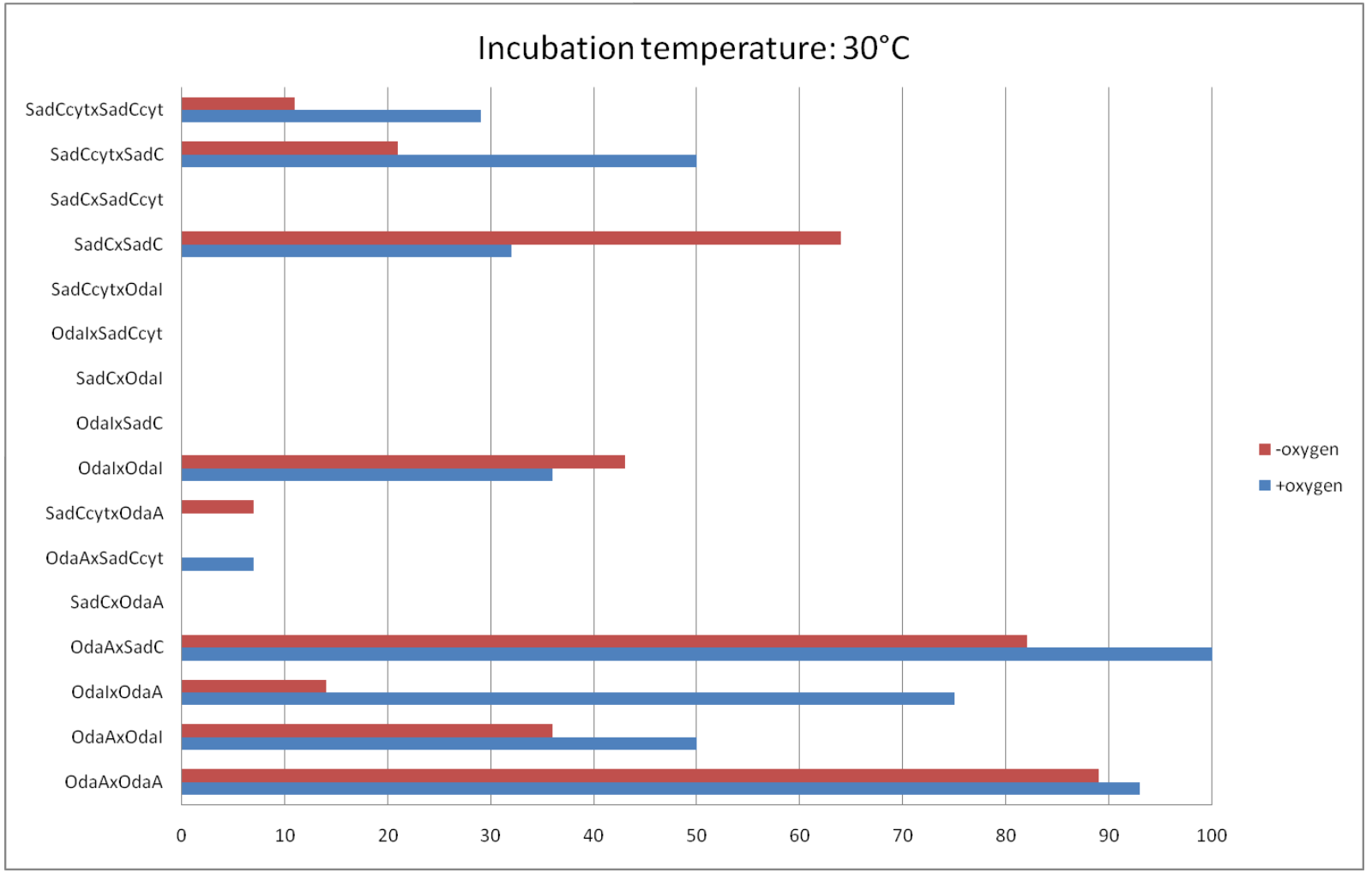

Figure 16 Results of the BACTH System experiment performed at 30°C in aerobic and anaerobic conditions. Descriptions on the *y*-axis refer to plasmids' combination - pKNT25 x pUT18 - carrying listed genes, and values on the *x*-axis refer to a percentage of the maximal possible score in the experiment. The presented results are averages from three independent experiments.

8.2 Analysis of cysteine residues in $SadC_{cyt}$

To deepen understanding of SadC's function in modulating alginate synthesis when *P. aeruginosa* is subjected to anaerobic environments, an examination of the potential role of four cysteine residues within the cytosolic part of SadC in oxygen detection was performed. Considering the prevailing knowledge that SadC does not possess any recognizable domains linked to oxygen sensing, these cysteine residues were identified as candidates for investigation. Oxidation of at least one of the cysteine residues could hypothetically result in, for example, conformational changes of SadC, resulting in altered activity, interaction with other proteins, or localization within a cell.

Cysteine residues can function as redox switches in response to the oxidative stress in the oxidative posttranslational modifications (Ox-PTM) of protein. Cysteine contains a thiol functional group (-SH), which is highly reactive and can be modified by reactive oxygen species. Under normal conditions, molecular oxygen (O_2) is not particularly reactive with cysteine residues. However, when molecular oxygen is partially reduced, it can give rise to various ROS, such as superoxide, hydrogen peroxide, or hydroxyl radicals. It is these ROS, rather than molecular oxygen itself, that are typically involved in the modification of cysteine residues (Chung et al., 2013).

Thiol functional group of cysteine (-SH) can be modified by S-nitrosylation (SNO), sulfhydration (SSH), S-glutathionylation (SSG), disulphide bonds formation (RS-SR), sulfenylation (SOH) and modification to sulfinic acid (SO_2H) and sulfonic acid (SO_3H). Formulation of specific modification depends on the reactivity of specific cysteine residue, its surrounding environment, and the current state of the local redox-environment. All reactions besides the formation of sulfonic acid can be reversed by antioxidant defense systems or converted to another Ox-PTM (Chung et al., 2013). Therefore, we substituted all cysteine residues to alanine in the cytosolic part of SadC (mutations: C390A; C420A and C421A; C748A) to verify its effect on the regulation of SadC function.

First set of expression constructs was prepared (pMCSG19::MBP-$SadC_{cyt\ C390A}$, pMCSG19::MBP-$SadC_{cyt\ C420A\ C421A}$ and pMCSG19::MBP-$SadC_{cyt\ C478A}$) and transformed into *E. coli* BL21. In all experiments, as a control, plasmid pMCSG19::MBP-$SadC_{cyt}$ harboring all native cysteine residues was used. Strains containing all listed plasmids were cultured under aerobic conditions, MBP-$SadC_{cyt}$ protein variants were purified by amylose affinity chromatography and size exclusion chromatography. The presence of protein variants in crude lysates (Figure 17), after amylose affinity chromatography and size exclusion chromatography was proved by Western blotting using a specific

antibody for MBP-SadC$_{cyt}$ as the primary antibody, followed by a secondary HRP-conjugated antibody. The samples were concentrated, and the buffer was exchanged to 50 mM Tris-HCl or 20 mM phosphate buffer using Amicon Ultra-15 50K centrifugal filter units. Next, obtained protein samples were tested in dimerization and GTP binding assays, which were performed under aerobic conditions. Each assay was performed using the same concentration of each protein variant, as described in detail in chapter 7.3.4.7 and chapter 7.3.4.8.

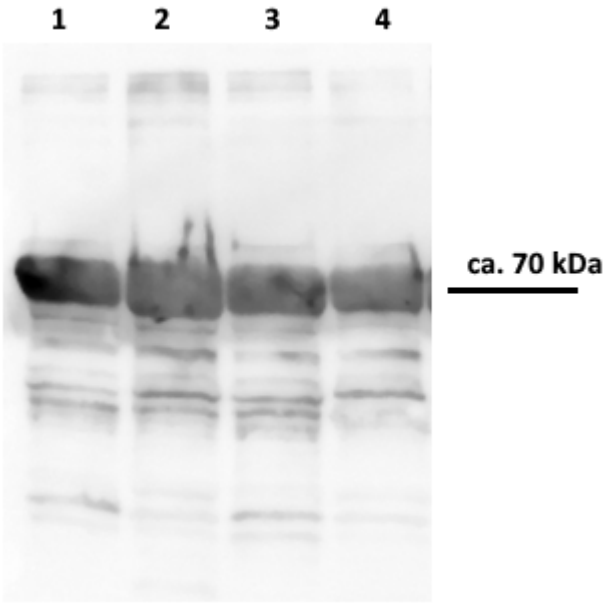

Figure 17 Western blot of crude lysates of cell pellet from *E. coli* carrying pMCSG19::MBP-His-PA4332$_{883-1464}$ mutants (approx. size of 70 kDa), in order: wild type (lane 1); C390A (lane 2); C420A C421A (lane 3); C478A (lane 4). To perform the Western blot, a specific antibody for MBP-SadCcyt was used as the primary antibody, followed by a secondary HRP-conjugated antibody.

8.2.1 MBP-SadC$_{cyt}$ cysteine mutants show different elution profiles in size exclusion chromatography

MBP-SadC$_{cyt}$ protein mutants, obtained in affinity chromatography, were subsequently purified in size exclusion chromatography. Collected fractions were analyzed using SDS PAGE and Western blotting to confirm the presence of MBP-SadC$_{cyt}$. The absorbance at 280 nm of eluent was monitored constantly. MBP-SadC$_{cyt}$ as well as its variants was detected in two peaks (with maximum absorbance value around 50 ml (peak 1) and 80 ml (peak 2) of a retention volume (Figure 18).

We hypothesize that those two peaks contain MBP-SadC$_{cyt}$ in two different conformations: dimeric (retention volume 50 ml) or monomeric (retention volume 80 ml). Wild type and mutants of cytosolic part of SadC: C390A and C478A showed elution profiles in which most of MBP-SadC$_{cyt}$ is eluted in peak 2 (respectively: 3.5; 3.71 and 2.61 times more). That may suggest that those mutants occur in a sample mainly in

a monomeric state. Interestingly, the mutant $SadC_{cyt\ C420A\ C421A}$ showed a different ratio between peaks. In that case, the protein was eluted from the column mostly in a peak 1, hypothetically as a dimer.

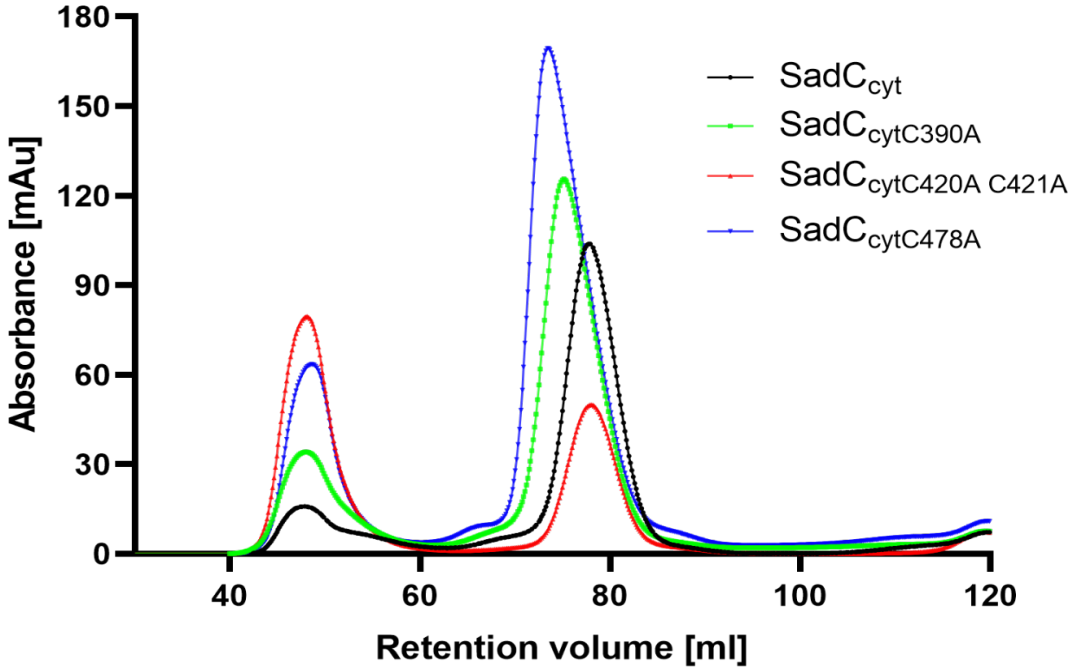

Figure 18 Elution profile of MBP-Sad_{cyt} and its mutants (C390A, C420A C421A, C478A) on a size exclusion chromatography. Proteins were expressed in *E. coli* BL21, cultivated under aerobic conditions, and purified by affinity chromatography using amylose resins. MBP-$SadC_{cyt}$ and its mutants were detected in two peaks: around 50 ml and 80 ml of retention volume. The absorbance was monitored at 280 nm.

8.2.2 Performed cysteine substitutions do not influence the ability of MBP-$SadC_{cyt}$ to self-interact

Despite the unresolved molecular structure of SadC, research on other DGCs indicates that dimerization is critical for their catalytic activation, as evidenced by prior research (Chan et al., 2004; Paul et al., 2007). Dimerization assay was used to investigate if prepared substitutions of cysteine to alanine influence the self-interaction of the cytosolic part of SadC fused to MBP. A cross-linking agent DSS crosslinks primary amine groups (-NH_2) of lysine was used.

It was observed that cysteine substitutions in cytosolic part of SadC do not influence the ability of MBP-$SadC_{cyt}$ to self-interact (Figure 18). The Western blot analysis conducted on samples from the dimerization assay showed additional bands with higher molecular weights when $SadC_{cyt}$ variants (wild type, C390A, C420A, C421A, and C478A) were treated with DSS as compared to their respective untreated controls. This indicates that the ability to self-interact is retained across all tested variants, akin

to the wild type. This result implies that MBP-SadC$_{cyt}$ and its protein variants are hypothetically capable of dimerization, which aligns with the known behavior of diguanylate cyclases (DGCs) that require dimerization for catalytic activation. Therefore, it can be inferred that replacing cysteine with alanine does not impede SadC$_{cyt}$'s self-interaction and in consequence hypothetical dimerization when it is expressed and processed in the presence of oxygen.

This experiment showed that SadC$_{cyt}$ variants are able to self-interact. It goes along with the data from the elution profile from size exclusion chromatography where each variant was eluted in two peaks, which hypothetically represented monomeric and dimeric state of SadC$_{cyt}$. The presence of the peak representing the dimeric state of SadC$_{cyt}$ confirms results from the dimerization experiment that each variant of SadC can self-interact (Figure 19).

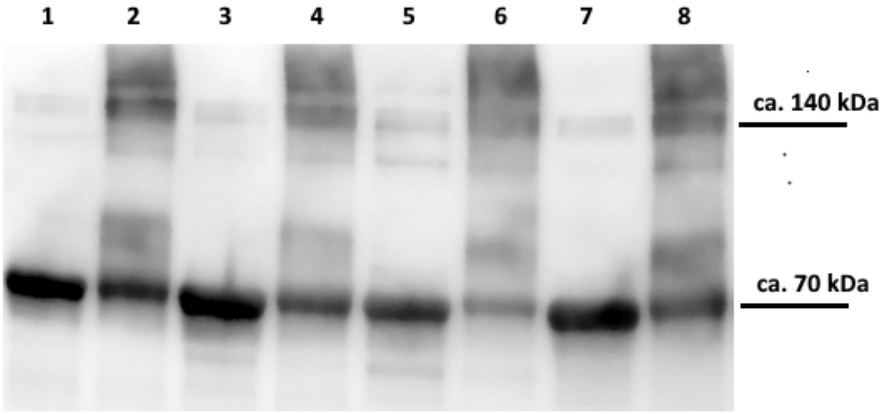

Figure 19 Western blot of dimerization assay using purified MBP-SadC$_{cyt}$ variants (approx. size of 70 kDa), in order: wild type (lanes 1,2); C390A (lanes 3,4); C420A C421A (lanes 5,6); C478A (lanes 7,8). Samples were incubated without (lanes 1,3,5,7) or with an addition of a cross-linker DSS (lanes 2,4,6,8). Western blot was performed using a specific antibody for MBP-SadC$_{cyt}$ and a secondary HRP-conjugated antibody.

8.2.3 MANT-GTP binding by MBP-SadC$_{cyt}$ differs for cysteine mutants

To assess whether cysteine substitution affects the active center of SadC and hypothetically its enzymatic activity, an experiment utilizing MANT-GTP was conducted. MANT-GTP serves as a GTP analogue, a substrate for SadC, enabling the validation of substrate binding to the active centre of SadC. The binding of MANT-GTP is designed to be reversible; thus, introducing GTP into the reaction should reduce the fluorescence signal. This reduction occurs due to the competition between MANT-GTP and GTP, further confirming the original functionality of SadC's active centre. MANT-GTP, when bound to the active centre of DGCs, including SadC, is characterized by an increased

fluorescence emission peaking at 450 nm when excited at 350 nm. This increase in fluorescence is a result of the enhanced hydrophobic environment created upon binding to the enzyme's active site. Additionally, this method allows for the measurement of the binding capacity of the protein, as the fluorescence of MANT-GTP can be quantified and compared, providing a reliable indicator of substrate interaction (Schmidt, 2015; Spangler et al., 2011).

We checked if cysteine substitutions in MBP-$SadC_{cyt}$ alter MANT-GTP's binding and its competition for binding with GTP in comparison to the native MBP-$SadC_{cyt}$. In all the cases, MANT-GTP's binding to SadC was reversible and could be decreased by the addition of GTP. All cysteine substitutions in SadC caused an alteration of the fluorescence signal of tested samples at 450 nm (Figure 21, Figure 22 and Figure 23) in comparison to WT (Figure 20). While exposed to MANT-GTP, mutants $SadC_{cyt\ C390A}$ and $SadC_{cyt\ C478A}$ displayed enhanced fluorescence emission at 450 nm compared to $SadC_{cyt}$ by respectively 49,5% and 63.9% which suggests increased binding of MANT-GTP to the active centre of SadC. In the case of mutant $SadC_{cyt\ C420A\ C421A}$ signal in comparison to WT was lower by 41,2%, which can be caused by the lower binding capacity of MANT-GTP. The performed experiment showed that the binding of GTP to SadC and its variants remained reversible in all tested protein mutants and that the cysteine residues in $SadC_{cyt}$ can alter the binding efficiency of GTP and therefore influence the enzymatic activity of c-di-GMP synthesis, which can hypothetically impact alginate synthesis. This could be caused e. g. by conformational changes due to cysteine mutation. Furthermore, the ability of SadC variants to bind MANT-GTP reversibly demonstrates that they can form dimers, thereby creating an active center capable of binding its substrate. This aligns with the results from the dimerization assay, which showed that each tested SadC variant was able to dimerize.

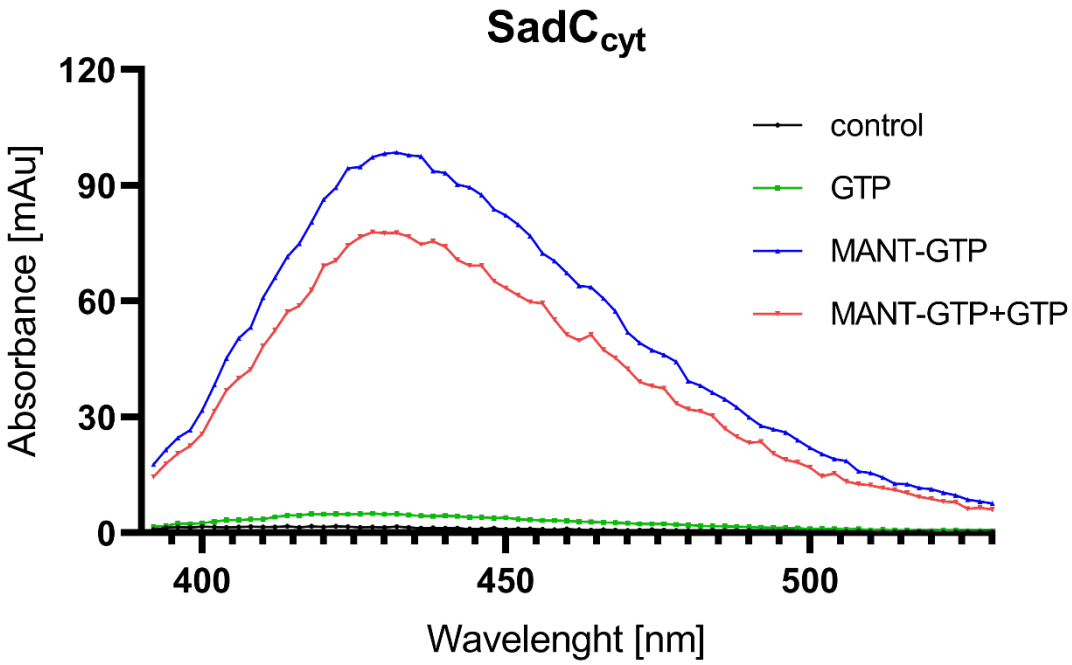

Figure 20 Analysis of GTP and MANT-GTP binding efficiency to MBP-SadC$_{cyt}$. The fluorescence was measured using an emission and excitation wavelength of 350 nm and 380 to 540 nm, respectively. Samples contained: control –protein sample in a buffer; GTP –protein sample and GTP in a buffer; MANT-GTP - protein sample and MANT-GTP in a buffer; MANT-GTP + GTP protein sample, MANT-GTP, and GTP in a buffer. The presented results are averages from three independent experiments.

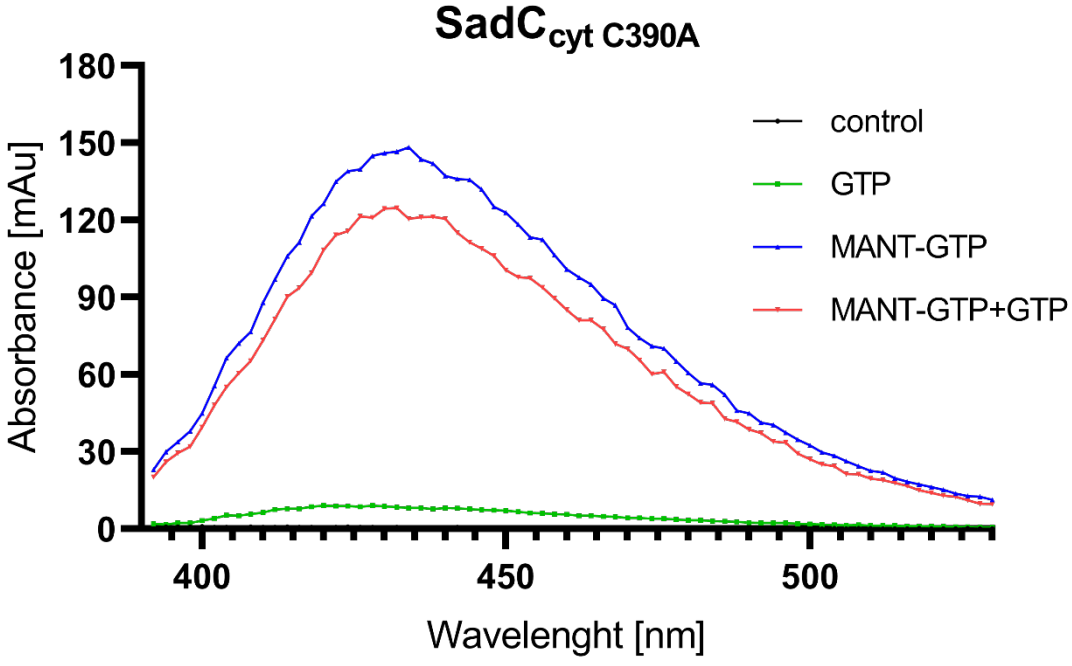

Figure 21 Analysis of GTP and MANT-GTP binding efficiency to MBP-SadC$_{cyt\ C390A}$. The fluorescence was measured using an emission and excitation wavelength of 350 nm and 380 to 540 nm, respectively. Samples contained: control –protein sample in a buffer; GTP –protein sample and GTP in a buffer; MANT-GTP - protein sample and MANT-GTP in a buffer; MANT-GTP + GTP protein sample, MANT-GTP, and GTP in a buffer. The presented results are averages from three independent experiments.

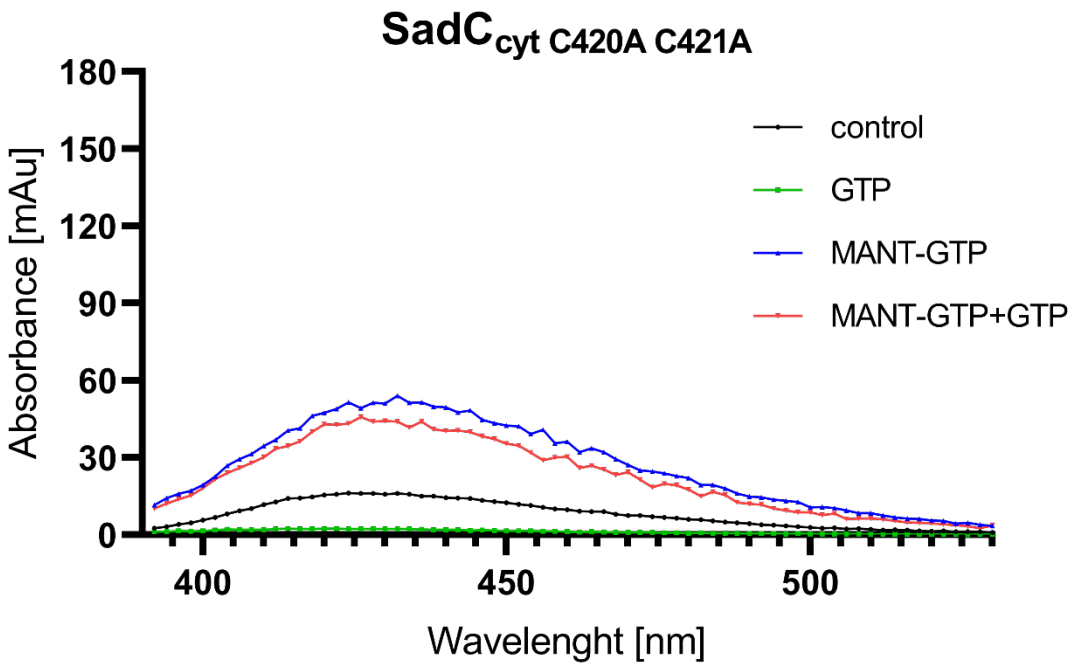

Figure 22 Analysis of GTP and MANT-GTP binding efficiency to MBP-SadC$_{cyt\ C420A\ C421A}$. The fluorescence was measured using an emission and excitation wavelength of 350 nm and 380 to 540 nm, respectively. Samples contained: control –protein sample in a buffer; GTP –protein sample and GTP in a buffer; MANT-GTP - protein sample and MANT-GTP in a buffer; MANT-GTP + GTP protein sample, MANT-GTP, and GTP in a buffer. The presented results are averages from three independent experiments.

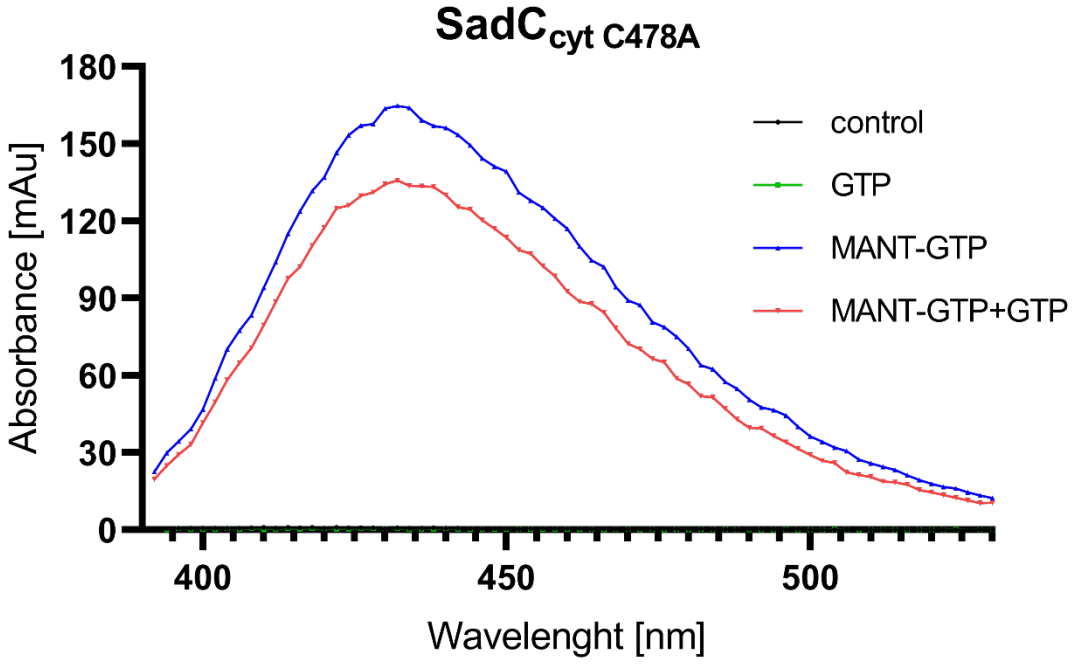

Figure 23 Analysis of GTP and MANT-GTP binding efficiency to MBP-SadC$_{cyt\ C478A}$. The fluorescence was measured using an emission and excitation wavelength of 350 nm and 380 to 540 nm, respectively. Samples contained: control –protein sample in a buffer; GTP –protein sample and GTP in a buffer; MANT-GTP - protein sample and MANT-GTP in a buffer; MANT-GTP + GTP protein sample, MANT-GTP, and GTP in a buffer. The presented results are averages from three independent experiments.

8.3 mRNA sequencing of *P. aeruginosa* WT and Δ*sadC* grown under aerobic and anaerobic conditions

It has been demonstrated that SadC is essential for increased alginate synthesis when *P. aeruginosa* is exposed to anaerobic conditions. The MBP-SadC$_{cyt}$ fusion protein, expressed and purified from *E. coli* under anaerobic conditions, exhibits significantly higher activity compared to that purified from cultures grown in the presence of oxygen. Notably, the alginate synthesis undergoes a noticeable increase after already 60 minutes of exposure to anaerobic conditions, indicating that this duration allows *P. aeruginosa* to adapt to anaerobic conditions (Schmidt, 2015; Schmidt et al., 2016). One plausible explanation for this phenomenon is c-di-GMP-dependent activation of alginate synthesis for example by activating Alg44. Since the regulation of alginate synthesis is complex and transcriptional regulation cannot be ruled out and the global effect of SadC is not known, transcriptome analysis was performed. To delve deeper into this phenomenon, the mRNA sequencing experiment was conducted to investigate the impact of SadC on gene expression levels under aerobic and anaerobic conditions.

To carry out this experiment, both *P. aeruginosa* PAO1 – WT and Δ*sadC* strains were cultured in a fermentor under planktonic conditions containing nitrate as an electron acceptor during anaerobic growth. The same cultures were grown under both aerobic and anaerobic conditions. Initially, the cells were cultivated in aerobic conditions until they reached an OD_{600} of 1.0±0.2. At this point, a sample for mRNA sequencing was collected into DNA/RNA Shield™, and nitrogen flushing was performed to create anaerobic conditions within minutes. After 2 hours of anaerobic incubation, aliquots of the cultures were again aseptically collected into DNA/RNA Shield™.

It's important to note that the data presented here are based on a single biological replicate, and therefore, statistical significance tests were not conducted due to the limited sample size. When working with only one sample per condition per strain, the statistical power to detect differences in gene expression is reduced, making it more challenging to confidently identify genes that exhibit significant differences in expression between conditions. After obtaining the raw sequencing data, the results were normalized based on TPM (transcripts per million). The results were subjected to pairwise comparisons across the tested conditions (Figure 24). Additionally, Table 29-34 present the twenty most upregulated genes in pairwise comparisons between the experimental setups.

Figure 25 provides an enriched pathway analysis comparing *P. aeruginosa* PAO1 (WT) to Δ*sadC*, both cultured under anaerobic conditions. Genes exhibiting at least

a two-fold enrichment were considered for the analysis of enriched pathways. GO enrichment analysis was conducted to identify significantly overrepresented pathways. Table 33 displays the fold change of genes involved in the synthesis and regulation of alginate synthesis.

8.3.1 Deletion of SadC has an impact on gene expression levels in both aerobic and anaerobic conditions

Obtained data were analyzed using pairwise comparisons, a methodological approach that allows for the direct examination of the differential expression between two conditions or states (Figure 24). This technique offers the advantage of isolating the specific effects of a single variable - in this case, the presence or absence of SadC – by comparing gene expression levels between the wild-type (WT) and SadC deletion mutant (Δ*sadC*) strains of *P. aeruginosa*. Such comparisons are invaluable in elucidating the influence of specific genetic alterations on the organism's overall regulatory mechanisms. The focus was placed on genes with a fold change in expression greater than 2 or less than 0.5, focusing specifically on the most significantly impacted genes and disregarding those with subtle or negligible expression changes.

Under aerobic conditions, the analysis revealed several differences in gene expression profiles between the WT and Δ*sadC* strains. Some genes for example showed sixfold higher expression in the WT. Moreover, the transition to anaerobic conditions showed an even higher effect of SadC on gene regulation. The Δ*sadC* mutant showed considerable changes in gene expression, with alarge number of genes exhibiting fold changes beyond the established thresholds. This contrasted with the more stable expression profile observed in the WT strain under the same conditions.

The stark differences in gene expression between the Δ*sadC* mutant and WT strain, particularly in the absence of oxygen, underline the importance of SadC in response of *P. aeruginosa* to anaerobic stress. While the WT maintains gene expression profile more stable, the Δ*sadC* mutant displays a disrupted profile, indicating that SadC plays a significant role in regulating a vast array of genes critical for survival and adaptation to anaerobic environments.

The results, drawn from a single biological replicate, suggest that SadC may act as a key regulatory element in the adaptation to oxygen-limited conditions. To confirm these findings and fully understand the regulatory scope of SadC, further investigations with more biological replicates and robust statistical analyses are required.

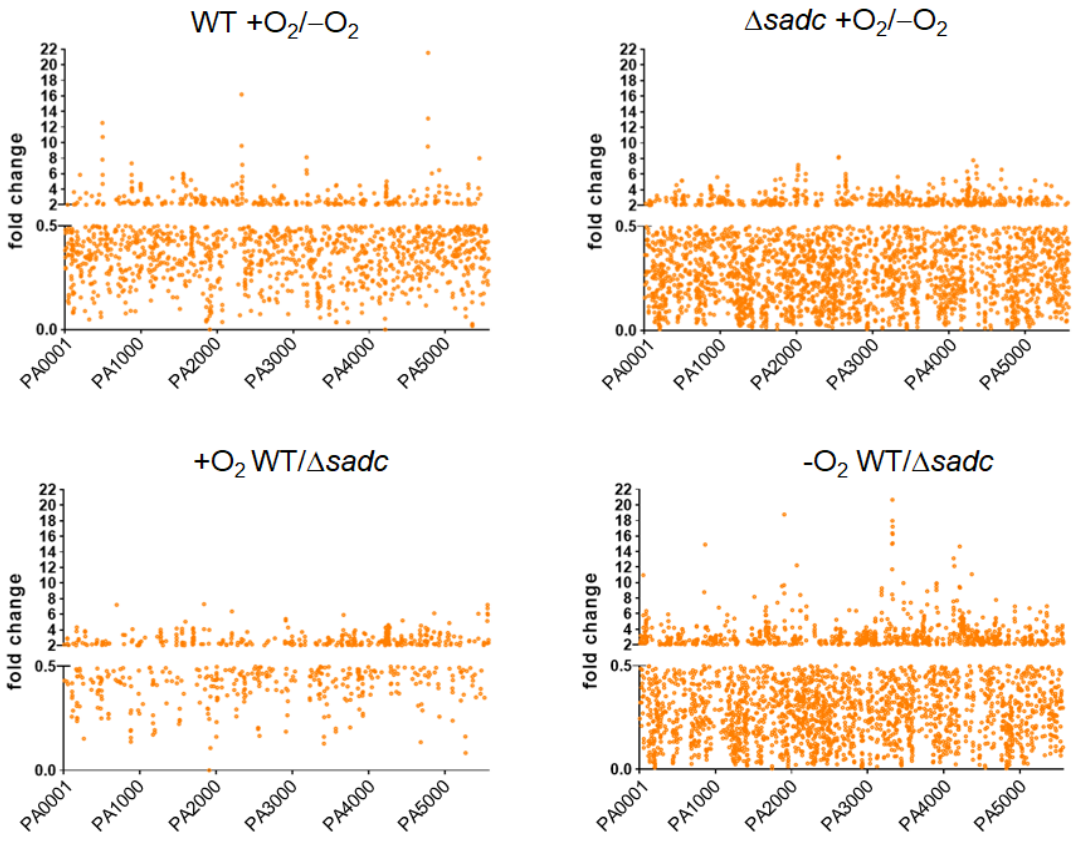

Figure 24 Impact of SadC deletion on gene expression in *P. aeruginosa* under aerobic and anaerobic conditions. This figure illustrates the fold change in gene expression of *P. aeruginosa* PAO1 wild-type (WT) and the SadC deletion mutant (Δ*sadC*) when subjected to both aerobic and anaerobic conditions. The y-axis represents the fold change in gene expression, focusing on those genes with changes greater than two-fold. Each point on the graph corresponds to a single gene, with its position reflecting the magnitude of expression change relative to the baseline condition. The data were derived from a single biological replicate, highlighting the preliminary nature of the results. The four panels represent different comparisons: the top left panel shows the WT response to oxygen availability, the top right panel the Δ*sadC* response to oxygen availability, the bottom left panel the comparison of WT and Δ*sadC* in the presence of oxygen, and the bottom right panel the comparison of WT and Δ*sadC* in the absence of oxygen. This figure serves as a visual representation of the gene expression modulation that occurs following the deletion of SadC and under different respiratory conditions.

8.3.2 The most upregulated genes in *P. aeruginosa* WT and Δ*sadC* when cultured under aerobic and anaerobic conditions

The following chapter aims to spotlight the genes that are most upregulated in *P. aeruginosa* WT and Δ*sadC* cultured in the presence and absence of oxygen and compared pairwise. The intent is to present and list the genes that exhibit the highest levels of upregulation across four setups: the Δ*sadC* mutant and WT in both aerobic and anaerobic conditions, and direct comparisons of the wild type and Δ*sadC* mutant in each oxygen environment. By presenting the genes with the greatest expression increases, it is possible to identify which genes are most responsive to the loss of SadC and the shift

in oxygen conditions. The following tables (Table 29-32) provide the fold changes and gene identities, serving as a reference for the most affected genes in the bacterial genome under the experimental conditions described.

Table 29 presents the top genes that are upregulated in the *P. aeruginosa* Δ*sadC* strain under anaerobic and aerobic conditions. The genes with the most significant increase under anaerobic conditions include a probable binding protein component of ABC transporter (PA0203) with a fold change of 0.006, a histidine transport protein HisP (PA2926) with a fold change of 0.008, and a ferric enterobactin transport protein FepD (PA4160) with a fold change of 0.008. Under aerobic conditions, notable upregulations include a probable AMP-binding enzyme (PA2555) with a fold change of 8.189, and a probable short-chain dehydrogenase (PA2554) with a fold change of 8.100.

The most upregulated genes in the wild type strain of *P. aeruginosa* under anaerobic and aerobic conditions are presented in Table 30. Under anaerobic conditions, there is upregulation in genes such as those involved in glycolate metabolism, with glycolate oxidase subunit GlcE (PA5353) showing a fold change of 0.017 and GlcF (PA5354) showing a fold change of 0.022. Under aerobic conditions, there is a significant increase in genes related to iron transport and metabolism, such as the probable ferredoxin (PA4772) with a fold change of 21.523. Genes involved in the central metabolic pathways, like gluconate permease GntP (PA3272) with a fold change of 16.188, and several cytochrome c oxidase subunits, are also notably upregulated, indicating active aerobic respiration.

In anaerobic conditions, significant gene upregulation is observed when comparing wild type to Δ*sadC* strains of *P. aeruginosa*, as detailed in Table 31. Notably, in the Δ*sadC* strain, genes like *hcpB* and *nrdD* exhibit increased expression levels. The *hcpE* gene encodes a secreted protein, while *nudD* is a class III (anaerobic) ribonucleoside-triphosphate reductase subunit. These genes show fold changes of approximately 0.083 and 0.107, respectively, indicating a moderate increase in expression. Conversely, in the wild-type strain, there is a pronounced upregulation of the *sadC* gene itself, with a fold change of approximately 107.071. This upregulation serves as evidence of a successful deletion of the sadC gene. Additionally, other genes such as *exbD2*, implicated in transport, and various subunits of ATP synthase, crucial for energy metabolism under anaerobic conditions, exhibit significant upregulation with fold changes of approximately 7.302.

Table 32 presents a list of the twenty most upregulated genes in *P. aeruginosa* WT compered to Δ*sadC* under anaerobic conditions. In the Δ*sadC* strain, genes such as PA4549, encoding a type 4 fimbrial biogenesis protein, and PA2924, a histidine transport system permease, are among those with increased expression levels, with fold

changes of 0.009 and 0.010, respectively. For the wild type, the gene *sadC* (PA4332) itself shows a high fold change of 116.210, indicating successful deletion of this gene in the Δ*sadC* strain. Other genes with significant upregulation include *lasB* (PA3724), a gene encoding elastase, and *acpP* (PA1869), a probable acyl carrier protein, with fold changes of 39.196 and 23.426, respectively.

Table 29 Differential gene expression in *P. aeruginosa* Δ*sadC* mutant under anaerobic and aerobic conditions. The table lists the top twenty upregulated genes under each condition, with their corresponding gene ID, gene name, product description, and fold change (FC). The fold change represents the ratio of gene expression under aerobic conditions to that under anaerobic conditions, highlighting the genes most responsive to oxygen levels in the Δ*sadC* background. [a] – data source: https://www.pseudomonas.com.

Gene ID	Gene name	Product description[a]	FC (O_2/N_2)
Upregulated under anaerobic conditions			
PA0203	-	probable binding protein component of ABC transporter (P)	0.006
PA0202	-	probable amidase	0.007
PA2926	*hisP*	histidine transport protein HisP (CM)	0.008
PA4160	*fepD*	ferric enterobactin transport protein FepD (CM)	0.008
PA1743	-	hypothetical	0.008
PA2923	*hisJ*	periplasmic histidine-binding protein HisJ (P)	0.008
PA3446	-	hypothetical	0.009
PA4549	*fimT*	type 4 fimbrial biogenesis protein FimT (P)	0.009
PA4823	-	hypothetical	0.010
PA3445	-	hypothetical	0.011
PA3126	*ibpA*	heat-shock protein IbpA	0.011
PA4471	-	hypothetical	0.011
PA4832	-	probable short-chain dehydrogenase	0.013
PA3449	-	hypothetical	0.013
PA3448	-	probable permease of ABC transporter (CM)	0.013
PA3125	-	putative transferase	0.014
PA2472	-	probable major facilitator superfamily (MFS) transporter (CM)	0.014
PA2933	-	probable major facilitator superfamily (MFS) transporter (CM)	0.014
PA2924	*hisQ*	histidine transport system permease HisQ (CM)	0.014
PA1599	-	probable transcriptional regulator	0.015
Upregulated under aerobic conditions			
PA2555	-	probable AMP-binding enzyme	8.189
PA2554	-	probable short-chain dehydrogenase	8.100
PA4315	*mvaT*	transcriptional regulator MvaT, P16 subunit	7.775
PA2016	*liuR*	regulator of *liu* genes	7.177
PA4359	-	hypothetical	7.019
PA2015	*liuA*	putative isovaleryl-CoA dehydrogenase	6.840
PA4687	*hitA*	ferric iron-binding periplasmic protein HitA (E)	6.569
PA2014	*liuB*	methylcrotonyl-CoA carboxylase, beta-subunit	6.560
PA4237	*rplQ*	50S ribosomal protein L17	6.328
PA4357	-	hypothetical	6.109
PA2646	*nuoK*	NADH dehydrogenase I chain K (CM)	6.044
PA2116	-	hypothetical (C)	6.025
PA2013	*liuC*	putative 3-methylglutaconyl-CoA hydratase (C)	5.874
PA2644	*nuoI*	NADH Dehydrogenase I chain I (C)	5.644
PA3331	-	cytochrome P450 (C)	5.635
PA0958	*oprD*	basic amino acid, basic peptide and imipenem outer membrane porin OprD precursor (O)	5.617
PA4252	*rplX*	50S ribosomal protein L24	5.477
PA4366	*sodB*	superoxide dismutase (P)	5.443
PA3919	-	hypothetical (C)	5.422
PA1787	*acnB*	aconitate hydratase 2 (C)	5.419

Table 30 Differential gene expression in *P. aeruginosa* wild type mutant under anaerobic and aerobic conditions. The table lists the top twenty upregulated genes under each condition, with their corresponding gene ID, gene name, product description, and fold change (FC). The fold change represents the ratio of gene expression under aerobic conditions to that under anaerobic conditions, highlighting the genes most responsive to oxygen levels in the wild-type background. [a] – data source: https://www.pseudomonas.com.

Gene ID	Gene name	Product description[a]	FC (O_2/N_2)
Upregulated under anaerobic conditions			
PA5353	*gclF*	glycolate oxidase subunit GlcF (CM)	0.017
PA5354	*gclE*	glycolate oxidase subunit GlcE	0.022
PA5352	-	hypothetical	0.022
PA5355	*gclD*	glycolate oxidase subunit GlcD (C)	0.028
PA3570	*mmsA*	methylmalonate-semialdehyde dehydrogenase (C)	0.035
PA3724	*lasB*	elastase (E)	0.035
PA3569	*mmsB*	3-hydroxyisobutyrate dehydrogenase (C)	0.036
PA2069	-	probable carbamoyltransferase (C)	0.036
PA1856	-	probable cytochrome oxidase subunit (CM)	0.038
PA1855	-	hypothetical	0.046
PA1869	*acp1*	probable acyl carrier protein (CM)	0.049
PA0320	*carO*	calcium-regulated OB-fold protein CarO	0.049
PA4210	*phzA1*	probable phenazine biosynthesis protein (C)	0.052
PA3361	*lecB*	fucose-binding lectin PA-IIL	0.058
PA0472	*fiuI*	FiuI (C)	0.061
PA5267	*hcpB*	secreted protein Hcp (E)	0.063
PA1899	*phzA2*	probable phenazine biosynthesis protein (C)	0.066
PA2300	*chiC*	chitinase (E)	0.069
PA3479	*rhlA*	rhamnosyltransferase chain A (C)	0.072
PA2570	*lecA*	PA-I galactophilic lectin	0.075
Upregulated under aerobic conditions			
PA4772	-	probable ferredoxin (C)	21.523
PA2322	*gntP*	gluconate permease (CM)	16.188
PA4771	*lldD*	L-lactate dehydrogenase (C)	13.107
PA0493	-	probable biotin-requiring enzyme	12.519
PA0494	-	probable acyl-CoA carboxylase subunit (C)	10.732
PA2321	*gntK*	gluconate kinase	9.573
PA4770	*lldP*	L-lactate permease (CM)	9.483
PA3182	*pgl*	6-phosphogluconolactonase	8.110
PA5446	-	hypothetical	7.997
PA0492	-	hypothetical (C)	7.802
PA0878	-	hypothetical (C)	7.319
PA2331	-	hypothetical	7.140
PA4918	*pcnA*	nicotinamidase (C)	6.469
PA3181	-	2-keto-3-deoxy-6-phosphogluconate aldolase (C)	6.466
PA4823	-	hypothetical	6.044
PA1555	*ccop2*	cytochrome c oxidase, cbb3-type, CcoP subunit	6.017
PA3183	*zwf*	glucose-6-phosphate 1-dehydrogenase (C)	6.004
PA1556	*ccoO2*	cytochrome c oxidase, cbb3-type, CcoO subunit (C)	5.891
PA0200	-	hypothetical	5.872
PA0496	-	hypothetical (C)	5.871

Table 31 Differential gene expression in *P. aeruginosa* wild-type and Δ*sadC* mutant under aerobic conditions. This table delineates the twenty most upregulated genes for the wild type and Δ*sadC* mutant, respectively, detailing their gene ID, gene name, and product description. Fold change (FC) is calculated as the ratio of expression in the wild type to the Δ*sadC* mutant. [a] – data source: https://www.pseudomonas.com.

Gene ID	Gene name	Product description[a]	FC (WT/□)
Upregulated in ΔsadC			
PA5267	*hcpB*	secreted protein Hcp (E)	0.083
PA1920	*nrdD*	class III (anaerobic) ribonucleoside-triphosphate reductase subunit, NrdD (C)	0.107
PA3415	-	probable dihydrolipoamide acetyltransferase (C)	0.129
PA4683	-	hypothetical	0.136
PA0881	-	hypothetical (C)	0.138
PA0263	*hcpC*	secreted protein Hcp (E)	0.153
PA0880	-	probable ring-cleaving dioxygenase (C)	0.157
PA1999	*dhcA*	dehydrocarnitine CoA transferase, subunit A (C)	0.161
PA3416	-	probable pyruvate dehydrogenase E1 component, beta chain	0.162
PA5266	*vgrG6*	VgrG6	0.163
PA2570	*lecA*	PA-I galactophilic lectin	0.166
PA1173	*napB*	cytochrome c-type protein NapB precursor (P)	0.171
PA1195	*ddaH*	dimethylarginine dimethylaminohydrolaseDdaH (C)	0.182
PA3570	*mmsA*	methylmalonate-semialdehyde dehydrogenase (C)	0.186
PA2916	-	hypothetical (CM)	0.186
PA0879	-	probable acyl-CoA dehydrogenase (C)	0.190
PA1194	-	probable amino acid permease (CM)	0.194
PA0882	-	hypothetical (C)	0.194
PA2553	-	probable acyl-CoA thiolase (C)	0.198
PA3569	*mmsB*	3-hydroxyisobutyrate dehydrogenase	0.201
Upregulated in the wild type			
[PA4332	*sadC*	SadC (CM)	107.071]
PA1837	-	hypothetical (C)	7.302
PA0694	*exbD2*	transport protein ExbD (CM)	7.220
PA5557	*atpH*	ATP synthase delta chain (C)	7.205
PA5558	*atpF*	ATP synthase B chain (CM)	6.749
PA2203	-	probable amino acid permease (CM)	6.358
PA4855	*purD*	phosphoribosylamine--glycine ligase (C)	6.137
PA5556	*atpA*	ATP synthase alpha chain (C)	6.088
PA5435	-	probable transcarboxylase subunit (C)	6.083
PA5559	*atpE*	ATP synthase C chain (CM)	5.963
PA3670	-	hypothetical (CM)	5.915
PA2912	-	probable ATP-binding component of ABC transporter (CM)	5.402
PA2913	-	hypothetical	5.202
PA4442	*cysN*	ATP sulfurylase GTP-binding subunit/APS kinase (C)	5.195
PA5555	*atpG*	ATP synthase gamma chain	5.142
PA1596	*htpG*	heat shock protein HtpG (C)	5.051
PA5054	*hslU*	heat shock protein HslU (C)	4.879
PA4259	*rpsS*	30S ribosomal protein S19 (C)	4.641
PA4686	-	hypothetical (C)	4.546
PA4258	*rplV*	50S ribosomal protein L22 (C)	4.461
PA4226	*pchE*	dihydroaeruginoic acid synthetase	4.328

Table 32 Differential gene expression in P. aeruginosa wild-type and ΔsadC mutant under anaerobic conditions. This table delineates the twenty most upregulated genes for the wild type and ΔsadC mutant, respectively, detailing their gene ID, gene name, and product description. Fold change (FC) is calculated as the ratio of expression in the wild type to the ΔsadC mutant. [a] – data source: https://www.pseudomonas.com.

Gene ID	Gene name	Product description [a]	FC (WT/□)
Upregulated in ΔsadC			
PA1743	-	hypothetical	0.004
PA4823	-	hypothetical	0.005
PA0202	-	probable amidase (C)	0.008
PA4549	*fimT*	type 4 fimbrialbiogenesisproteinFimT (CM)	0.009
PA0203	-	probable binding protein component of ABC transporter (P)	0.010
PA2924	*hisQ*	histidine transport system permease HisQ (CM)	0.010
PA4832	-	probable short-chain dehydrogenase (C)	0.011
PA2926	*hisP*	histidine transport protein HisP (CM)	0.012
PA2932	*morB*	morphinone reductase (C)	0.012
PA3125	-	putative transferase	0.012
PA1952	*fapE*	FapE (E)	0.013
PA0204	-	probable permease of ABC transporter (CM)	0.013
PA1744	-	hypothetical (CM)	0.015
PA2923	*hisJ*	periplasmic histidine-binding protein HisJ (P)	0.017
PA2922	-	probable hydrolase (C)	0.018
PA1419	-	probable transporter (CM)	0.018
PA4542	*clpB*	ClpB protein (C)	0.018
PA3449	-	hypothetical	0.019
PA2933	-	probable major facilitator superfamily (MFS) transporter (CM)	0.019
PA1417	-	probable decarboxylase (C)	0.020
Upregulated in the wild type			
[PA4332	*sadC*	SadC (CM)	116.210]
PA3724	*lasB*	elastase (E)	39.190
PA1869	*acp1*	probable acyl carrier protein (C)	23.426
PA3331	-	cytochrome P450 (CM)	20.656
PA1900	*phzB2*	probable phenazine biosynthesis protein (C)	18.778
PA3329	-	hypothetical (C)	17.961
PA3334	*acp3*	probable acyl carrier protein	17.220
PA3330	-	probable short chain dehydrogenase (C)	16.357
PA3333	*fabH2*	3-oxoacyl-[acyl-carrier-protein] synthase III (C)	16.236
PA3332	-	hypothetical (C)	15.081
PA3328	-	probable FAD-dependent monooxygenase	14.989
PA0865	*hpd*	4-hydroxyphenylpyruvate dioxygenase (C)	14.910
PA4211	*phzB1*	probable phenazine biosynthesis protein (C)	14.666
PA4133	-	cytochrome c oxidase subunit (cbb3-type) (C)	13.131
PA2069		probable carbamoyl transferase (C)	12.240
PA4141	-	hypothetical	12.147
PA3327	-	probable non-ribosomal peptide synthetase (C)	11.724
PA4370	*icmP*	insulin-cleaving metalloproteinase outer membrane protein precursor (OM)	11.078
PA0049	-	hypothetical	10.972
PA3472	-	hypothetical	9.931
PA3907	*tseT*	TOX-REase-5 domain-containing effector, TseT	9.924

8.3.3 Deletion of SadC influences expression profile of biosynthetic pathways and proteins exported by type III secretion system under anaerobic conditions

To elucidate the regulatory role of SadC under anaerobic conditions in *P. aeruginosa*, a Gene Ontology (GO) enrichment analysis was performed (Figure 25), contrasting the PAO1 wild-type with Δ*sadC* mutant cultured under anaerobic conditions. This endeavor aimed to shed light on SadC deletion effects on essential cellular processes, recognizing its potential impact on the organism's adaptability and pathogenicity.

Culturing the strains under anaerobic conditions was pivotal, as it reflects the bacterium's natural response in oxygen-limited environments, akin to those encountered in specific infection sites. The mRNA sequencing approach identified significant gene expression changes, employing a two-fold change as a threshold to ensure the focus on biologically significant alterations.

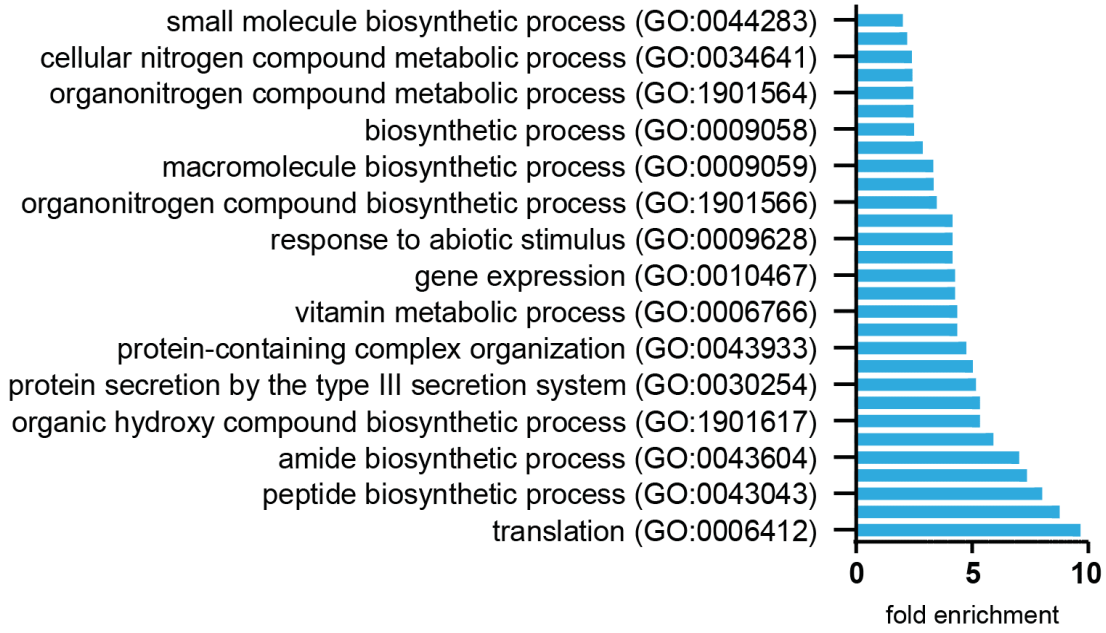

Figure 25 Gene Ontology (GO) enrichment analysis of affected pathways in P. *aeruginosa* (WT) versus Δ*sadC* strains under anaerobic conditions, as determined by mRNA sequencing. The figure emphasizes genes with a two-fold expression change, highlighting SadC's regulatory impact on translation, peptide synthesis, and key biosynthetic and type III secretion system pathways.

The analysis unveiled a marked enrichment in genes related to translation or peptide synthesis, indicating an influence of SadC deletion on the bacterium's protein production machinery. Additionally, the comprehensive examination revealed significant

changes in genes associated with the type III secretion system and biosynthetic pathways.

The findings underscore the importance of further investigations with additional biological replicates and robust statistical analyses to validate these preliminary results, thereby broadening our understanding of SadC's regulatory scope under anaerobic conditions.

8.3.4 Regulatory influence on alginate synthesis gene expression in *P. aeruginosa*: the role of SadC deletion under aerobic and anaerobic conditions

8.3.4.1 Influence of SadC and oxygen levels on OdaI and OdaA expression

The regulation of alginate synthesis in *P. aeruginosa* PAO1 under varying oxygen conditions is complex, involving both transcriptional and post-transcriptional mechanisms. SadC, OdaA and OdaI, as demonstrated by Schmidt (2015) and Schmidt et al. (2016), play pivotal roles in the regulation of alginate synthesis under different oxygen levels. The transcription analysis revealed a significant fold change in SadC expression under both aerobic (2,749 times, WT/Δ*sadC* +O_2) and anaerobic conditions (116,210 times, WT/Δ*sadC* -O_2), when comparing wild-type to Δ*sadC* mutant. This indicates that the deletion of *sadC* in the mutant was successful (Table 33).

In the wild type, OdaI expression under aerobic conditions surged remarkably (107,071-fold, WT/ΔsadC +O2) when compared with the ΔsadC mutant, underscoring the significant role of SadC in influencing OdaI expression in the presence of oxygen. Conversely, for OdaI under anaerobic conditions, and OdaA under both aerobic and anaerobic conditions, the expression changes were not markedly pronounced, indicating that SadC does not significantly impact the expression levels of these genes in anaerobic (for OdaA and OdaI) and aerobic (for OdaI) conditions.

8.3.4.2 Regulatory effects of SadC and oxygen on the alginate operon and associated regulatory genes.

In *P. aeruginosa* WT, the *algD-algA* operon, along with its associated regulatory genes (*algT*, *mucA*, *mucB,* and *mucC*), demonstrates a subtle yet noticeable response to oxygen availability. In the WT, expression levels of the majority of genes within the operon remain largely consistent across aerobic and anaerobic conditions. However, *algL* and *algF* show a slight upregulation under aerobic conditions, with *algL* increasing to 2.016-fold and *algF* to 2.218-fold in WT +/- O_2 scenarios, indicating a modest oxygen-related sensitivity (Table 33). This suggests that while oxygen does not

drastically influence the expression of the alginate operon, certain components do exhibit a slight induction in the presence of oxygen, which may be part of a delicate regulatory response to environmental cues.

When comparing the wild type to the Δ*sadC* mutant under aerobic conditions (WT/Δ*sadC* +O_2), the expression levels of the genes within the alginate operon and associated regulatory genes remain relatively stable, with no significant changes observed. This stability indicates that SadC does not exert a major influence on the expression of these genes in the presence of oxygen. The slight variations observed do not exceed the typically considered threshold of significance (2-fold change), suggesting that the regulatory role of SadC under these conditions may be limited or overshadowed by other regulatory mechanisms.

Most genes within the operon display reduced expression levels in the WT/Δ*sadC* -O_2 comparison, with fold changes below 0.5, indicating that SadC is indeed important for their expression under anaerobic conditions. The decreased expression in the absence of SadC confirms its role in upregulating these genes, except for *algQ* and *algC*, which do not show substantial change, with fold changes of 1.943 and 0.829, respectively. This indicates that, overall, SadC has a significant regulatory impact on the operon, particularly under anaerobic conditions.

8.3.4.3 Impact of SadC and oxygen conditions on competing alginate precursor genes

The genes *murA*, *wbpL*, *pslB*, and *wbpW* within *P. aeruginosa* PAO1 play critical roles in pathways that converge with alginate biosynthesis by competing for substrates with *algD*, the gene encoding GDP-mannose dehydrogenase which catalyzes the initial step of alginate production. Investigating the expression levels of these genes is crucial to determine if environmental conditions, such as oxygen availability, or genetic alterations, like SadC deletion, influence their activity. Overexpression of these genes might suggest a competitive advantage in substrate utilization over *algD*, potentially leading to decreased alginate synthesis. Conversely, the reduced expression could indicate an abundance of substrates for alginate production, enhancing the biosynthesis capacity of *algD*. Thus, understanding the expression dynamics of these genes provides insight into the intricate balance of substrate distribution and its impact on the process of alginate synthesis in *P. aeruginosa*.

The sequencing results reveal the expression patterns of *murA*, *wbpL*, *pslB*, and *wbpW* under aerobic and anaerobic conditions, as well as in the presence and absence of SadC. MurA, involved in peptidoglycan biosynthesis, demonstrates a slight increase in expression under aerobic conditions (WT +/- O_2) with a fold change of 0.365,

suggesting a modest increase in peptidoglycan production when oxygen is available. More notably, in anaerobic conditions and without SadC (WT/Δ*sadC* -O_2), *murA* expression significantly rises with a fold change of 2.949, implying that SadC may act to repress *murA* expression, possibly favoring alginate production by conserving substrates for *algD*. In contrast, *wbpL*, *pslB*, and *wbpW* show stable expression levels across both oxygenated and deoxygenated environments, as well as with and without SadC (Table 33).

Table 33 Comparative expression analysis of alginate biosynthesis-related genes in *P. aeruginosa* PAO1. This table details fold changes in expression for genes SadC, OdaA, OdaI, the *algD-algA* operon, associated regulatory genes (*algT, mucA, mucB, mucC*), and genes competing for alginate substrates (*murA, wbpL, pslB, wbpW*) under both aerobic (+O_2) and anaerobic (-O_2) conditions between the wild type (WT) and Δ*sadC* mutant strains.

Gene ID	Gene name	WT/ Δ*sadC* -O_2	WT/Δ*sadC* + O_2	WT +/- O_2	Δ*sadC* +/- O_2
PA4330	*odaA*	0,872	0,527	0,984	0,833
PA4331	*odaI*	0,905	107,071	0,643	1,106
PA4332	*sadC*	116,210	2,749	0,450	0,483
PA3540	*algD*	0,247	0,631	0,670	0,263
PA3541	*alg8*	0,186	0,873	0,904	0,193
PA3542	*alg44*	0,205	1,263	1,192	0,194
PA3543	*algK*	0,194	1,348	0,909	0,131
PA3544	*algE*	0,145	1,178	1,215	0,149
PA3545	*algG*	0,438	1,065	1,266	0,521
PA3546	*algX*	0,148	1,816	1,594	0,130
PA3547	*algL*	0,115	1,152	2,016	0,201
PA3548	*algI*	0,246	0,739	1,111	0,369
PA3549	*algJ*	0,124	0,981	1,737	0,220
PA3550	*algF*	0,383	1,291	2,218	0,658
PA3551	*algA*	0,269	0,958	1,720	0,483
PA5255	*algQ*	1,638	0,668	0,895	1,943
PA5322	*algC*	1,186	1,844	1,093	0,829
PA0762	*algT*	0,184	1,113	1,096	0,182
PA0763	*mucA*	0,232	0,978	0,989	0,234
PA0764	*mucB*	0,225	0,887	0,851	0,216
PA0765	*mucC*	0,408	1,057	1,148	0,443
PA0766	*mucD*	0,511	1,490	2,289	0,785
PA4450	*murA*	2,949	0,854	0,365	0,910
PA3145	*wbpL*	1,190	0,781	1,099	1,675
PA2232	*pslB*	0,541	0,491	0,965	1,064
PA5452	*wbpW*	1,297	0,892	0,645	1,085

8.3.5 Validation of RNA sequencing data through Western Blot analysis

To corroborate the RNA sequencing findings, Western Blot analysis was employed using an *α*LasB antibody (Figure 26). LasB, a protease pivotal for virulence and biofilm formation, exists as a preenzyme (~54 kDa) intracellularly and as a mature form (~30 kDa) in the extracellular supernatant. RNA sequencing data indicated a 39-fold increase in LasB expression in *P. aeruginosa* wild-type (WT) relative to the Δ*sadC* mutant under anaerobic conditions. A pronounced elevation in the secreted LasB (~30 kDa) was noted in the supernatant from the WT strain under anaerobic conditions, compared to aerobic conditions or the Δ*sadC* mutant under any condition, aligning with the RNA sequencing outcomes which highlighted *lasB* upregulation in the WT strain under anaerobic conditions.

The αRpoB antibody was meticulously selected as a control to ascertain cell integrity throughout the experimental procedure. RpoB, the β subunit of RNA polymerase (~150 kDa), is a critical enzyme confined within the bacterial cell, playing a central role in DNA transcription. Its detection exclusively in cellular fractions serves as a robust indicator of cell membrane integrity, ensuring that observed variations in extracellular protein levels are reflective of regulated secretion mechanisms rather than cellular lysis or damage. This approach underscores the validity of the Western Blot results by confirming that differential protein expressions are genuine outcomes of cellular regulation under varying conditions, rather than artifacts of cell disruption

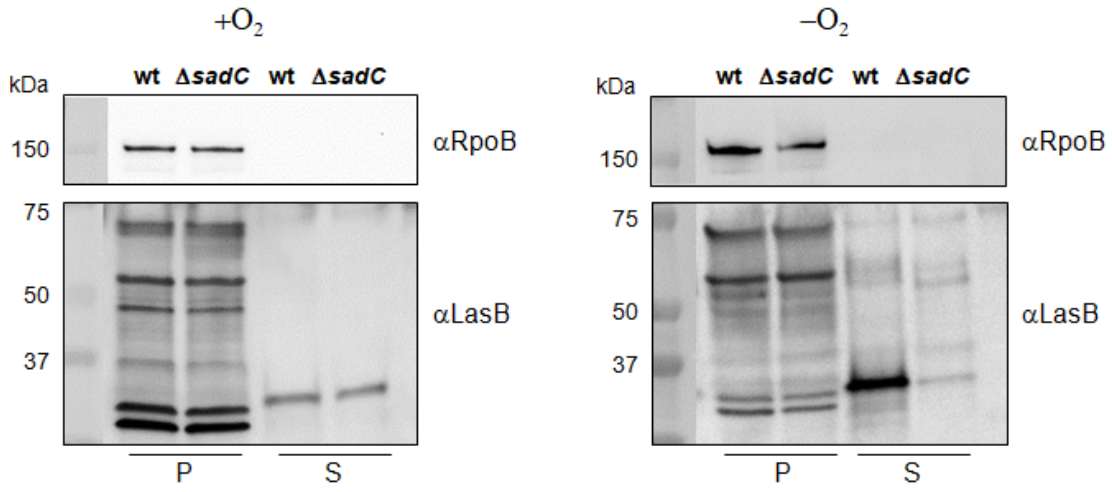

Figure 26 This figure contrasts the qualitative protein expression of LasB in *P. aeruginosa* (WT) against the Δ*sadC* mutant, under anaerobic and aerobic conditions, as informed by RNA sequencing data. The denser LasB band in WT under anaerobic conditions visually supports the RNA sequencing revelation of a 39-fold increase in *lasB* mRNA levels compared to the Δ*sadC* mutant, exclusively under these conditions. Presence of LasB preenzyme (~54 kDa) in the cell pellet and mature LasB (~30 kDa) in the supernatant, along with αRpoB bands (~150 kDa), verifies cell membrane integrity, ensuring that observed protein levels are not artifacts of cellular disruption.

9. Discussion

Cystic fibrosis is an autosomal recessive disorder caused by mutations in CFTR protein (cystic transmembrane conductance regulator), resulting in disturbed regulation of ion transport across the cell membrane (Elborn, 2016; Scotet et al., 2020). In CF patients' lungs, enormous amounts of thick, stagnant and dehydrated mucus results in decreased mucociliary clearance. Such an environment favors chronic bacterial infections, which are hard to eradicate and are the leading cause of CF patients' deaths (Elborn, 2016; Registry, 2020). Combination of stagnant mucus, infections, inflammations, and oxygen demands exceeding supply cause hypoxia in lungs epithelium and mucus (Page et al., 2021; Worlitzsch et al., 2002).

P. aeruginosa is the most often diagnosed pathogen in the lungs of adult CF patients. It can easily adapt to the environment encountered in CF lungs. The most common adaptations occur in DNA repair processes, energy metabolism, acquisition of limited nutrients, antibiotic and stress resistance, and biofilm formation (Rossi et al., 2021). Infections with mucoid variants of *P. aeruginosa* can be rarely eradicated and usually lead to chronic infections (Registry, 2020). Constitutive overproduction of exopolysaccharide alginate is caused by mucoidy. It is caused by mutations in genes involved in the regulation of alginate synthesis, the most often in the *mucA* gene. Alginate protects *P. aeruginosa* from antibiotics, host immune system response, reactive oxygen species, and maintains an optimal hydration level (Rossi et al., 2021). It was shown that nonmucoid *P. aeruginosa* synthesizes alginate *in vitro* and *in vivo* in the CF lungs with chronic infections under oxygen limitation (Bragonzi et al., 2005; Worlitzsch et al., 2002). Exact pathways controlling oxygen-dependent regulation of alginate synthesis are not known yet. Previous studies excluded the role of oxygen-dependent regulator ANR and revealed that a diguanylate cyclase SadC takes part in the regulation (Bastian, 2008; Schmidt, 2015; Schmidt et al., 2016).

SadC is essential in the oxygen-dependent synthesis of alginate. Deletion mutant of SadC was unable to synthetise alginate under anaerobic conditions. SadC consists of the transmembrane and GGEEF domain, synthesizing c-di-GMP, but no known oxygen-sensing domains were predicted, which means that other regulatory steps are required to control alginate synthesis under anaerobic conditions. SadC plays a role as a central regulator of surface mode growth (Merritt et al., 2007; Schmidt et al., 2016). It was shown that c-di-GMP is necessary for alginate synthesis under anaerobic conditions, and it was hypothesized that SadC synthesizes it to stimulate alginate production (Bastian, 2008; Bragonzi et al., 2005; Schmidt, 2015). Two proteins localized in the operon together with SadC, OdaA, and OdaI participate in the regulation.

OdaA is essential for alginate synthesis under anoxic growth conditions, whereas OdaI inhibits alginate synthesis in the presence of molecular oxygen. mRNA levels of SadC, OdaA, and OdaI do not change while changing conditions from aerobic to anaerobic. Therefore it was hypothesized that the regulation of alginate synthesis takes place on a posttranslational level (Schmidt, 2015; Schmidt et al., 2016).

Recently, OdaA was described as monofunctional enoyl-CoA isomerase, and its crystal structure was resolved. OdaA was proposed to be involved in synthesizing diffusible signal factors (DSFs), which were found to play a role in quorum sensing (Zhao et al., 2021). That finding excludes the hypothesis that OdaA can conduct proline dehydroxylation. Other proteins may likely take part in oxygen-dependent regulation of alginate synthesis by SadC.

In this study, we attempt to shed more light on alginate synthesis controlled by SadC in an oxygen-dependent manner. We studied interactions between SadC, OdaI, and OdaA and investigated the possible role of cysteine residues of the cytosolic part of SadC in an oxygen-dependent alginate synthesis.

9.1 The TM domain is essential for SadC functionality

It was shown that the TM domain of SadC is critical for promoting cell aggregation, biofilm formation, Psl synthesis, or inhibiting swimming and twitching motility. Moreover, it was found that the α-helix of amino acid residues 300-322 is necessary to assemble active oligomers of the cytosolic part of SadC (residues 300-487, $SadC_{300-487}$). The presence of the TM domain also impacted the localization of SadC-GFP fusions in the cell. Full-length SadC showed a periphery localization pattern, whereas $SadC_{300-487}$ was distributed within the cell. That means that full-length SadC is most likely associated with the cell membrane, whereas the cytosolic part is localized in the cytoplasm. Interestingly the total intracellular levels of c-di-GMP were significantly higher for full-length SadC than for $SadC_{300-487}$ (~220 versus 150 pmol/mg total protein when induced with 2% arabinose, and ~100 versus 25 pmol/mg total protein when induced with 0,1% arabinose) (Zhu et al., 2016). It is important to remark that all mentioned above data come from experiments performed in *P. aeruginosa* PAO1 in aerobic conditions.

In this work, we showed in BACTH analysis that an effective self-interaction (and possible dimerization) of SadC is only possible in the presence of the TM domain. It is worth noting that SadC self-interacts better in anaerobic (70% and 65% of maximal score at room temperature or 30°C respectively) than in aerobic conditions (10% and 30% of maximal score at room temperature or 30°C respectively). The analysis was

performed in *E. coli,* and obtained results may vary in the original background in *P. aeruginosa*. We conclude that the TM domain is critical for the efficient dimerization and functionality of SadC. It goes in line with the finding that total intracellular levels of c-di-GMP were higher when full-length SadC was overexpressed instead of $SadC_{300-487}$ (Zhu et al., 2016). Zhu et al. (2016) found that the cytosolic part of SadC containing the α-helix of amino acid residues 300-322 possesses enzymatic activity. Possibly, mentioned α -helix is required for SadC to obtain any catalytic activity of the cytosolic part of the protein, but only the presence of the TM domain guarantees full functionality. Hypothetically, the α-helix of amino acid residues 300-322 can participate in oxygen-dependent alginate synthesis regulation since Schmidt et al. (2016) showed that the enzymatic activity of MBP-$SadC_{cyt}$ is influenced by oxygen. These experiments were performed in *E.coli,* where OdaA and OdaI were absent. Even though MBP-$SadC_{cyt}$ showed enzymatic activity only in aerobic conditions, which can be caused by similarities in enzymatic machinery in *E.coli* and *P. aeruginosa*.

It was shown before that SadC is essential for alginate synthesis in the lack of oxygen (Bastian, 2008; Schmidt, 2015; Schmidt et al., 2016). Our results indicate a more robust self-interaction of full-length SadC under anaerobic conditions. We hypothesize that full-length SadC dimerizes and activates alginate synthesis in the so far not defined way in the lack of oxygen. It is still to answer if SadC directly triggers alginate synthesis by supplying c-di-GMP, which binds to the PilZ domain of Alg44, or if the response pathway to anoxia is more complex and involves more steps in-between. It is also possible that the start of alginate production in response to oxygen tensions does not include c-di-GMP binding to Alg44, but another regulation takes place instead.

In BACTH analysis, $SadC_{cyt}$ self-interacted at a low level at room temperature, and the signal was higher for anaerobic conditions. Surprisingly, at 30°C, $SadC_{cyt}$ self-interacted more stronger in the presence of oxygen. That contradicts results obtained in an *in vitro* assay, where MBP-Sad_{cyt} purified from *E. coli* (Schmidt et al., 2016) and *P. aeruginosa* (data not published, Dr. Annika Schmidt, University of Tübingen) was significantly more enzymatically active under anoxic conditions. The most likely is that the expression level of proteins at 30°C was too robust and caused an unspecific signal in BACTH analysis. On the other hand, these data may suggest that the self-interaction and enzymatic activity of $SadC_{cyt}$ are influenced differently by oxygen tensions than full-length SadC. That could be explained by the so far unknown role of the TM domain in the oxygen-dependent regulation of SadC activity and alginate synthesis. Additionally, we cannot exclude the possibility that dimerization of SadC is not the only step required in oxygen-dependent regulation of alginate synthesis or does not take part directly in that regulation process at all.

9.2 OdaA interacts with full-length SadC, but not with Sad_{cyt}

It was already shown that the TM domain of SadC is crucial for direct interactions with other proteins. It interacts with type 4 pili alignment complex protein, PilO (SadC residues T83 and L172). PilO-SadC interaction took place in the planktonic mode of growth and was shown to decrease the enzymatic activity of SadC. Upon the switch to the surface-associated mode of growth, the inhibitory effect of PilO in SadC reduces, and SadC's activity additionally becomes positively stimulated by MotC (interacts with SadC residues L82, L94, L134, and F136), which is a part of MotCD flagellar stator. MotCD and MotAB possibly dynamically compete for motor occupancy due to, e. g., environmental cues or growth mode, which modifies c-di-GMP signaling within the cell(Baker et al., 2019; Webster et al., 2021).

Here we demonstrated an interaction between full-length SadC and OdaA. It shows the importance of the TM domain in the functionality of SadC since $SadC_{cyt}$ did not interact with OdaA. The signal was strong only in a combination of pKNT25::OdaA and pUT18::SadC, independent of oxygen tensions and temperature. That corresponds with our results from co-immunoprecipitation of $SadC_{cyt}$-3xFLAG and OdaA-His, where we could not pull out $SadC_{cyt}$ together with OdaA by using amylose resins (data not published).

OdaA was found to be necessary for alginate synthesis in anaerobic conditions (Schmidt et al., 2016). Recently crystal structure of OdaA was resolved and showed that OdaA forms a homotrimer and functions as a mono-functional enoyl-CoA isomerase. Authors showed that OdaA can bind Co-A thioesters and hypothesized that OdaA could be involved in quorum sensing signaling by synthesizing diffusible signal factors (DFS) (Zhao et al., 2021). DFFs take part in regulating biofilm formation, antibiotic resistance, or virulence. So far, only one DFS was described in *P. aeruginosa,* which is cis-2-decenoid acid (CDA). CDA triggers biofilm dispersal in *P. aeruginosa* and is hypothetically synthesized and sensed by a cluster of genes PA4978-PA4983. Interestingly CDA was shown to regulate the expression of OdaA and SadC in a microarray assay (Dow, 2017; Rahmani-Badi et al., 2015).

It is worth noticing that our analysis indicates strong self-interaction of OdaA independently of tested conditions in BACTH experiment. Most likely, OdaA oligomerizes in anaerobic and aerobic conditions, and that process is not involved in oxygen-dependent regulation of alginate synthesis in *P. aeruginosa.* Still, the exact function of OdaA remains unknown, and it is also to investigate if OdaA regulates the activity of SadC in c-di-GMP synthesis or, e.g., instead stimulates alginate synthesis directly.

9.3 OdaI does not interact with SadC but interacts with OdaA

OdaI was shown to be essential for inhibiting alginate synthesis under aerobic conditions *in vivo* and necessary for the enzymatic activity of MBP-SadC$_{cyt}$ in an *in vitro* assay. Surprisingly, the BACTH system analysis did not show an interaction between SadC and OdaI. We observed only a weak signal at room temperature for *E. coli* strains carrying pKNT25::OdaI and pUT18:SadC plasmids. Moreover, that interaction was more vital under anaerobic conditions. Data published by Schmidt (2015) suggested that we would observe strong signal interaction in the case of SadC and OdaI. The lack of evidence for that interaction in the BACTH assay excludes the possible regulation of SadC by OdaI by steric hindrance, as proposed before (Schmidt, 2015). It is still possible that OdaI modifies SadC enzymatically in an oxygen-dependent manner and that those proteins interact together too short to result in detection by BACTH assay.

Here we also found proof of a self-interaction of OdaI. Our data showed the high signal strength of interaction, but it is impossible to conclude if the interaction of OdaI is oxygen-dependent. At room temperature signal is stronger in anaerobic conditions, but at 30°C the other way around.

The last interesting observation from the BACTH experiment is an interaction between OdaI and OdaA. The obtained data again are inconclusive about the oxygen-dependent nature of that interaction. Up to date, we do not have enough information about OdaA and OdaI to hypothesize about the role of that interaction. It is essential to perform more experiments on those proteins to reveal their activity and function in an oxygen-dependent regulation of alginate synthesis.

9.4 Cysteine substitutions in SadC$_{cyt}$ alter the binding affinity of GTP

P. aeruginosa encounters reactive oxygen species (ROS) produced by the host's immune system, but ROS are also a side product of aerobic respiration and the presence of molecular oxygen in the environment (Boronat et al., 2014). It was shown that *P. aeruginosa* prefers microaerophilic conditions in the environment. Interestingly, while cultured in a bath bioreactor under aerobic conditions, it synthesized substances that decreased oxygen transfer to the growth medium (Sabra et al., 2002). Moreover, *Azotobacter vinelandii*, cultured aerobically in a phosphate-limited and nitrogen-free medium, started to produce alginate to protect from oxygen a nitrogenase, which is crucial for growth in tested conditions (Sabra et al., 2000).

Considering the above pieces of information and the fact that cysteine residues are highly reactive due to the presence of a thiol functional group (-SH), which ROS can oxidize (Boronat et al., 2014), we sought to determine the impact of cysteine residues on the cytosolic part of SadC (residues C390, C420, C421, and C478) and the possible role of ROS in the regulation of SadC and further alginate synthesis under anaerobic conditions. Our results indicated that the elution profile of a size exclusion chromatography of the mutant MBP-SadC$_{cyt\ C420A\ C421A}$ was changed. The protein was eluted primarily on a peak that most likely contains a dimeric form of SadC$_{cyt}$. Two other mutants showed an elution profile similar to WT. A crosslinking assay using DSS showed that all the mutants dimerize similarly to WT. Interestingly, GTP binding affinity was altered for all mutants. Mutants MBP-SadC$_{cyt\ C390A}$ and MBP-SadC$_{cyt\ C478A}$ bonded GTP, respectively ~50% and ~60% better than WT. On the other hand, mutant MBP-SadC$_{cyt\ C420A\ C421A}$ was deficient in binding GTP by ~40% compared to WT.

MBP-SadC$_{cyt}$ was eluted from a size exclusion chromatography in two peaks, corresponding with this protein's mono- and dimeric form. It was shown that protein samples from a peak with a dimeric form of MBP-SadC$_{cyt}$ are enzymatically less active (Schmidt, 2015). Interestingly, in our experiment, we observed decreased GTP binding efficiency of mutant MBP-SadC$_{cyt\ C420A\ C421A}$, which was eluted on a size exclusion chromatography mainly in the peak containing dimeric protein. The mutant MBP-SadC$_{cyt\ C420A\ C421A}$ would possibly show lower enzymatic activity.

On the other hand, two other mutants (MBP-SadC$_{cyt\ C390A}$ and MBP-SadC$_{cyt\ C478A}$) showed increased binding efficiency of GTP and were eluted mainly in a monomeric state. It is still to test, but possibly they are also enzymatically more active. That would mean that the substitution of cysteine residues C390 and C478 influence the activity of SadC$_{cyt}$ under aerobic conditions, which is decreased in a WT.

9.5 SadC as a hypothetical master regulator of gene expression and its influence on alginate synthesis genes' expression under anaerobic conditions in *P. aeruginosa*

The differential expression analysis between wild-type (WT) and SadC deletion mutant (Δ*sadC*) strains of *P. aeruginosa* underlines the pivotal role of SadC, especially under anaerobic conditions. While aerobic conditions showed several differences in gene expression profiles between the WT and Δ*sadC* strains, indicating a role for SadC in the presence of oxygen, the transition to anaerobic conditions revealed its significant

impact. The Δ*sadC* mutant displayed extensive changes in gene expression, with a notable number of genes surpassing the fold change thresholds, contrasting sharply with relatively stable expression observed in the WT strain. This stark difference underscores the essential function of SadC in regulating gene expression critical for adaptation and survival in oxygen-limited environments.

Further analysis revealed that the deletion of SadC significantly influences the transcriptional regulation of alginate biosynthesis genes' expression under anaerobic conditions. Moreover, the absence of SadC led to significant transcriptional alterations across a wide array of genes, suggesting a central role as a regulatory hub under anaerobic stress. These transcriptional changes indicate that SadC may act as an important regulator and suggest the possibility of a complex regulatory mechanism. This implies the need for further investigation.

Particularly noteworthy is the slight transcriptional variation observed in *murA* in the context of SadC deletion. This variation hints at an indirect effect of SadC on the competition for substrates required for alginate biosynthesis, potentially affecting the levels of alginate synthesis. Such a finding underscores the nuanced impact of SadC on metabolic pathways of *P. aeruginosa*, especially under anaerobic conditions, and raises questions about the broader implications of this regulatory mechanism on bacterial physiology and pathogenicity.

The insights gained from this investigation shed light on the adaptive strategies employed by *P. aeruginosa* in response to anaerobic stress, positioning SadC as a regulatory figure. Despite the progress made, further research is essential to delineate the mechanisms behind SadC-mediated gene regulation, its post-transcriptional control influences, and its interactions within the cellular network. Such endeavors will deepen our understanding of bacterial adaptation and pathogenesis, potentially leading to innovative therapeutic approaches targeting these mechanisms.

9.6 Further perspectives

P. aeruginosa is one of the most relevantclinical pathogens. In many niches, it encounters an anaerobic environment, which successfully colonizes. One of the virulence factors, alginate, was shown to be synthesized in the lack of oxygen. SadC is essential for activating alginate synthesis under anaerobic conditions (Bastian, 2008; Bragonzi et al., 2005; Schmidt, 2015; Schmidt et al., 2016; Worlitzsch et al., 2002). Besides that, SadC was shown to influence many processes in the cell, like swimming, swarming and twitching motilities, biofilm formation, Psl synthesis, stress response, regulation of liposaccharide modifications, and more (Baker et al., 2019;

Chen et al., 2015; Chua et al., 2015; Kuchma et al., 2010; Kuchma et al., 2012; Lewis et al., 2019; Merritt et al., 2007; Moscoso et al., 2014; Schmidt et al., 2016; Webster et al., 2021; Zhu et al., 2016). SadC was shown to act downstream of Gac/Rsm pathway and upstream of SadB, to interact with MotC, PilO, PilY1, or WarA. Our knowledge about SadC and its importance for *P. aeruginosa* is still limited, but we can assume that SadC intermediates and regulates many different processes within the cell.

The oxygen-dependent regulation of alginate synthesis by SadC seems to be a multi-step process involving other proteins like OdaA or OdaI. During further research, it is crucial to distinguish between the regulation of SadC activity, activation of alginate synthesis, and hypothetically other steps that may take place in-between. That is because, e. g., the c-di-GMP synthesized by SadC can hypothetically not directly activate alginate synthesis. Or the synthesis of alginate is activated in such conditions not by binding c-di-GMP to a PilZ domain of Alg44 but by another mechanism.

A recent study about OdaA describing the protein as a mono-functional enoyl-CoA isomerase (Zhao et al., 2021), a paper showing that OdaA is essential for alginate synthesis in anoxia (Schmidt et al., 2016), and our results showing an interaction between SadC and OdaA suggest that also quorum sensing could be involved in oxygen-dependent regulation of alginate synthesis. Furthermore, interactions between SadC and proteins building up a type 4 pili and flagellum mean that surface attachment and proton gradient within a cell membrane can also influence alginate synthesis. The lack of precise techniques seems to be the bottleneck limiting our understanding of such complex regulation and answering the most emerging questions.

Here it was demonstrated that TM is crucial for the self-interaction of SadC. Therefore, it seems that results from experiments where only the cytosolic part of SadC is used can be misleading and not fully show the features of SadC. Up to date, the purification of full-length SadC has not been successful. Purifying a native full-length SadC would allow further study of the protein *in vitro*. Still, SadC could be studied indirectly. It was demonstrated that the BACTH system is suitable for that purpose (this work, Webster et al., 2021). Importantly, we showed in this work that the BACTH system could also be used to study SadC under anaerobic conditions.

It is emerging to develop techniques that allow us to monitor the activity of SadC directly, not by observations of a final phenotype (e.g., alginate synthesis or biofilm formation). It is widely used to quantify total levels of c-di-GMP concentration in the cell by HPLC coupled with MS/MS. This method does not precisely inform us about the specific activity of SadC due to the presence of multiple different diguanylate cyclases and phosphodiesterases in *P. aeruginosa* or *E. coli*. A fluorescent-based

reporter plasmid pCdrA::*gfp*(ASV) was used in *P. aeruginosa* PAO1 to track the timing and level of SadC expression of SadC (Zhu et al., 2016). SadC activity was also investigated in a strain of *Salmonella typhimurium* deficient in c-di-GMP synthesis (Bastian, 2008). In that case, the activity of SadC was estimated indirectly on the synthesis of cellulose, which in that strain takes place only when the c-di-GMP is produced. All of the instanced methods have drawbacks, e.g., measurement of c-di-GMP cannot be tracked over time (total levels of c-di-GMP concentration in the cell), are not suitable for anoxic conditions (usage of GFP-based sensors) or estimate the activity of SadC indirectly (cellulose levels in *S. typhimurium*)

SadC activity could be directly measured using a strain of *Salmonella typhimurium* deficient in the c-di-GMP synthesis where RNA-based fluoresce c-di-GMP biosensor is expressed (Wang et al., 2016). For quantifying the fluorescence, flow cytometry or microscopy could be used. That method would allow us to measure the enzymatic activity of SadC under anaerobic conditions directly and to track the activity of SadC in time and place.

Another emerging question is the role of OdaA and OdaI in an oxygen-dependent regulation of alginate synthesis. OdaI was proved to inhibit alginate synthesis under aerobic conditions and also to inhibit the enzymatic activity of SadC in the presence of oxygen. OdaI is predicted to be cytoplasmic ferredoxin reductase and was also shown to share high similarity with a benzoate dioxygenase reductase (1KRH) from *Acinetobacter sp*.

As already mentioned, we found that OdaI interacts with OdaA. OdaA was experimentally found to be mono-functional enoyl-CoA isomerase, possibly taking part in synthetizing DFS, which takes part in quorum sensing (Zhao et al., 2021). It remains to investigate why OdaA is necessary for alginate synthesis under anaerobic conditions and if OdaA is engaged in activating SadC enzymatic functions or another step in the oxygen-dependent regulation of alginate synthesis.

The last subject we want to stress due to the further studies of oxygen-dependent regulation of alginate synthesis in *P. aeruginosa* is reference conditions in which experiments are performed. Up to date, this regulation was tested under aerobic and anaerobic conditions. In past experiments, it was not found that *P.aeruginosa* synthesizes alginate under aerobic conditions (Schmidt, 2015; Schmidt et al., 2016). Although it was found that a closely related bacterium, *Azotobacter vinelandii* produces alginate to protect the enzymatic machinery when cultured aerobically (Sabra et al., 2000). Another study found that aerobically grown *P. aeruginosa* releases

some substances into the medium, which inhibit oxygen transfer and that microaerophilic conditions are the most suitable for P. aeruginosa to grow (Sabra et al., 2002). We also showed that the substitution of cysteine to alanine residues C390 and C478 might enhance the activity of $SadC_{cyt}$ purified from an aerobically grown culture. Therefore, hypothetically the activity of WT SadC could potentially be suppressed under aerobic conditions due to cysteine oxidation. Taken all together, it may mean that in further experiments, *P. aeruginosa* should be cultured in microaerophilic conditions as a reference, and it should be studied how aerobic and anaerobic conditions influence oxygen-dependent regulation of alginate synthesis (and also another process).

10. References

Allen, P., Borick, J., & Borick, J. (2020). Acute and Chronic Infection Management in CF. Cystic Fibrosis in Primary Care: An Essential Guide to a Complex, Multi-System Disease, 69–87.

Alonso, A., Rojo, F., & Martinez, J. L. (1999). Environmental and clinical isolates of *Pseudomonas aeruginosa* show pathogenic and biodegradative properties irrespective of their origin. *Environ Microbiol*, *1*(5), 421-430.

Alvarez-Ortega, C., & Harwood, C. S. (2007). Responses of *Pseudomonas aeruginosa* to low oxygen indicate that growth in the cystic fibrosis lung is by aerobic respiration. *Mol Microbiol*, *65*(1), 153-165.

Anderson, D. H. (1938). Cystic fibrosis of the pancreas and its relation to celiac disease. A clinical and pathologic study. *Am. J. Dis. Child.*, *56*, 344-399.

Andersson, D. I., Nicoloff, H., & Hjort, K. (2019). Mechanisms and clinical relevance of bacterial heteroresistance. *Nat Rev Microbiol*, *17*(8), 479-496.

Antoniou, S., & Elston, C. (2016). Cystic fibrosis. *Medicine*, *44*(5), 321-325.

Baker, A. E., Webster, S. S., Diepold, A., Kuchma, S. L., Bordeleau, E., Armitage, J. P., & O'Toole, G. A. (2019). Flagellar Stators Stimulate c-di-GMP Production by *Pseudomonas aeruginosa*. *J Bacteriol*, *201*(18).

Baker, E. H., Clark, N., Brennan, A. L., Fisher, D. A., Gyi, K. M., Hodson, M. E., Philips, B. J., Baines, D. L., & Wood, D. M. (2007). Hyperglycemia and cystic fibrosis alter respiratory fluid glucose concentrations estimated by breath condensate analysis. *J Appl Physiol (1985)*, *102*(5), 1969-1975.

Balaban, N. Q., Helaine, S., Lewis, K., Ackermann, M., Aldridge, B., Andersson, D. I., Brynildsen, M. P., Bumann, D., Camilli, A., Collins, J. J., Dehio, C., Fortune, S., Ghigo, J. M., Hardt, W. D., Harms, A., Heinemann, M., Hung, D. T., Jenal, U., Levin, B. R., Zinkernagel, A. (2019). Definitions and guidelines for research on antibiotic persistence. *Nat Rev Microbiol*, *17*(7), 441-448.

Bastian, M. (2008). Identification of oxygen sensor systems regulating the production of exopolysaccharides in *Staphylococcus aureus* and *Pseudomonas aeruginosa.*

Baynham, P. J., Ramsey, D. M., Gvozdyev, B. V., Cordonnier, E. M., & Wozniak, D. J. (2006). The *Pseudomonas aeruginosa* ribbon-helix-helix DNA-binding protein AlgZ (AmrZ) controls twitching motility and biogenesis of type IV pili. *J Bacteriol*, *188*(1), 132-140.

Bhat, S. A., Singh, N., Trivedi, A., Kansal, P., Gupta, P., & Kumar, A. (2012). The mechanism of redox sensing in *Mycobacterium tuberculosis*. *Free Radic Biol Med*, *53*(8), 1625-1641.

Bjarnsholt, T., Jensen, P. O., Fiandaca, M. J., Pedersen, J., Hansen, C. R., Andersen, C. B., Pressler, T., Givskov, M., & Hoiby, N. (2009). *Pseudomonas aeruginosa* biofilms in the respiratory tract of cystic fibrosis patients. *Pediatr Pulmonol*, *44*(6), 547-558.

Blanchard, A. C., & Waters, V. J. (2019). Microbiology of Cystic Fibrosis Airway Disease. *Semin Respir Crit Care Med*, *40*(6), 727-736.

Boronat, S., Domenech, A., Paulo, E., Calvo, I. A., Garcia-Santamarina, S., Garcia, P., Encinar Del Dedo, J., Barcons, A., Serrano, E., Carmona, M., & Hidalgo, E. (2014). Thiol-based H_2O_2 signaling in microbial systems. *Redox Biol*, *2*, 395-399.

Botelho, J., Grosso, F., & Peixe, L. (2019). Antibiotic resistance in *Pseudomonas aeruginosa* - Mechanisms, epidemiology and evolution. *Drug Resist Updat*, *44*, 100640.

Boucher, J. C., Martinez-Salazar, J., Schurr, M. J., Mudd, M. H., Yu, H., & Deretic, V. (1996). Two distinct loci affecting conversion to mucoidy in *Pseudomonas aeruginosa* in cystic fibrosis encode homologs of the serine protease HtrA. *J Bacteriol*, *178*(2), 511-523.

Boucher, J. C., Schurr, M. J., & Deretic, V. (2000). Dual regulation of mucoidy in *Pseudomonas aeruginosa* and sigma factor antagonism. *Mol Microbiol*, *36*(2), 341-351.

Boucher, J. C., Yu, H., Mudd, M. H., & Deretic, V. (1997). Mucoid *Pseudomonas aeruginosa* in cystic fibrosis: characterization of muc mutations in clinical isolates and analysis of clearance in a mouse model of respiratory infection. *Infect Immun*, *65*(9), 3838-3846.

Boyle, M. P., & De Boeck, K. (2013). A new era in the treatment of cystic fibrosis: correction of the underlying CFTR defect. *Lancet Respir Med*, *1*(2), 158-163.

Bragonzi, A., Paroni, M., Nonis, A., Cramer, N., Montanari, S., Rejman, J., Di Serio, C., Doring, G., & Tummler, B. (2009). *Pseudomonas aeruginosa* microevolution during cystic fibrosis lung infection establishes clones with adapted virulence. *Am J Respir Crit Care Med*, *180*(2), 138-145.

Bragonzi, A., Worlitzsch, D., Pier, G. B., Timpert, P., Ulrich, M., Hentzer, M., Andersen, J. B., Givskov, M., Conese, M., & Doring, G. (2005). Nonmucoid *Pseudomonas aeruginosa* expresses alginate in the lungs of patients with cystic fibrosis and in a mouse model. *J Infect Dis*, *192*(3), 410-419.

Brennan, A. L., Gyi, K. M., Wood, D. M., Johnson, J., Holliman, R., Baines, D. L., Philips, B. J., Geddes, D. M., Hodson, M. E., & Baker, E. H. (2007). Airway glucose concentrations and effect on growth of respiratory pathogens in cystic fibrosis. *J Cyst Fibros*, *6*(2), 101-109.

Byrd, M. S., Sadovskaya, I., Vinogradov, E., Lu, H., Sprinkle, A. B., Richardson, S. H., Ma, L., Ralston, B., Parsek, M. R., Anderson, E. M., Lam, J. S., & Wozniak, D. J. (2009). Genetic and biochemical analyses of the *Pseudomonas aeruginosa* Psl exopolysaccharide reveal overlapping roles for polysaccharide synthesis enzymes in Psl and LPS production. *Mol Microbiol*, *73*(4), 622-638.

Cetin, E. T., Toereci, K., & Ang, O. (1965). Encapsulated *Pseudomonas Aeruginosa* (*Pseudomonas Aeruginosa Mucosus*) Strains. *J Bacteriol*, *89*, 1432-1433.

Chan, C., Paul, R., Samoray, D., Amiot, N. C., Giese, B., Jenal, U., & Schirmer, T. (2004). Structural basis of activity and allosteric control of diguanylate cyclase. *Proc Natl Acad Sci U S A*, *101*(49), 17084-17089.

Chang, A. L., Tuckerman, J. R., Gonzalez, G., Mayer, R., Weinhouse, H., Volman, G., Amikam, D., Benziman, M., & Gilles-Gonzalez, M. A. (2001). Phosphodiesterase A1, a regulator of cellulose synthesis in *Acetobacter xylinum*, is a heme-based sensor. *Biochemistry*, *40*(12), 3420-3426.

Chen, H. J., Li, N., Luo, Y., Jiang, Y. L., Zhou, C. Z., Chen, Y., & Li, Q. (2018). The GDP-switched GAF domain of DcpA modulates the concerted synthesis/hydrolysis of c-di-GMP in *Mycobacterium smegmatis*. *Biochem J*, *475*(7), 1295-1308.

Chen, Y., Yuan, M., Mohanty, A., Yam, J. K., Liu, Y., Chua, S. L., Nielsen, T. E., Tolker-Nielsen, T., Givskov, M., Cao, B., & Yang, L. (2015). Multiple diguanylate cyclase-coordinated regulation of pyoverdine synthesis in *Pseudomonas aeruginosa*. *Environ Microbiol Rep*, *7*(3), 498-507.

Chua, S. L., Sivakumar, K., Rybtke, M., Yuan, M., Andersen, J. B., Nielsen, T. E., Givskov, M., Tolker-Nielsen, T., Cao, B., Kjelleberg, S., & Yang, L. (2015). C-di-GMP regulates *Pseudomonas aeruginosa* stress response to tellurite during both planktonic and biofilm modes of growth. *Sci Rep*, *5*, 10052.

Chung, H. S., Wang, S. B., Venkatraman, V., Murray, C. I., & Van Eyk, J. E. (2013). Cysteine oxidative posttranslational modifications: emerging regulation in the cardiovascular system. *Circ Res*, *112*(2), 382-392.

Ciofu, O., Lee, B., Johannesson, M., Hermansen, N. O., Meyer, P., & Hoiby, N. (2008). Investigation of the *algT* operon sequence in mucoid and non-mucoid *Pseudomonas aeruginosa* isolates from 115 Scandinavian patients with cystic fibrosis and in 88 in vitro non-mucoid revertants. *Microbiology (Reading)*, *154*(Pt 1), 103-113.

Ciofu, O., & Tolker-Nielsen, T. (2019). Tolerance and Resistance of *Pseudomonas aeruginosa* Biofilms to Antimicrobial Agents-How P. aeruginosa Can Escape Antibiotics. *Front Microbiol*, *10*, 913.

Clark, S. T., Diaz Caballero, J., Cheang, M., Coburn, B., Wang, P. W., Donaldson, S. L., Zhang, Y., Liu, M., Keshavjee, S., Yau, Y. C., Waters, V. J., Elizabeth Tullis, D., Guttman, D. S., & Hwang, D. M. (2015). Phenotypic diversity within a *Pseudomonas aeruginosa* population infecting an adult with cystic fibrosis. *Sci Rep*, *5*, 10932.

Colgan, S. P., Furuta, G. T., & Taylor, C. T. (2020). Hypoxia and Innate Immunity: Keeping Up with the HIFsters. *Annu Rev Immunol*, *38*, 341-363.

Cowley, E. S., Kopf, S. H., LaRiviere, A., Ziebis, W., & Newman, D. K. (2015). Pediatric Cystic Fibrosis Sputum Can Be Chemically Dynamic, Anoxic, and Extremely Reduced Due to Hydrogen Sulfide Formation. *mBio*, *6*(4), e00767.

Crabbe, A., Jensen, P. O., Bjarnsholt, T., & Coenye, T. (2019). Antimicrobial Tolerance and Metabolic Adaptations in Microbial Biofilms. *Trends Microbiol*, *27*(10), 850-863.

Dahlstrom, K. M., Collins, A. J., Doing, G., Taroni, J. N., Gauvin, T. J., Greene, C. S., Hogan, D. A., & O'Toole, G. A. (2018). A Multimodal Strategy Used by a Large c-di-GMP Network. *J Bacteriol*, *200*(8).

Dahlstrom, K. M., & O'Toole, G. A. (2017). A Symphony of Cyclases: Specificity in Diguanylate Cyclase Signaling. *Annu Rev Microbiol*, *71*, 179-195.

Damkiaer, S., Yang, L., Molin, S., & Jelsbak, L. (2013). Evolutionary remodeling of global regulatory networks during long-term bacterial adaptation to human hosts. *Proc Natl Acad Sci USA*, *110*(19), 7766-7771.

Davidson, D. J., & Porteous, D. J. (1998). Genetics and pulmonary medicine. 1. The genetics of cystic fibrosis lung disease. *Thorax*, *53*(5), 389-397.

Delgado-Nixon, V. M., Gonzalez, G., & Gilles-Gonzalez, M. A. (2000). Dos, a heme-binding PAS protein from *Escherichia coli*, is a direct oxygen sensor. *Biochemistry*, *39*(10), 2685-2691.

Delic-Attree, I., Toussaint, B., Garin, J., & Vignais, P. M. (1997). Cloning, sequence and mutagenesis of the structural gene of *Pseudomonas aeruginosa* CysB, which can activate algD transcription. *Mol Microbiol*, *24*(6), 1275-1284.

DeVries, C. A., & Ohman, D. E. (1994). Mucoid-to-nonmucoid conversion in alginate-producing *Pseudomonas aeruginosa* often results from spontaneous mutations in algT, encoding a putative alternate sigma factor, and shows evidence for autoregulation. *J Bacteriol*, *176*(21), 6677-6687.

Dickinson, R. S., Murphy, F., Doherty, C., Williams, S., Mirchandani, A., Willson, J., Scotti, J. S., Preston, G., Schofield, C. J., Whyte, M. K. B., & Walmsley, S. R. (2017). *Pseudomonas* expression of an oxygen sensing prolyl hydroxylase homologue regulates neutrophil host responses in vitro and in vivo. *Wellcome Open Res*, *2*, 104.

Donlan, R. M. (2002). Biofilms: microbial life on surfaces. *Emerg Infect Dis*, *8*(9), 881-890.

Donnelly, M. I., Zhou, M., Millard, C. S., Clancy, S., Stols, L., Eschenfeldt, W. H., Collart, F. R., & Joachimiak, A. (2006). An expression vector tailored for large-scale, high-throughput purification of recombinant proteins. *Protein Expr Purif*, *47*(2), 446-454.

Douglas, T. A., Brennan, S., Gard, S., Berry, L., Gangell, C., Stick, S. M., Clements, B. S., & Sly, P. D. (2009). Acquisition and eradication of *P. aeruginosa* in young children with cystic fibrosis. *Eur Respir J*, *33*(2), 305-311.

Dow, J. M. (2017). Diffusible signal factor-dependent quorum sensing in pathogenic bacteria and its exploitation for disease control. *J Appl Microbiol*, *122*(1), 2-11.

Elborn, J. S. (2016). Cystic fibrosis. *Lancet*, *388*(10059), 2519-2531.

Elphick, H. E., & Southern, K. W. (2014). Antifungal therapies for allergic bronchopulmonary aspergillosis in people with cystic fibrosis. *Cochrane Database Syst Rev*(11), CD002204.

Emerson, J., Rosenfeld, M., McNamara, S., Ramsey, B., & Gibson, R. L. (2002). Pseudomonas aeruginosa and other predictors of mortality and morbidity in young children with cystic fibrosis. *Pediatr Pulmonol*, *34*(2), 91-100.

Eschbach, M., Schreiber, K., Trunk, K., Buer, J., Jahn, D., & Schobert, M. (2004). Long-term anaerobic survival of the opportunistic pathogen *Pseudomonas aeruginosa* via pyruvate fermentation. *J Bacteriol*, *186*(14), 4596-4604.

Euromedex. *Bacterial Adenylate Cyclase Two-Hybrid System Kit*

Flight, W. G., Bright-Thomas, R. J., Tilston, P., Mutton, K. J., Guiver, M., Morris, J., Webb, A. K., & Jones, A. M. (2014). Incidence and clinical impact of respiratory viruses in adults with cystic fibrosis. *Thorax*, *69*(3), 247-253.

Frede, S., Stockmann, C., Freitag, P., & Fandrey, J. (2006). Bacterial lipopolysaccharide induces HIF-1 activation in human monocytes via p44/42 MAPK and NF-kappaB. *Biochem J*, *396*(3), 517-527.

Fritz, L. B., Ouellette, H. A., O'Hanley, T. A., Kassarjian, A., & Palmer, W. E. (2007). Cystic changes at supraspinatus and infraspinatus tendon insertion sites: association with age and rotator cuff disorders in 238 patients. *Radiology*, *244*(1), 239-248.

Fritzsching, B., Zhou-Suckow, Z., Trojanek, J. B., Schubert, S. C., Schatterny, J., Hirtz, S., Agrawal, R., Muley, T., Kahn, N., Sticht, C., Gunkel, N., Welte, T., Randell, S. H., Langer, F., Schnabel, P., Herth, F. J., & Mall, M. A. (2015). Hypoxic epithelial necrosis triggers neutrophilic inflammation via IL-1 receptor signaling in cystic fibrosis lung disease. *Am J Respir Crit Care Med*, *191*(8), 902-913.

Galinier, A., Garnerone, A. M., Reyrat, J. M., Kahn, D., Batut, J., & Boistard, P. (1994). Phosphorylation of the *Rhizobium meliloti* FixJ protein induces its binding to a compound regulatory region at the fixK promoter. *J Biol Chem*, *269*(38), 23784-23789.

Gao, R., & Stock, A. M. (2009). Biological insights from structures of two-component proteins. *Annu Rev Microbiol*, *63*, 133-154.

Garrett, E. S., Perlegas, D., & Wozniak, D. J. (1999). Negative control of flagellum synthesis in *Pseudomonas aeruginosa* is modulated by the alternative sigma factor AlgT (AlgU). *J Bacteriol*, *181*(23), 7401-7404.

Ghaz-Jahanian, M. A., Khodaparastan, F., Berenjian, A., & Jafarizadeh-Malmiri, H. (2013). Influence of small RNAs on biofilm formation process in bacteria. *Mol Biotechnol*, *55*(3), 288-297.

Gibbs, D. F., Shanley, T. P., Warner, R. L., Murphy, H. S., Varani, J., & Johnson, K. J. (1999). Role of matrix metalloproteinases in models of macrophage-dependent acute lung injury. Evidence for alveolar macrophage as source of proteinases. *Am J Respir Cell Mol Biol*, *20*(6), 1145-1154.

Gilles-Gonzalez, M. A., & Gonzalez, G. (1993). Regulation of the kinase activity of heme protein FixL from the two-component system FixL/FixJ of Rhizobium meliloti. *J Biol Chem*, *268*(22), 16293-16297.

Gorres, K. L., & Raines, R. T. (2010). Prolyl 4-hydroxylase. *Crit Rev Biochem Mol Biol*, *45*(2), 106-124.

Gouet, P., Fabry, B., Guillet, V., Birck, C., Mourey, L., Kahn, D., & Samama, J. P. (1999). Structural transitions in the FixJ receiver domain. *Structure*, *7*(12), 1517-1526.

Grigg, J., Miyashita, L., & Suri, R. (2017). Pneumococcal infection of respiratory cells exposed to welding fumes; Role of oxidative stress and HIF-1 alpha. *PLoS One*, *12*(3), e0173569.

Ha, D. G., & O'Toole, G. A. (2015). c-di-GMP and its Effects on Biofilm Formation and Dispersion: a *Pseudomonas Aeruginosa* Review. *Microbiol Spectr*, *3*(2), MB-0003-2014.

Halfon, Y., Jimenez-Fernandez, A., La Rosa, R., Espinosa Portero, R., Krogh Johansen, H., Matzov, D., Eyal, Z., Bashan, A., Zimmerman, E., Belousoff, M., Molin, S., & Yonath, A. (2019). Structure of *Pseudomonas aeruginosa* ribosomes from an aminoglycoside-resistant clinical isolate. *Proc Natl Acad Sci U S A*, *116*(44), 22275-22281.

Harutyunyan, M., Huang, Y., Mun, K. S., Yang, F., Arora, K., & Naren, A. P. (2018). Personalized medicine in CF: from modulator development to therapy for cystic fibrosis patients with rare CFTR mutations. Am J Physiol Lung Cell Mol Physiol, 314(4), L529-L543.

Hassett, D. J. (1996). Anaerobic production of alginate by *Pseudomonas aeruginosa*: alginate restricts diffusion of oxygen. *J Bacteriol*, *178*(24), 7322-7325.

Hauser, A. R., Jain, M., Bar-Meir, M., & McColley, S. A. (2011). Clinical significance of microbial infection and adaptation in cystic fibrosis. *Clin Microbiol Rev*, *24*(1), 29-70.

Hay, I. D., Gatland, K., Campisano, A., Jordens, J. Z., & Rehm, B. H. (2009). Impact of alginate overproduction on attachment and biofilm architecture of a supermucoid *Pseudomonas aeruginosa* strain. *Appl Environ Microbiol*, *75*(18), 6022-6025.

Hay, I. D., Ur Rehman, Z., Moradali, M. F., Wang, Y., & Rehm, B. H. (2013). Microbial alginate production, modification and its applications. Microb Biotechnol, 6(6), 637-650.

Hay, I. D., Remminghorst, U., & Rehm, B. H. (2009). MucR, a novel membrane-associated regulator of alginate biosynthesis in *Pseudomonas aeruginosa*. *Appl Environ Microbiol*, *75*(4), 1110-1120.

Hay, I. D., Wang, Y., Moradali, M. F., Rehman, Z. U., & Rehm, B. H. (2014). Genetics and regulation of bacterial alginate production. *Environ Microbiol*, *16*(10), 2997-3011.

He, J., Jia, X., Yang, S., Xu, X., Sun, K., Li, C., Yang, T., & Zhang, L. (2018). Heteroresistance to carbapenems in invasive *Pseudomonas aeruginosa* infections. *Int J Antimicrob Agents*, *51*(3), 413-421.

Hecht, G. B., & Newton, A. (1995). Identification of a novel response regulator required for the swarmer-to-stalked-cell transition in *Caulobacter crescentus*. *J Bacteriol*, *177*(21), 6223-6229.

Hendricks, M. R., Lashua, L. P., Fischer, D. K., Flitter, B. A., Eichinger, K. M., Durbin, J. E., Sarkar, S. N., Coyne, C. B., Empey, K. M., & Bomberger, J. M. (2016). Respiratory syncytial virus infection enhances *Pseudomonas aeruginosa* biofilm growth through dysregulation of nutritional immunity. *Proc Natl Acad Sci U S A*, *113*(6), 1642-1647.

Hengge, R. (2009). Principles of c-di-GMP signalling in bacteria. *Nat Rev Microbiol*, *7*(4), 263-273.

Hengge, R. (2016). Trigger phosphodiesterases as a novel class of c-di-GMP effector proteins. *Philos Trans R Soc Lond B Biol Sci*, *371*(1707).

Hermes, D. M., Pormann Pitt, C., Lutz, L., Teixeira, A. B., Ribeiro, V. B., Netto, B., Martins, A. F., Zavascki, A. P., & Barth, A. L. (2013). Evaluation of heteroresistance to polymyxin B among carbapenem-susceptible and -resistant *Pseudomonas aeruginosa*. *J Med Microbiol*, *62*(Pt 8), 1184-1189.

Hodges, N. A., & Gordon, C. A. (1991). Protection of *Pseudomonas aeruginosa* against ciprofloxacin and beta-lactams by homologous alginate. *Antimicrob Agents Chemother*, *35*(11), 2450-2452.

Hogardt, M., & Heesemann, J. (2013). Microevolution of *Pseudomonas aeruginosa* to a chronic pathogen of the cystic fibrosis lung. Curr Top Microbiol Immunol, 358, 91-118.

Hooper, D. C., & Jacoby, G. A. (2015). Mechanisms of drug resistance: quinolone resistance. *Ann N Y Acad Sci*, *1354*, 12-31.

Hou, S., Larsen, R. W., Boudko, D., Riley, C. W., Karatan, E., Zimmer, M., Ordal, G. W., & Alam, M. (2000). Myoglobin-like aerotaxis transducers in Archaea and Bacteria. *Nature*, *403*(6769), 540-544.

Jenal, U., Reinders, A., & Lori, C. (2017). Cyclic di-GMP: second messenger extraordinaire. *Nat Rev Microbiol*, *15*(5), 271-284.

Johansen, H. K., & Hoiby, N. (1992). Seasonal onset of initial colonisation and chronic infection with *Pseudomonas aeruginosa* in patients with cystic fibrosis in Denmark. *Thorax*, *47*(2), 109-111.

Kakishima, K., Shiratsuchi, A., Taoka, A., Nakanishi, Y., & Fukumori, Y. (2007). Participation of nitric oxide reductase in survival of *Pseudomonas aeruginosa* in LPS-activated macrophages. *Biochem Biophys Res Commun*, *355*(2), 587-591.

Karimova, G., Pidoux, J., Ullmann, A., & Ladant, D. (1998). A bacterial two-hybrid system based on a reconstituted signal transduction pathway. Proceedings of the National Academy of Sciences of the United States of America, 95(10), 5752–5756.

Kerem, B., Rommens, J. M., Buchanan, J. A., Markiewicz, D., Cox, T. K., Chakravarti, A., Buchwald, M., & Tsui, L. C. (1989). Identification of the cystic fibrosis gene: genetic analysis. *Science*, *245*(4922), 1073-1080.

Kiley, P. J., & Beinert, H. (1998). Oxygen sensing by the global regulator, FNR: the role of the iron-sulfur cluster. *FEMS Microbiol Rev*, *22*(5), 341-352.

Kim, E. J., Sabra, W., & Zeng, A. P. (2003). Iron deficiency leads to inhibition of oxygen transfer and enhanced formation of virulence factors in cultures of *Pseudomonas aeruginosa* PAO1. *Microbiology (Reading)*, *149*(Pt 9), 2627-2634.

Klauck, G., Serra, D. O., Possling, A., & Hengge, R. (2018). Spatial organization of different sigma factor activities and c-di-GMP signalling within the three-dimensional landscape of a bacterial biofilm. *Open Biol*, *8*(8).

Klockgether, J., Cramer, N., Fischer, S., Wiehlmann, L., & Tummler, B. (2018). Long-Term Microevolution of *Pseudomonas aeruginosa* Differs between Mildly and Severely Affected Cystic Fibrosis Lungs. *Am J Respir Cell Mol Biol*, *59*(2), 246-256.

Kordes, A., Preusse, M., Willger, S. D., Braubach, P., Jonigk, D., Haverich, A., Warnecke, G., & Haussler, S. (2019). Genetically diverse *Pseudomonas aeruginosa* populations display similar transcriptomic profiles in a cystic fibrosis explanted lung. *Nat Commun*, *10*(1), 3397.

Kuchma, S. L., Ballok, A. E., Merritt, J. H., Hammond, J. H., Lu, W., Rabinowitz, J. D., & O'Toole, G. A. (2010). Cyclic-di-GMP-mediated repression of swarming motility by *Pseudomonas aeruginosa*: the *pilY1* gene and its impact on surface-associated behaviors. *J Bacteriol*, *192*(12), 2950-2964.

Kuchma, S. L., Griffin, E. F., & O'Toole, G. A. (2012). Minor pilins of the type IV pilus system participate in the negative regulation of swarming motility. *J Bacteriol*, *194*(19), 5388-5403.

La Rosa, R., Johansen, H. K., & Molin, S. (2018). Convergent Metabolic Specialization through Distinct Evolutionary Paths in *Pseudomonas aeruginosa. mBio*, *9*(2).

LaFemina, M. J., Sutherland, K. M., Bentley, T., Gonzales, L. W., Allen, L., Chapin, C. J., Rokkam, D., Sweerus, K. A., Dobbs, L. G., Ballard, P. L., & Frank, J. A. (2014). Claudin-18 deficiency results in alveolar barrier dysfunction and impaired alveologenesis in mice. *Am J Respir Cell Mol Biol*, *51*(4), 550-558.

Lalaouna, D., Fochesato, S., Sanchez, L., Schmitt-Kopplin, P., Haas, D., Heulin, T., & Achouak, W. (2012). Phenotypic switching in *Pseudomonas brassicacearum* involves GacS- and GacA-dependent Rsm small RNAs. *Appl Environ Microbiol*, *78*(6), 1658-1665.

Laventie, B. J., Sangermani, M., Estermann, F., Manfredi, P., Planes, R., Hug, I., Jaeger, T., Meunier, E., Broz, P., & Jenal, U. (2019). A Surface-Induced Asymmetric Program Promotes Tissue Colonization by *Pseudomonas aeruginosa*. *Cell Host Microbe*, *25*(1), 140-152 e146.

Learn, D. B., Brestel, E. P., & Seetharama, S. (1987). Hypochlorite scavenging by *Pseudomonas aeruginosa* alginate. *Infect Immun*, *55*(8), 1813-1818.

Leech, A. J., Sprinkle, A., Wood, L., Wozniak, D. J., & Ohman, D. E. (2008). The NtrC family regulator AlgB, which controls alginate biosynthesis in mucoid *Pseudomonas aeruginosa*, binds directly to the *algD* promoter. *J Bacteriol*, *190*(2), 581-589.

Lewis, K. A., Baker, A. E., Chen, A. I., Harty, C. E., Kuchma, S. L., O'Toole, G. A., & Hogan, D. A. (2019). Ethanol Decreases *Pseudomonas aeruginosa* Flagellar Motility through the Regulation of Flagellar Stators. *J Bacteriol*, *201*(18).

Li, X., Nielsen, L., Nolan, C., & Halverson, L. J. (2010). Transient alginate gene expression by *Pseudomonas putida* biofilm residents under water-limiting conditions reflects adaptation to the local environment. *Environ Microbiol*, *12*(6), 1578-1590.

Li, Y., Heine, S., Entian, M., Sauer, K., & Frankenberg-Dinkel, N. (2013). NO-induced biofilm dispersion in Pseudomonas aeruginosa is mediated by an MHYT domain-coupled phosphodiesterase. *J Bacteriol*, *195*(16), 3531-3542.

Limoli, D. H., Rockel, A. B., Host, K. M., Jha, A., Kopp, B. T., Hollis, T., & Wozniak, D. J. (2014). Cationic antimicrobial peptides promote microbial mutagenesis and pathoadaptation in chronic infections. *PLoS Pathog*, *10*(4), e1004083.

Lipuma, J. J. (2010). The changing microbial epidemiology in cystic fibrosis. *Clin Microbiol Rev*, *23*(2), 299-323.

Lori, C., Ozaki, S., Steiner, S., Bohm, R., Abel, S., Dubey, B. N., Schirmer, T., Hiller, S., & Jenal, U. (2015). Cyclic di-GMP acts as a cell cycle oscillator to drive chromosome replication. *Nature*, *523*(7559), 236-239.

M, T., T, A., B, S., Ak, G., & Sks, S. (2020). Curcumin prophylaxis refurbishes alveolar epithelial barrier integrity and alveolar fluid clearance under hypoxia. *Respiratory Physiology & Neurobiology*, *274*, 103336.

Ma, L., Wang, J., Wang, S., Anderson, E. M., Lam, J. S., Parsek, M. R., & Wozniak, D. J. (2012). Synthesis of multiple *Pseudomonas aeruginosa* biofilm matrix exopolysaccharides is post-transcriptionally regulated. *Environ Microbiol*, *14*(8), 1995-2005.

Malhotra, S., Hayes, D., Jr., & Wozniak, D. J. (2019). Cystic Fibrosis and *Pseudomonas aeruginosa*: the Host-Microbe Interface. *Clin Microbiol Rev*, *32*(3).

Malhotra, S., Limoli, D. H., English, A. E., Parsek, M. R., & Wozniak, D. J. (2018). Mixed Communities of Mucoid and Nonmucoid *Pseudomonas aeruginosa* Exhibit Enhanced Resistance to Host Antimicrobials. *mBio*, *9*(2).

Mall, M. A. (2016). Unplugging Mucus in Cystic Fibrosis and Chronic Obstructive Pulmonary Disease. *Ann Am Thorac Soc*, *13 Suppl 2*, S177-185.

Martin, D. W., Schurr, M. J., Yu, H., & Deretic, V. (1994). Analysis of promoters controlled by the putative sigma factor AlgU regulating conversion to mucoidy in *Pseudomonas aeruginosa*: relationship to sigma E and stress response. *J Bacteriol*, *176*(21), 6688-6696.

Marvig, R. L., Johansen, H. K., Molin, S., & Jelsbak, L. (2013). Genome analysis of a transmissible lineage of pseudomonas aeruginosa reveals pathoadaptive mutations and distinct evolutionary paths of hypermutators. *PLoS Genet*, *9*(9), e1003741.

Marvig, R. L., Sommer, L. M., Molin, S., & Johansen, H. K. (2015). Convergent evolution and adaptation of *Pseudomonas aeruginosa* within patients with cystic fibrosis. *Nat Genet*, *47*(1), 57-64.

Matsuyama, B. Y., Krasteva, P. V., Baraquet, C., Harwood, C. S., Sondermann, H., & Navarro, M. V. (2016). Mechanistic insights into c-di-GMP-dependent control of the biofilm regulator FleQ from *Pseudomonas aeruginosa*. *Proc Natl Acad Sci U S A*, *113*(2), E209-218.

McCarthy, R. R., Mazon-Moya, M. J., Moscoso, J. A., Hao, Y., Lam, J. S., Bordi, C., Mostowy, S., & Filloux, A. (2017). Cyclic-di-GMP regulates lipopolysaccharide

modification and contributes to *Pseudomonas aeruginosa* immune evasion. *Nat Microbiol*, *2*, 17027.

Merighi, M., Lee, V. T., Hyodo, M., Hayakawa, Y., & Lory, S. (2007). The second messenger bis-(3'-5')-cyclic-GMP and its PilZ domain-containing receptor Alg44 are required for alginate biosynthesis in *Pseudomonas aeruginosa*. *Mol Microbiol*, *65*(4), 876-895.

Merritt, J. H., Brothers, K. M., Kuchma, S. L., & O'Toole, G. A. (2007). SadC reciprocally influences biofilm formation and swarming motility via modulation of exopolysaccharide production and flagellar function. *J Bacteriol*, *189*(22), 8154-8164.

Moll, S., Schneider, D. J., Stodghill, P., Myers, C. R., Cartinhour, S. W., & Filiatrault, M. J. (2010). Construction of an rsmX co-variance model and identification of five rsmX non-coding RNAs in *Pseudomonas syringae pv. tomato* DC3000. *RNA Biol*, *7*(5), 508-516.

Monson, E. K., Weinstein, M., Ditta, G. S., & Helinski, D. R. (1992). The FixL protein of Rhizobium meliloti can be separated into a heme-binding oxygen-sensing domain and a functional C-terminal kinase domain. *Proc Natl Acad Sci U S A*, *89*(10), 4280-4284.

Moradali, M. F., Ghods, S., & Rehm, B. H. A. (2017). Activation Mechanism and Cellular Localization of Membrane-Anchored Alginate Polymerase in *Pseudomonas aeruginosa. Appl Environ Microbiol*, *83*(9).

Moscoso, J. A., Jaeger, T., Valentini, M., Hui, K., Jenal, U., & Filloux, A. (2014). The diguanylate cyclase SadC is a central player in Gac/Rsm-mediated biofilm formation in *Pseudomonas aeruginosa*. *J Bacteriol*, *196*(23), 4081-4088.

Mullner, M., Hammel, O., Mienert, B., Schlag, S., Bill, E., & Unden, G. (2008). A PAS domain with an oxygen labile [4Fe-4S](2+) cluster in the oxygen sensor kinase NreB of *Staphylococcus carnosus*. *Biochemistry*, *47*(52), 13921-13932.

Nair, H. A., Periasamy, S., Yang, L., Kjelleberg, S., & Rice, S. A. (2017). Real Time, Spatial, and Temporal Mapping of the Distribution of c-di-GMP during Biofilm Development. *J Biol Chem*, *292*(2), 477-487.

Ng, C., Nadig, T., Smyth, A. R., & Flume, P. (2020). Treatment of pulmonary exacerbations in cystic fibrosis. Curr Opin Pulm Med, 26(6), 679-684.

Nguyen, A. T., & Oglesby-Sherrouse, A. G. (2016). Interactions between *Pseudomonas aeruginosa* and *Staphylococcus aureus* during co-cultivations and polymicrobial infections. *Appl Microbiol Biotechnol*, *100*(14), 6141-6148.

Nishimura, T., Teramoto, H., Vertes, A. A., Inui, M., & Yukawa, H. (2008). ArnR, a novel transcriptional regulator, represses expression of the *narKGHJI* operon in *Corynebacterium glutamicum*. *J Bacteriol*, *190*(9), 3264-3273.

Nivens, D. E., Ohman, D. E., Williams, J., & Franklin, M. J. (2001). Role of alginate and its O acetylation in formation of *Pseudomonas aeruginosa* microcolonies and biofilms. *J Bacteriol*, *183*(3), 1047-1057.

Oglesby, L. L., Jain, S., & Ohman, D. E. (2008). Membrane topology and roles of *Pseudomonas aeruginosa* Alg8 and Alg44 in alginate polymerization. *Microbiology (Reading)*, *154*(Pt 6), 1605-1615.

Page, L. K., Staples, K. J., Spalluto, C. M., Watson, A., & Wilkinson, T. M. A. (2021). Influence of Hypoxia on the Epithelial-Pathogen Interactions in the Lung: Implications for Respiratory Disease. *Front Immunol*, *12*, 653969.

Palmer, K. L., Aye, L. M., & Whiteley, M. (2007). Nutritional cues control *Pseudomonas aeruginosa* multicellular behavior in cystic fibrosis sputum. *J Bacteriol*, *189*(22), 8079-8087.

Paul, R., Abel, S., Wassmann, P., Beck, A., Heerklotz, H., & Jenal, U. (2007). Activation of the diguanylate cyclase PleD by phosphorylation-mediated dimerization. *J Biol Chem*, *282*(40), 29170-29177.

Petchiappan, A., Naik, S. Y., & Chatterji, D. (2020). Tracking the homeostasis of second messenger cyclic-di-GMP in bacteria. *Biophys Rev*, *12*(3), 719-730.

Pier, G. B., Coleman, F., Grout, M., Franklin, M., & Ohman, D. E. (2001). Role of alginate O acetylation in resistance of mucoid *Pseudomonas aeruginosa* to opsonic phagocytosis. *Infect Immun*, *69*(3), 1895-1901.

Platt, M. D., Schurr, M. J., Sauer, K., Vazquez, G., Kukavica-Ibrulj, I., Potvin, E., Levesque, R. C., Fedynak, A., Brinkman, F. S., Schurr, J., Hwang, S. H., Lau, G. W., Limbach, P. A., Rowe, J. J., Lieberman, M. A., Barraud, N., Webb, J., Kjelleberg, S., Hunt, D. F., & Hassett, D. J. (2008). Proteomic, microarray, and signature-tagged mutagenesis analyses of anaerobic *Pseudomonas aeruginosa* at pH 6.5, likely representing chronic, late-stage cystic fibrosis airway conditions. *J Bacteriol*, *190*(8), 2739-2758.

Price-Whelan, A., Dietrich, L. E., & Newman, D. K. (2007). Pyocyanin alters redox homeostasis and carbon flux through central metabolic pathways in *Pseudomonas aeruginosa* PA14. *J Bacteriol*, *189*(17), 6372-6381.

Pullan, S. T., Monk, C. E., Lee, L., & Poole, R. K. (2008). Microbial responses to nitric oxide and nitrosative stress: growth, "omic," and physiological methods. *Methods Enzymol*, *437*, 499-519.

Qiu, D., Eisinger, V. M., Head, N. E., Pier, G. B., & Yu, H. D. (2008). ClpXP proteases positively regulate alginate overexpression and mucoid conversion in *Pseudomonas aeruginosa*. *Microbiology (Reading)*, *154*(Pt 7), 2119-2130.

Qiu, D., Eisinger, V. M., Rowen, D. W., & Yu, H. D. (2007). Regulated proteolysis controls mucoid conversion in *Pseudomonas aeruginosa*. *Proc Natl Acad Sci U S A*, *104*(19), 8107-8112.

Rahmani-Badi, A., Sepehr, S., Fallahi, H., & Heidari-Keshel, S. (2015). Dissection of the cis-2-decenoic acid signaling network in *Pseudomonas aeruginosa* using microarray technique. *Front Microbiol*, *6*, 383.

Registry, C. F. F. P. (2022). 2019 Annual Data Report. *©2023 Cystic Fibrosis Foundation*.

Rietsch, A., Vallet-Gely, I., Dove, S. L., & Mekalanos, J. J. (2005). ExsE, a secreted regulator of type III secretion genes in *Pseudomonas aeruginosa*. Proc Natl Acad Sci U S A, 102(22), 8006-8011.

Riordan, J. R., Rommens, J. M., Kerem, B., Alon, N., Rozmahel, R., Grzelczak, Z., Zielenski, J., Lok, S., Plavsic, N., Chou, J. L., & et al. (1989). Identification of the cystic fibrosis gene: cloning and characterization of complementary DNA. *Science*, *245*(4922), 1066-1073.

Rodesney, C. A., Roman, B., Dhamani, N., Cooley, B. J., Katira, P., Touhami, A., & Gordon, V. D. (2017). Mechanosensing of shear by *Pseudomonas aeruginosa* leads to increased levels of the cyclic-di-GMP signal initiating biofilm development. *Proc Natl Acad Sci U S A*, *114*(23), 5906-5911.

Rommens, J. M., Iannuzzi, M. C., Kerem, B., Drumm, M. L., Melmer, G., Dean, M., Rozmahel, R., Cole, J. L., Kennedy, D., Hidaka, N., & et al. (1989). Identification of the cystic fibrosis gene: chromosome walking and jumping. *Science*, *245*(4922), 1059-1065.

Rosales-Reyes, R., Vargas-Roldán, S. Y., Lezana-Fernández, J. L., & Santos-Preciado, J. I. (2021). *Pseudomonas Aeruginosa*: Genetic Adaptation, A Strategy for its Persistence in Cystic Fibrosis. *Archives of Medical Research*, *52*(4), 357-361.

Ross, P., Weinhouse, H., Aloni, Y., Michaeli, D., Weinberger-Ohana, P., Mayer, R., Braun, S., de Vroom, E., van der Marel, G. A., van Boom, J. H., & Benziman, M. (1987). Regulation of cellulose synthesis in *Acetobacter xylinum* by cyclic diguanylic acid. *Nature*, *325*(6101), 279-281.

Rossi, E., Falcone, M., Molin, S., & Johansen, H. K. (2018). High-resolution in situ transcriptomics of *Pseudomonas aeruginosa* unveils genotype independent patho-phenotypes in cystic fibrosis lungs. *Nat Commun*, *9*(1), 3459.

Rossi, E., La Rosa, R., Bartell, J. A., Marvig, R. L., Haagensen, J. A. J., Sommer, L. M., Molin, S., & Johansen, H. K. (2021). *Pseudomonas aeruginosa* adaptation and evolution in patients with cystic fibrosis. *Nat Rev Microbiol*, *19*(5), 331-342.

Ryder, C., Byrd, M., & Wozniak, D. J. (2007). Role of polysaccharides in *Pseudomonas aeruginosa* biofilm development. *Curr Opin Microbiol*, *10*(6), 644-648.

Sabra, W., Kim, E. J., & Zeng, A. P. (2002). Physiological responses of *Pseudomonas aeruginosa* PAO1 to oxidative stress in controlled microaerobic and aerobic cultures. *Microbiology (Reading)*, *148*(Pt 10), 3195-3202.

Sabra, W., Zeng, A. P., Lunsdorf, H., & Deckwer, W. D. (2000). Effect of oxygen on formation and structure of *Azotobacter vinelandii* alginate and its role in protecting nitrogenase. *Appl Environ Microbiol*, *66*(9), 4037-4044.

Saiman, L., Siegel, J. D., LiPuma, J. J., Brown, R. F., Bryson, E. A., Chambers, M. J., Downer, V. S., Fliege, J., Hazle, L. A., Jain, M., Marshall, B. C., O'Malley, C., Pattee, S. R., Potter-Bynoe, G., Reid, S., Robinson, K. A., Sabadosa, K. A., Schmidt, H. J., Tullis, E., Webber, J., Weber, D. J., Cystic Fibrous, F., & Society for Healthcare Epidemiology of, A. (2014). Infection prevention and control guideline for cystic fibrosis: 2013 update. Infect Control Hosp Epidemiol, 35 Suppl 1, S1-S67.

Sarenko, O., Klauck, G., Wilke, F. M., Pfiffer, V., Richter, A. M., Herbst, S., Kaever, V., & Hengge, R. (2017). More than Enzymes That Make or Break Cyclic Di-GMP-Local Signaling in the Interactome of GGDEF/EAL Domain Proteins of *Escherichia coli*. *mBio*, *8*(5).

Sautter, R., Ramos, D., Schneper, L., Ciofu, O., Wassermann, T., Koh, C. L., Heydorn, A., Hentzer, M., Hoiby, N., Kharazmi, A., Molin, S., Devries, C. A., Ohman, D. E., & Mathee, K. (2012). A complex multilevel attack on *Pseudomonas aeruginosa* algT/U expression and algT/U activity results in the loss of alginate production. *Gene*, *498*(2), 242-253.

Schaible, B., Crifo, B., Schaffer, K., & Taylor, C. T. (2020). The putative bacterial oxygen sensor Pseudomonas prolyl hydroxylase (PPHD) suppresses antibiotic resistance and pathogenicity in *Pseudomonas aeruginosa*. *J Biol Chem*, *295*(5), 1195-1201.

Schaible, B., Rodriguez, J., Garcia, A., von Kriegsheim, A., McClean, S., Hickey, C., Keogh, C. E., Brown, E., Schaffer, K., Broquet, A., & Taylor, C. T. (2017). Hypoxia Reduces the Pathogenicity of *Pseudomonas aeruginosa* by Decreasing the Expression of Multiple Virulence Factors. *J Infect Dis*, *215*(9), 1459-1467.

Scherhag, A., Raschle, M., Unbehend, N., Venn, B., Glueck, D., Muhlhaus, T., Keller, S., Perez Patallo, E., Zehner, S., & Frankenberg-Dinkel, N. (2023). Characterization of a soluble library of the *Pseudomonas aeruginosa* PAO1 membrane proteome with emphasis on c-di-GMP turnover enzymes. Microlife, 4, uqad028.

Schirmer, T., & Jenal, U. (2009). Structural and mechanistic determinants of c-di-GMP signalling. *Nat Rev Microbiol*, *7*(10), 724-735.

Schmidt, A. (2015). *Oxygen-dependent regulation of alginate export in Pseudomonas aeruginosa*

Schmidt, A., Hammerbacher, A. S., Bastian, M., Nieken, K. J., Klockgether, J., Merighi, M., Lapouge, K., Poschgan, C., Kolle, J., Acharya, K. R., Ulrich, M., Tummler, B., Unden, G., Kaever, V., Lory, S., Haas, D., Schwarz, S., & Doring, G. (2016). Oxygen-dependent regulation of c-di-GMP synthesis by SadC controls alginate production in *Pseudomonas aeruginosa*. *Environ Microbiol*, *18*(10), 3390-3402.

Schnicker, N. J., Razzaghi, M., Guha Thakurta, S., Chakravarthy, S., & Dey, M. (2017). Bacillus anthracis Prolyl 4-Hydroxylase Interacts with and Modifies Elongation Factor Tu. *Biochemistry*, *56*(43), 5771-5785.

Schobert, M., & Jahn, D. (2010). Anaerobic physiology of *Pseudomonas aeruginosa* in the cystic fibrosis lung. *Int J Med Microbiol*, *300*(8), 549-556.

Schogler, A., Stokes, A. B., Casaulta, C., Regamey, N., Edwards, M. R., Johnston, S. L., Jung, A., Moeller, A., Geiser, T., & Alves, M. P. (2016). Interferon response of the cystic fibrosis bronchial epithelium to major and minor group rhinovirus infection. *J Cyst Fibros*, *15*(3), 332-339.

Scotet, V., Gutierrez, H., & Farrell, P. M. (2020). Newborn Screening for CF across the Globe-Where Is It Worthwhile? *Int J Neonatal Screen*, *6*(1), 18.

Scotti, J. S., Leung, I. K., Ge, W., Bentley, M. A., Paps, J., Kramer, H. B., Lee, J., Aik, W., Choi, H., Paulsen, S. M., Bowman, L. A., Loik, N. D., Horita, S., Ho, C. H., Kershaw, N. J., Tang, C. M., Claridge, T. D., Preston, G. M., McDonough, M. A., & Schofield, C. J. (2014). Human oxygen sensing may have origins in prokaryotic elongation factor Tu prolyl-hydroxylation. *Proc Natl Acad Sci U S A*, *111*(37), 13331-13336.

Shang L, Yan Y, Zhan Y, Ke X, Shao Y, Liu Y, Yang H, Wang S, Dai S, Lu J, Yan N, Yang Z, Lu W, Liu Z, Chen S, Elmerich C, Lin M. A regulatory network involving Rpo, Gac and Rsm for nitrogen-fixing biofilm formation by *Pseudomonas stutzeri*. NPJ Biofilms Microbiomes. 2021 Jul 1;7(1):54.

Shinabarger, D., Berry, A., May, T. B., Rothmel, R., Fialho, A., & Chakrabarty, A. M. (1991). Purification and characterization of phosphomannose isomerase-guanosine diphospho-D-mannose pyrophosphorylase. A bifunctional enzyme in the alginate biosynthetic pathway of *Pseudomonas aeruginosa*. *J Biol Chem*, *266*(4), 2080-2088.

Shukla, S. D., Sohal, S. S., O'Toole, R. F., Eapen, M. S., & Walters, E. H. (2015). Platelet activating factor receptor: gateway for bacterial chronic airway infection in chronic obstructive pulmonary disease and potential therapeutic target. *Expert Rev Respir Med*, *9*(4), 473-485.

Simon, R., Priefer, U., & Pühler, A. (1983). A Broad Host Range Mobilization System for In Vivo Genetic Engineering: Transposon Mutagenesis in Gram Negative Bacteria. Bio/Technology, 1(9), 784-791.

Son, M. S., Matthews, W. J., Jr., Kang, Y., Nguyen, D. T., & Hoang, T. T. (2007). In vivo evidence of *Pseudomonas aeruginosa* nutrient acquisition and pathogenesis in the lungs of cystic fibrosis patients. *Infect Immun*, *75*(11), 5313-5324.

Southern, K. W., Munck, A., Pollitt, R., Travert, G., Zanolla, L., Dankert-Roelse, J., Castellani, C., & Group, E. C. N. S. W. (2007). A survey of newborn screening for cystic fibrosis in Europe. *J Cyst Fibros*, *6*(1), 57-65.

Spangler, C., Kaever, V., & Seifert, R. (2011). Interaction of the diguanylate cyclase YdeH of *Escherichia coli* with 2',(3')-substituted purine and pyrimidine nucleotides. *J Pharmacol Exp Ther*, *336*(1), 234-241.

Spiro, S. (2007). Regulators of bacterial responses to nitric oxide. *FEMS Microbiol Rev*, *31*(2), 193-211.

Stevens, D. A., Moss, R. B., Kurup, V. P., Knutsen, A. P., Greenberger, P., Judson, M. A., Denning, D. W., Crameri, R., Brody, A. S., Light, M., Skov, M., Maish, W., Mastella, G., & Participants in the Cystic Fibrosis Foundation Consensus, C. (2003). Allergic bronchopulmonary aspergillosis in cystic fibrosis--state of the art: Cystic Fibrosis Foundation Consensus Conference. *Clin Infect Dis*, *37 Suppl 3*, S225-264.

Stoltz, D. A., Meyerholz, D. K., & Welsh, M. J. (2015). Origins of cystic fibrosis lung disease. *N Engl J Med*, *372*(16), 1574-1575.

Sutton, V. R., Mettert, E. L., Beinert, H., & Kiley, P. J. (2004). Kinetic analysis of the oxidative conversion of the [4Fe-4S]2+ cluster of FNR to a [2Fe-2S]2+ Cluster. *Journal of bacteriology*, *186*(23), 8018-8025.

Taabazuing, C. Y., Hangasky, J. A., & Knapp, M. J. (2014). Oxygen sensing strategies in mammals and bacteria. *J Inorg Biochem*, *133*, 63-72.

Tai, A. S., Sherrard, L. J., Kidd, T. J., Ramsay, K. A., Buckley, C., Syrmis, M., Grimwood, K., Bell, S. C., & Whiley, D. M. (2017). Antibiotic perturbation of mixed-strain *Pseudomonas aeruginosa* infection in patients with cystic fibrosis. *BMC Pulm Med*, *17*(1), 138.

Thi, M. T. T., Wibowo, D., & Rehm, B. H. A. (2020). *Pseudomonas aeruginosa* Biofilms. *Int J Mol Sci*, *21*(22).

Trimble, M. J., & McCarter, L. L. (2011). Bis-(3'-5')-cyclic dimeric GMP-linked quorum sensing controls swarming in *Vibrio parahaemolyticus*. *Proc Natl Acad Sci U S A*, *108*(44), 18079-18084.

Turcios, N. L. (2020). Cystic Fibrosis Lung Disease: An Overview. *Respir Care*, *65*(2), 233-251.

Unden, G., Nilkens, S., & Singenstreu, M. (2013). Bacterial sensor kinases using Fe-S cluster binding PAS or GAF domains for O_2 sensing. *Dalton Trans*, *42*(9), 3082-3087.

Urtuvia, V., Maturana, N., Acevedo, F., Pena, C., & Diaz-Barrera, A. (2017). Bacterial alginate production: an overview of its biosynthesis and potential industrial production. World J Microbiol Biotechnol, 33(11), 198. https://doi.org/10.1007/s11274-017-2363-x

Valentini, M., & Filloux, A. (2016). Biofilms and Cyclic di-GMP (c-di-GMP) Signaling: Lessons from *Pseudomonas aeruginosa* and Other Bacteria. *J Biol Chem*, *291*(24), 12547-12555.

Valentini, M., Gonzalez, D., Mavridou, D. A., & Filloux, A. (2018). Lifestyle transitions and adaptive pathogenesis of *Pseudomonas aeruginosa*. Curr Opin Microbiol, 41, 15-20.

Walmsley, S. R., Print, C., Farahi, N., Peyssonnaux, C., Johnson, R. S., Cramer, T., Sobolewski, A., Condliffe, A. M., Cowburn, A. S., Johnson, N., & Chilvers, E. R. (2005). Hypoxia-induced neutrophil survival is mediated by HIF-1alpha-dependent NF-kappaB activity. *J Exp Med*, *201*(1), 105-115.

Wang, X. C., Wilson, S. C., & Hammond, M. C. (2016). Next-generation RNA-based fluorescent biosensors enable anaerobic detection of cyclic di-GMP. *Nucleic Acids Res*, *44*(17), e139.

Wang, Y., Hay, I. D., Rehman, Z. U., & Rehm, B. H. (2015). Membrane-anchored MucR mediates nitrate-dependent regulation of alginate production in *Pseudomonas aeruginosa*. *Appl Microbiol Biotechnol*, *99*(17), 7253-7265.

Wat, D., & Doull, I. (2003). Respiratory virus infections in cystic fibrosis. *Paediatr Respir Rev*, *4*(3), 172-177.

Webster, S. S., Lee, C. K., Schmidt, W. C., Wong, G. C. L., & O'Toole, G. A. (2021). Interaction between the type 4 pili machinery and a diguanylate cyclase fine-tune c-di-GMP levels during early biofilm formation. *Proc Natl Acad Sci U S A*, *118*(26).

Wong, B. W., Kuchnio, A., Bruning, U., & Carmeliet, P. (2013). Emerging novel functions of the oxygen-sensing prolyl hydroxylase domain enzymes. *Trends Biochem Sci*, *38*(1), 3-11.

Wood, L. F., & Ohman, D. E. (2015). Cell wall stress activates expression of a novel stress response facilitator (SrfA) under sigma22 (AlgT/U) control in *Pseudomonas aeruginosa. Microbiology (Reading)*, *161*(Pt 1), 30-40.

Worlitzsch, D., Tarran, R., Ulrich, M., Schwab, U., Cekici, A., Meyer, K. C., Birrer, P., Bellon, G., Berger, J., Weiss, T., Botzenhart, K., Yankaskas, J. R., Randell, S., Boucher, R. C., & Doring, G. (2002). Effects of reduced mucus oxygen concentration in airway *Pseudomonas* infections of cystic fibrosis patients. *J Clin Invest*, *109*(3), 317-325.

Wozniak, D. J., Wyckoff, T. J., Starkey, M., Keyser, R., Azadi, P., O'Toole, G. A., & Parsek, M. R. (2003). Alginate is not a significant component of the extracellular polysaccharide matrix of PA14 and PAO1 *Pseudomonas aeruginosa* biofilms. *Proc Natl Acad Sci U S A*, *100*(13), 7907-7912.

Xie, L., Xiao, K., Whalen, E. J., Forrester, M. T., Freeman, R. S., Fong, G., Gygi, S. P., Lefkowitz, R. J., & Stamler, J. S. (2009). Oxygen-regulated beta(2)-adrenergic receptor hydroxylation by EGLN3 and ubiquitylation by pVHL. *Sci Signal*, *2*(78), ra33.

Yin, Y., Withers, T. R., Wang, X., & Yu, H. D. (2013). Evidence for sigma factor competition in the regulation of alginate production by *Pseudomonas aeruginosa. PLoS One*, *8*(8), e72329.

Young, R. L., Malcolm, K. C., Kret, J. E., Caceres, S. M., Poch, K. R., Nichols, D. P., Taylor-Cousar, J. L., Saavedra, M. T., Randell, S. H., Vasil, M. L., Burns, J. L., Moskowitz, S. M., & Nick, J. A. (2011). Neutrophil extracellular trap (NET)-mediated killing of *Pseudomonas aeruginosa:* evidence of acquired resistance within the CF airway, independent of CFTR. *PLoS One*, *6*(9), e23637.

Zahringer, F., Lacanna, E., Jenal, U., Schirmer, T., & Boehm, A. (2013). Structure and signaling mechanism of a zinc-sensory diguanylate cyclase. *Structure*, *21*(7), 1149-1157.

Zhao, N. L., Zhang, Q. Q., Zhao, C., Liu, L., Li, T., Li, C. C., He, L. H., Zhu, Y. B., Song, Y. J., Liu, H. X., & Bao, R. (2021). Structural and molecular dynamic studies of *Pseudomonas aeruginosa* OdaA reveal the regulation role of a C-terminal hinge element. *Biochim Biophys Acta Gen Subj*, *1865*(1), 129756.

Zheng, H., Korendovych, I. V., & Luk, Y. Y. (2016). Quantification of alginate by aggregation induced by calcium ions and fluorescent polycations. *Anal Biochem*, *492*, 76-81.

Zhu, B., Liu, C., Liu, S., Cong, H., Chen, Y., Gu, L., & Ma, L. Z. (2016). Membrane association of SadC enhances its diguanylate cyclase activity to control exopolysaccharides synthesis and biofilm formation in *Pseudomonas aeruginosa*. *Environ Microbiol*, *18*(10), 3440-3452.

Zumft, W. G. (1997). Cell biology and molecular basis of denitrification. *Microbiol Mol Biol Rev*, *61*(4), 533-616.